Elsevier Editorial System(tm) for Energy Conversion and Management

Manuscript Draft

Manuscript Number: ECM-D-18-07830R1

Title: Unbalanced mass flow rate of packed bed thermal energy storage and its influence on the Joule-Brayton based Pumped Thermal Electricity Storage

Article Type: Original research paper

Section/Category: 3. Clean Energy and Sustainability

Keywords: pumped thermal electricity storage; thermal energy storage; packed bed; energy storage; unbalanced mass flow

Corresponding Author: Professor Haisheng Chen,

Corresponding Author's Institution: Institute of Engineering Thermophysics, Chinese Academy of Sciences

First Author: Liang Wang, Ph.D

Order of Authors: Liang Wang, Ph.D; Xipeng Lin, Ph.D; Lei Chai, Ph.D; Long Peng, Ph.D; Dong Yu, Ph.D; Jia Liu, Ph.D; Haisheng Chen

Abstract: As the most suitable thermal energy storage manner for the Joule-Brayton based Pumped Thermal Electricity Storage (PTES), packed beds thermal energy storage has the natural feature that a steep thermal front propagates with great difference of temperature and density, which lead to an unbalanced mass flow rate of packed bed reservoirs and the PTES close loop. In this paper, the expression of thermal front propagation and unbalanced mass flow rates between the inflow and the outflow of packed beds is developed and validated experimentally. The result indicates that there are 0.62%, 0.26% and 0.36% unbalanced mass flow for the hot reservoir, the cold reservoir and the PTES close loop respectively. The sensitivities of the factors such as pressure ratio, heat capacity of TES material and porosity on the unbalanced mass flow rate and the round-trip efficiency of PTES system considering mass flow rate is discussed. Furthermore, a feasible and self-balancing PTES system without buffer vessel is proposed, with a round-trip efficiency 0.12% higher than the buffer vessel balancing PTES system.

Research Data Related to this Submission

There are no linked research data sets for this submission. The following reason is given:
Data will be made available on request

Dear Editor :

We thank you very much for your attention and the reviewers' evaluation and comments on our paper entitled "Unbalanced mass flow rate of packed bed thermal energy storage and its influence on the Joule-Brayton based Pumped Thermal Electricity Storage" (No.ECM-D-18-07830). We have revised the manuscript according to your kind advices and reviewers' detailed suggestions. All the revised parts have been marked in yellow.

We sincerely hope this manuscript will be finally acceptable to be published on Energy Conversion and Management. Thank you very much for all your help and looking forward to hearing from you soon.

Best regards

Sincerely yours

Dr. Liang Wang, Dr. Xipeng Lin, Dr. Lei Chai, Dr. Long Peng, Dr. Dong Yu, Dr. Jia Liu , Dr. Haisheng Chen

Highlights

- The mass flow rate ratio relation of outflow-to-inflow of packed bed was developed.
- Proportion of unbalanced flow is 0.62% for hot reservoir and 0.26% for cold.
- Impact of pressure ratio, porosity and TES material heat capacity was analyzed.
- Proportion of unbalanced mass flow is 0.36% in pumped heat electricity storage.
- A self-balance PTES system was proposed to void buffer vessel.

Unbalanced mass flow rate of packed bed thermal energy storage and its influence on the Joule-Brayton based Pumped Thermal Electricity Storage

Liang Wang[1, 2], Xipeng Lin[1], Lei Chai[3], Long Peng[1], Dong Yu[1], Jia Liu[4], Haisheng Chen[1, 2, *]

(1 Institute of Engineering Thermophysics, Chinese Academy of Sciences, Beijing 100190, China; 2 University of Chinese Academy of Sciences, Beijing 100049, China
3 RCUK National Centre for Sustainable Energy Use in Food Chain (CSEF), Brunel University London, Uxbridge, Middlesex UB8 3PH, UK
4 China Huanqiu Contracting & Engineering Corporation, Beijing 100012, China)

*Corresponding author. Tel.: +86 10 82543148, E-mail: chen_hs@iet.cn

Abstract

As the most suitable thermal energy storage manner for the Joule-Brayton based Pumped Thermal Electricity Storage (PTES), packed beds thermal energy storage has the natural feature that a steep thermal front propagates with great difference of temperature and density, which lead to an unbalanced mass flow rate of packed bed reservoirs and the PTES close loop. In this paper, the expression of thermal front propagation and unbalanced mass flow rates between the inflow and the outflow of packed beds is developed and validated experimentally. The result indicates that there are 0.62%, 0.26% and 0.36% unbalanced mass flow for the hot reservoir, the cold reservoir and the PTES close loop respectively. The sensitivities of the factors such as

pressure ratio, heat capacity of TES material and porosity on the unbalanced mass flow rate and the round–trip efficiency of PTES system considering mass flow rate is discussed. Furthermore, a feasible and self-balancing PTES system without buffer vessel is proposed, with a round-trip efficiency 0.12% higher than the buffer vessel balancing PTES system.

Keywords*:* pumped thermal electricity storage; thermal energy storage; packed bed; energy storage; unbalanced mass flow

Nomenclature

Abbreviations

CAES	Compressed air energy storage
CHEST	Compressed heat energy storage
DSC	Differential scanning calorimetry
EES	Electrical energy storage
ORC	Organic rankine cycle
PHS	Pumped hydro storage
PHES	Pumped heat electricity storage
PTES	Pumped thermal electricity storage
TES	Thermal energy storage

Symbols

C_F	Inertial coefficient of packed bed

1	c_p	Specific heat capacity, J K^{-1} kg^{-1}
2	D	Diameter of particles, m
3	E	Internal energy per unit mass, J kg^{-1}
4	G	Coefficient relating particles size ratio
5	h	Volumetric heat transfer coefficient, W m^{-3} K^{-1}
6	K	Intrinsic permeability of the porous medium
7	L	Length scale, m
8	m	Mass of gas, kg
9	V	Specific volume
10	r	Pressure/expansion ratio of compressor/expander
11	R	Size ratio of particles
12	S	The surface area, m^2
13	t	Time, s
14	T	Temperature, K
15	X	Volume fraction
16	u	Velocity, m s^{-1}
17	γ	Adiabatic exponent of gas
18	δ	A parameter, $\varepsilon/(1-\varepsilon)$
19	ε	Porosity of packed bed
20	η	Polytropic efficiency of compressor/expander
21	κ	A parameter, $(\gamma-1)/\gamma$
22	μ	Dynamic viscosity, Pa s

ρ	Density, kg m^{-3}	
χ	Round trip efficiency	
Ψ	Sphericity of particles	

Subscripts

BV_chg	Buffer vessel during charging
BV_dis	Buffer vessel during discharging
c_chg	Compressor during charging
c_dis	Compressor during discharging
e_dis	Expander during discharging
e_chg	Expander during charging
g	Gas
i	Inlet
L	Large
Nom	Nominal
o	Outlet
S	Small
v	Volume
x	X axial

1. Introduction

Over the past years, renewable power has grown rapidly: 161 GW of renewable

power (excluding hydro) capacity were added with the increase rate of nearly 9% in 2016, to almost 2017 GW [1, 2]. However, large quantities of grid-connected renewable energy bring challenges to the security and stability of the power network due to the fact that most renewable energy resources are characterized by intermittency and instability. Electrical Energy Storage (EES), which transforms electrical energy to another form of energy for storage and is later converted back to electrical energy when needed, has been referred to as one of the most promising approaches [3, 4]. Also, EES can provide substantial benefits for the conventional electricity industry, including load following, peaking power and standby reserve, hence improving the utilization rate of the power grid and the efficiency of thermal power generation [5, 6].

Nowadays, there are a lot of storage technologies of different maturation stages, including Pumped Hydro Storage (PHS), Compressed Air Energy Storage (CAES), Thermal energy storage (TES), and batteries including lithium ion, vanadium redox flow-cell etc. [3, 4]. Among the available storage technologies, only PHS and CAES are considered to be large-scale stand-alone electricity storage technologies with capacities over 100MW [3, 4, 7]. PHS is a mature technology with high capacity, long storage period, high efficiency and relatively low cost per unit of energy. With a round trip efficiency of about 71% to 85%, there are over 170GW of PHS in operation worldwide, which is about 94% of global energy storage capacity [3, 8]. The major constraints of PHS are suitable topological conditions for two large reservoirs with a certain fall head and one or two dams, as well as a long time and high cost for

construction. CAES is the other available technology suited for large scale energy storage. There are two CAES units under commercial operation in the world and they are 290 MW/2 h CAES in Huntorf, Germany and 110 MW/26 h CAES in McIntosh, Alabama, USA, with underground storage caverns of ~310,000 m^3 and ~500,000 m^3, respectively [4, 9]. Similar to PHS, appropriate geographical conditions for the enormous volume of storage caves is the main barrier for the construction of CAES systems. By storing air at the liquid state to overcome this barrier, Highview Power Storage Ltd built a small pilot (350 kW/2.5 MWh) and a medium prototype LAES plant (5 MW/15 WMh) in UK [10,11], and the Institute of Engineering Thermophysics, Chinese Academy of Sciences built a 1.5 MW and a 10MW advanced CAES demonstration in China [12, 13].

In recent years, relatively new energy storage technologies for large scale applications were studied, including "Pumped Heat Electricity Storage (PHES)" [14], "Pumped Thermal Electricity Storage (PTES)" [15-18], "Thermo-electric Energy Storage" [19-21], and "Compressed Heat Energy Storage (CHEST)" [22] etc. And the term PTES will be employed in this paper. Such technologies share similar working principles: in the charging process thermal (heat/cold) energy is generated by electricity through a heat pump cycle and stored; at the discharging process electricity is generated by the stored thermal energy through the heat-work conversion cycle. Such systems have the advantages of high efficiency, high energy storage density and no geographical restrictions.

There are two main PTES systems which have been investigated so far, based on

Joule-Brayton cycles and Rankine cycles. Few investigations have been made on the Carnot cycles although, Thess and Guo et al. carried out theoretical analysis on PHES and PCES systems using finite-time thermodynamics approaches and predicted the maximum round-trip efficiency with varying storage temperatures and other parameters, respectively [14, 23].

After the PTES system based on supercritical CO_2 Rankine cycle was firstly by ABB company [19], the PTES systems based on different thermodynamic cycles including subcritical NH_3 Rankine cycle [16, 17, 25], steam Rankine cycle [22], supercritical CO_2 Rankine cycle [20, 21, 24], supercritical air [24], supercritical argon [24] and the organic Rankine cycles (ORC) [15] were developed and the results show that the stand-alone round trip efficiency is between 51% and 70% under different temperatures of the hot and cold reservoirs [16, 17, 20-22], and achieve 130% when integrated with an 80°C~110°C heat source [15]. Roskosch et al. found the round trip efficiency of a PHES system consists of a compression heat pump and an ORC is between 56% and 37% and decrease with increasing storage temperatures [26].

On the Brayton based PTES, Desrues et al. firstly presented a PTES system based on the Joule-Brayton cycle consisting of two TES reservoirs connected by two compressor-turbine-pairs (one for charging and one for discharging) and two heat exchangers using argon as the working gas [27]. During the charging process, the hot reservoir is heated from 25°C to 1000°C under a pressure of 4.6 bar while the cold reservoir is cooled down from 500°C to -70°C under a pressure of 1.0 bar utilizing refractory material. By the numerical simulations and optimizations, a round-trip

efficiency of 66.7% was obtained for the 602.6 MWh PTES system based on the turbo machines' polytropic efficiency of 0.9. Based on the experimental studies on a series of working prototypes of Brayton based PTES, Howes developed a hypothetical 2 MW/16 MWh PTES system with the calculated round-trip efficiency of 72% [28]. White et al.'s thermodynamic study indicates that the round-trip efficiency and energy storage density increase with increasing temperature ratio between the hot and cold TES reservoirs [29]. Furthermore, McTigue et al. presented the theoretical analysis coupled with a Schumann-style packed bed model of the hot and cold reservoirs for the Brayton based PTES system. A buffer vessel was introduced in order to balance the total mass of gas in the hot and cold reservoirs [30]. For the 2 MW/16 MWh PTES system, the extension study indicates that the radial-flow packed beds have a comparable thermodynamic performance to the axial-flow packed beds, but require additional volume [31]. Davenne et al. introduced a liquid isopentane thermocline TES technology for cold storage for the PTES system driven by wind energy whose exergy loss was deduced to be smaller than the packed bed thermocline [32]. Benato proposed a new Brayton cycle based PTES system in which an electric heater is used after the compressor in order to maintain the hot tank temperature during the charging process with the cost ranges between 50 and 200 Euro/kWh while the energy density is from 60 to 285 kWh/m^3 [33, 34]. The first 2 MW/16 MWh grid-scale Brayton cycle based PTES demonstration was designed and manufactured by Isentropic Ltd and is being commissioned by Newcastle University [35, 36]. Based on the PTES demonstration plant, Smallbone et al. found the levelised cost of PHES is between

0.089 and 0.114 Euro/kWh [37]. And PTES become economically more competitive than LAES over a buy price of ~0.15 USD/kWh, primarily due to the higher round trip efficiency [38]. Detailed reviews of the principles and characteristics of these state of the art PHES technologies are presented in Refs. [39] and [40].

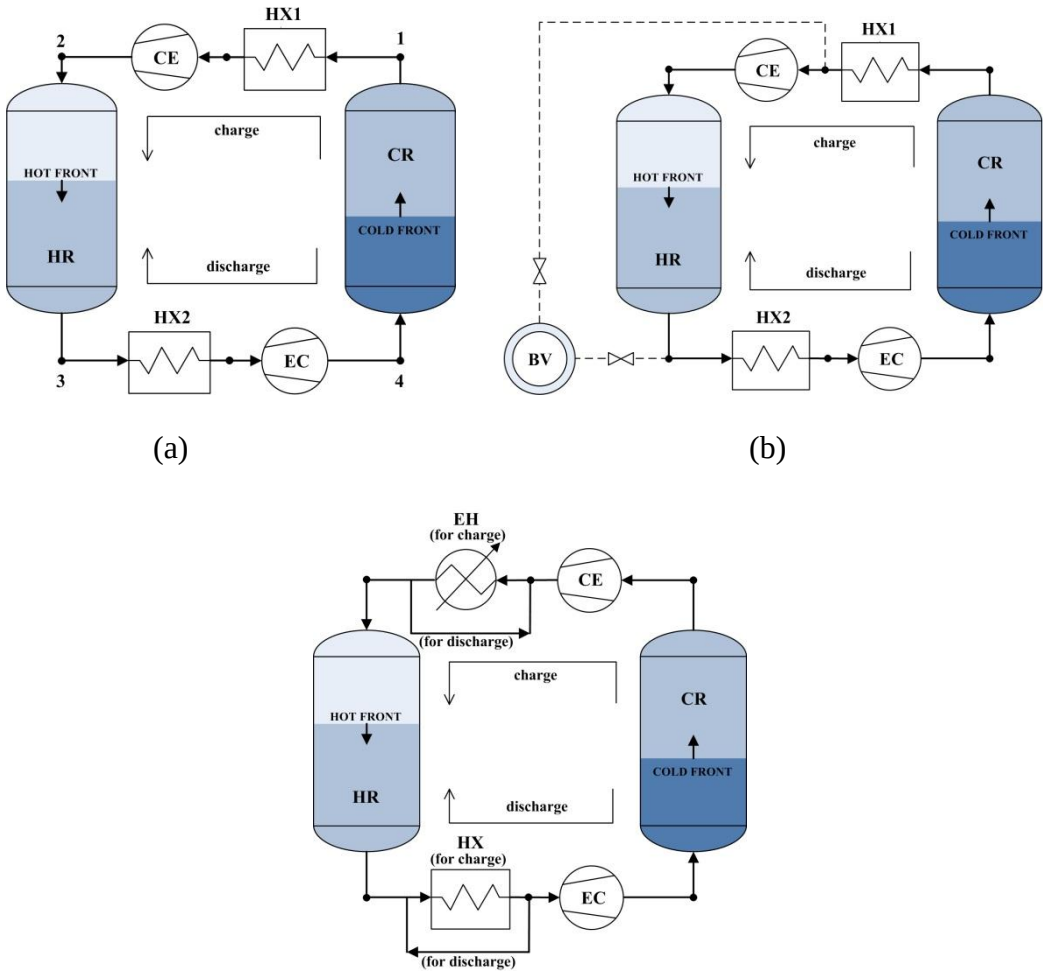

Fig.1. Layout of the Joule-Brayton cycle PTES system proposed by (a) Desrues et al. [27] and White et al.[29], (b) McTigue et al.[30], (c) Benato [33].

Low cost, high efficiency and high energy density TES is vital for the PTES system in order to compete with PHS and CAES. There are mainly three categories of heat storage: sensible, latent, and chemical heat storage [41]. Due to its low cost, wide

applicable temperature range (-200°C ~1000+°C), large specific surface area (which results in small temperature differences in heat transfer), non-toxicity, long life and other practical advantages, packed bed sensible TES has been identified as the most suitable technology for the PTES system [33]. The performance of PTES combining heat and cold packed bed reservoirs of different materials were adequately simulated and analyzed to determine round trip efficiency [27, 30, 33], energy density [33, 34], costs [33, 34] and other factors.

The existing studies on packed beds mainly focus on the thermal storage and thermodynamic loss [27-30, 34], whereas the characteristics of mass variation of gas has not been discussed before which is a basic but worthy to be noticed issue. During the charge/delivery process of packed bed TES, a large amount of heat transfer gas is stored or released in the pore volume of packed beds due to the great change in gas density owing to the translation of thermocline. In the PTES system, the total mass of argon in the hot reservoir decreases by about 60%, while that of the cold reservoir increases by about 150% [29, 30]. The mass variation of packed bed heat and cold reservoirs would certainly cause an unbalanced mass flow rate between the inflow and outflow in closed loop PTES systems, further lead to different gas flow rates between compressor and expander. Furthermore, taking the unbalanced mass flow rate into consideration would lead to an accurate calculation of round-trip efficiency and system optimization of PTES.

In this paper, therefore, both theoretical studies and experimental studies have been carried out on the propagation of the thermal front and the relation for the mass

flow rate ratio of packed bed between the outflow and the inflow. The unbalanced mass flow behavior of the packed bed reservoirs and Joule-Brayton based PTES system is found, and a series of related factors, such as PTES pressure ratio, packed bed porosity and heat capacity of TES materials, are investigated to understand their impact on unbalanced mass flow rate. Furthermore, the expression of the round-trip efficiency is proposed taking the unbalanced mass flow into account. Lastly, and a feasible and self-balancing PTES system are proposed, which can void the buffer vessel and have a little higher performance for future applications.

2. Theoretical Analysis

The packed bed region in the reservoir is chosen as the computational domain, and the x axis is the axial direction from the tank bottom to the tank top with $x = 0$ at the bottom of the packed bed region. The governing equations for heat transfer and fluid dynamics within the packed bed region include the continuity equation, the momentum equation, and the energy equations of the gas phase and the solid phase, which are Eqs. (1)–(4), shown below:

$$\varepsilon \frac{\partial \rho_{\mathrm{g}}}{\partial t} + \frac{\partial \left(\rho_{\mathrm{g}} u_{\mathrm{x}} \right)}{\partial x} = 0 \tag{1}$$

$$\frac{\partial \left(\rho_{\mathrm{g}} u_{\mathrm{x}} \right)}{\varepsilon \partial t} + \frac{\partial \left(\rho_{\mathrm{g}} u_{\mathrm{x}} u_{\mathrm{x}} \right)}{\varepsilon^2 \partial x} = \frac{\partial}{\partial x}\left(\mu \frac{\partial u_{\mathrm{x}}}{\partial x} \right) - \frac{\partial p}{\partial x} - \rho_{\mathrm{g}} g - \left(\frac{\mu}{K} + \frac{C_{\mathrm{F}}}{\sqrt{K}} \left| u_{\mathrm{x}} \right| \right) u_{\mathrm{x}} \tag{2}$$

$$\varepsilon \frac{\partial \left(\rho_{\mathrm{g}} c_{\mathrm{p,g}} T_{\mathrm{g}} \right)}{\partial t} + \frac{\partial \left(\rho_{\mathrm{g}} c_{\mathrm{p,g}} u_{\mathrm{x}} T_{\mathrm{g}} \right)}{\partial x} = h_{\mathrm{v}} \left(T_{\mathrm{s}} - T_{\mathrm{g}} \right) \tag{3}$$

$$\left(1 - \varepsilon \right) \frac{\partial \left(\rho_{\mathrm{s}} c_{\mathrm{p,s}} T_{\mathrm{s}} \right)}{\partial t} = h_{\mathrm{v}} \left(T_{\mathrm{g}} - T_{\mathrm{s}} \right) \tag{4}$$

where ε is the porosity of the packed bed, u_x represents the superficial velocity based on the total cross-sectional area of gas and porous medium, K is the intrinsic permeability of the porous medium, μ is the dynamic viscosity of gas, C_F is the inertial coefficient of the packed bed, and h_v represents the volumetric interstitial heat transfer coefficient between gas and the packed bed.

Based on Eqs. (3) and (4), we have

$$\frac{\partial\left(\rho_g c_{p,g} u_x T_g\right)}{\partial x}+\varepsilon\frac{\partial\left(\rho_g c_{p,g} T_g\right)}{\partial t}+\left(1-\varepsilon\right)\frac{\partial\left(\rho_s c_{p,s} T_s\right)}{\partial t}=0 \tag{5}$$

Combining this equation with the progress of the thermal front in this ideal case determined with the wave propagation speed of the thermal front U by Eqs. (6) and (7) [41] we derive

$$\frac{\partial\left(\rho_g c_{p,g} T_g\right)}{\partial t}+U\frac{\partial\left(\rho_g c_{p,g} T_g\right)}{\partial x}=0 \tag{6}$$

$$\frac{\partial T_s}{\partial t}+U\frac{\partial T_s}{\partial x}=0 \tag{7}$$

Integrated in the region of thermocline, the propagation speed of the thermal front U can be obtained as shown in Eq. (8)

$$U=\frac{u_x\left(\rho_{g,o}e_{g,o}-\rho_{g,i}e_{g,i}\right)}{\left(1-\varepsilon\right)\rho_s\left(e_{s,o}-e_{s,i}\right)+\varepsilon\left(\rho_{g,o}e_{g,o}-\rho_{g,i}e_{g,i}\right)} \tag{8}$$

when neglecting the variation of density and internal energy of gas inside the packed bed pore, the thermal wave speed can be reduced to

$$U=\frac{u_x\left(\rho_{g,o}e_{g,o}-\rho_{g,i}e_{g,i}\right)}{\left(1-\varepsilon\right)\rho_s\left(e_{s,o}-e_{s,i}\right)}=\frac{u_x\rho_g c_{p,g}}{\left(1-\varepsilon\right)\rho_s c_s} \tag{9}$$

as achieved by White et al.[42].

For ideal cases of thermal front propagation in the packed bed as shown in Fig. 2,

during the charging process of cold energy, the thermal front moves upward with a distance of Δx over the time Δt. Under a constant pressure, the mass change of gas Δm for the whole reservoir due to temperature and density variation extend as shown in Eq. (10)

$$\Delta m=\left(\dot{m}_{\mathrm{i}}-\dot{m}_{\mathrm{o}}\right)\Delta t=\left(\rho_{\mathrm{g,i}}-\rho_{\mathrm{g,o}}\right)\varepsilon UA\Delta t \tag{10}$$

where A is the area of the cross section.

As to the energy balance of the whole reservoir, the energy change of the thermal storage reservoir ΔE is

$$\Delta E=\left(\dot{m}_{\mathrm{i}}e_{\mathrm{g,i}}-\dot{m}_{\mathrm{o}}e_{\mathrm{g,o}}\right)\Delta t=\left(\rho_{\mathrm{g,i}}e_{\mathrm{g,i}}-\rho_{\mathrm{g,o}}e_{\mathrm{g,o}}\right)u_{\mathrm{x}}A\Delta t \tag{11}$$

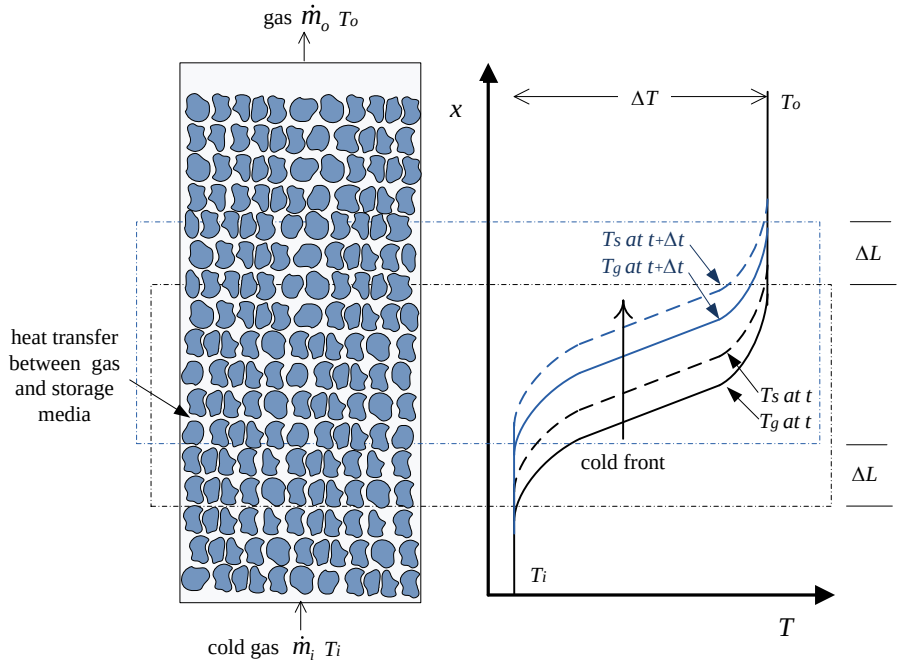

Fig. 2. Schematic diagram of thermal front in packed bed.

For thermal front propagation in the packed bed over time Δt, the variation of packed bed internal energy with volume of ΔxA including the packed solid storage medium and the gas in the pore, is as shown in Eq. (12) as below

$$\Delta E = \Delta L A\left[\rho_{\mathrm{s}}(1-\varepsilon)\left(e_{\mathrm{s,i}}-e_{\mathrm{s,o}}\right)+\varepsilon\left(\rho_{\mathrm{g,i}}e_{\mathrm{g,i}}-\rho_{\mathrm{o}}e_{\mathrm{g,o}}\right)\right] \tag{12}$$

From Eqs. (10) and (12), we have

$$U=\frac{\Delta L}{\Delta t}=\frac{u_{\mathrm{x}}\left(\rho_{\mathrm{g,o}}e_{\mathrm{g,o}}-\rho_{\mathrm{g,i}}e_{\mathrm{g,i}}\right)}{(1-\varepsilon)\rho_{\mathrm{s}}\left(e_{\mathrm{s,o}}-e_{\mathrm{s,i}}\right)+\varepsilon\left(\rho_{\mathrm{g,o}}e_{\mathrm{g,o}}-\rho_{\mathrm{g,i}}e_{\mathrm{g,i}}\right)} \tag{13}$$

which is as the same as Eq. (9). Combining Eqs. (10), (12) and (13), the mass flow ratio of the outflow to inflow for the packed bed reservoir is shown in Eq. (14) as

$$\frac{\dot{m}_o}{\dot{m}_i}=\frac{1+\dfrac{\rho_{\mathrm{g,o}}\bar{c}_{\mathrm{g}}}{\rho_{\mathrm{s}}\bar{c}_{\mathrm{s}}}\dfrac{\varepsilon}{1-\varepsilon}}{1+\dfrac{\rho_{\mathrm{g,i}}\bar{c}_{\mathrm{g}}}{\rho_{\mathrm{s}}\bar{c}_{\mathrm{s}}}\dfrac{\varepsilon}{1-\varepsilon}} \tag{14}$$

The mass flow ratio is mainly related to the gas density and gas heat capacity at the inlet and outlet, the volumetric heat capacity of TES material and the porosity of packed bed.

3 Validation experiment

In order to verify the mass flow correlations of Eq. (14) and study the cold thermal energy storage characteristics in the packed bed reservoir, the experimental study was performed using nitrogen as the working media.

3.1 Experimental apparatus

As shown in Fig. 3, the experimental system consists of two branches, i.e. the air branch and the nitrogen branch. In the air branch, dried air is first compressed from atmospheric pressure to the necessary pressure with a reciprocating compressor, and then goes through a surge tank to smooth the pulse air flow. Then it enters the packed bed reservoir from the top to provide the target pressure of the packed bed before the

cryogenic energy storage process. In order to decrease the thermal energy loss to the environment, high quality heat insulation material 100 mm thick was wrapped around the outer surface of the cryogenic storage packed bed reservoir, the cryogenic liquid pump and the corresponding connection tubes. In the nitrogen branch, liquid nitrogen forms a Dewar reservoir flow through a cryogenic flow meter to measure the flow rate, is pumped to the target pressure by a cryogenic liquid pump, and then enters the packed bed reservoir from the bottom. During the charging period, the valve at the outlet is adjusted by the feedback of a pressure signal to keep the pressure of the packed bed reservoir at a constant value. When the liquid nitrogen flows upward through the packed bed, the cryogenic energy is absorbed by packed pebbles, the liquid nitrogen changes to a gas state, and the flow rate is measured before delivered to the atmosphere. At the inlet and the outlet of the packed bed tank, the flow rate of liquid nitrogen is determined by a Shakic cryogenic electromagnetic flow meter with a range of 0-300 L/h and an accuracy of ±1%, and by a Collihigh vortex flow meter with a range of 36-320 m^3/h and an accuracy of ±1%. Three Collihigh piezoresistance pressure transducers with a range of 0-10 MPa and accuracies of ±0.5% are installed in the top and bottom of the cryogenic storage cylinder and at the end of the vent pipe.

The cryogenic storage cylinder is a 1500 mm height, 345 mm internal diameter and 32mm thickness stainless steel cylinder, wrapped with 200 mm thick magnesium silicate wool for insulation. The main apparatuses, such as the compressor, data acquisition system, cryogenic liquid pump, Dewar reservoir, and the cryogenic storage cylinder, are shown in Fig. 4. Granite pebbles of 7~11 mm in size with the

equivalent diameter of 9 mm are packed in the cryogenic storage cylinder. With the water saturation method, the porosity and the density of the granite pebbles are measured to 0.4±0.002 and 2688±11 kg/m^3, respectively. As shown in Fig. 5, the specific heat capacity of the pebbles is found to depend heavily on temperature from 0.45 kJ/(kgK) at -160°C to 0.82 kJ/(kgK) at 0°C, as measured by TA Q2000 DSC. Seven Pt100 platinum-thermal resistors with a range of -200 to 450^{o}C and accuracy of ±0.1% located in the interior of the packed bed at 0, 188, 376, 564, 752, 940 and 1128 mm below the upper surface of the pebble were used to measure the axial temperature distribution of the packed bed.

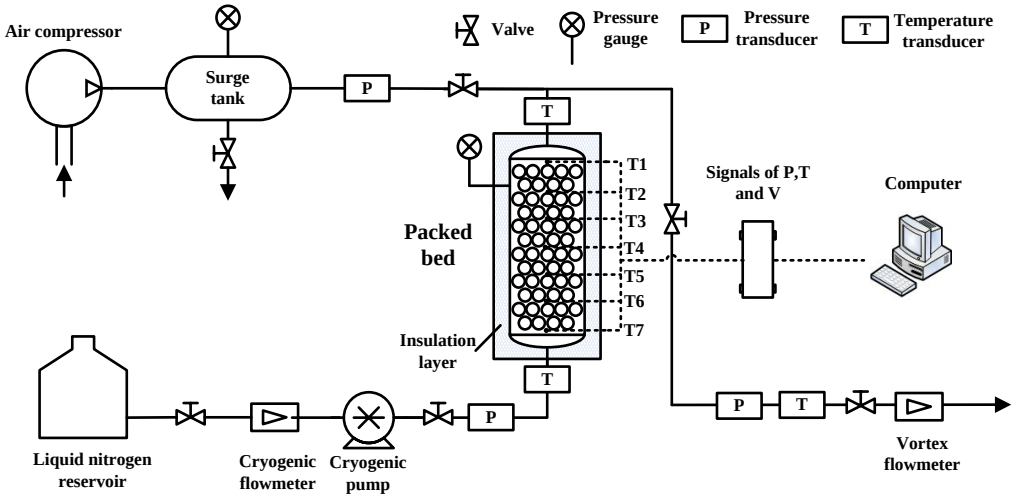

Fig. 3. Experiment setup and apparatus.

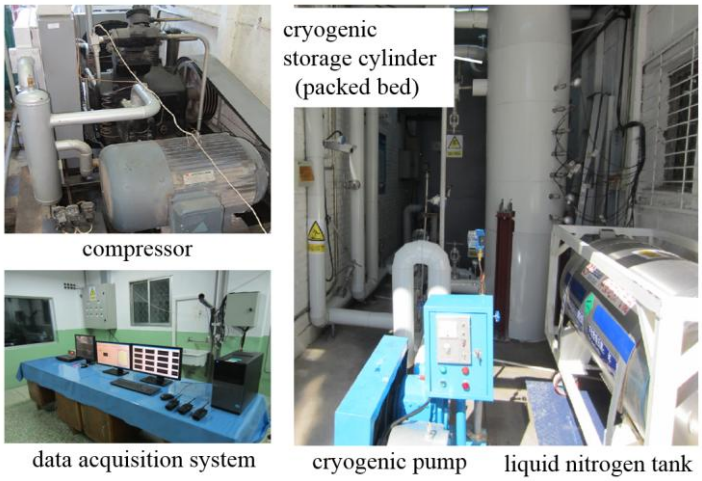

Fig. 4. Some of the experiment apparatus.

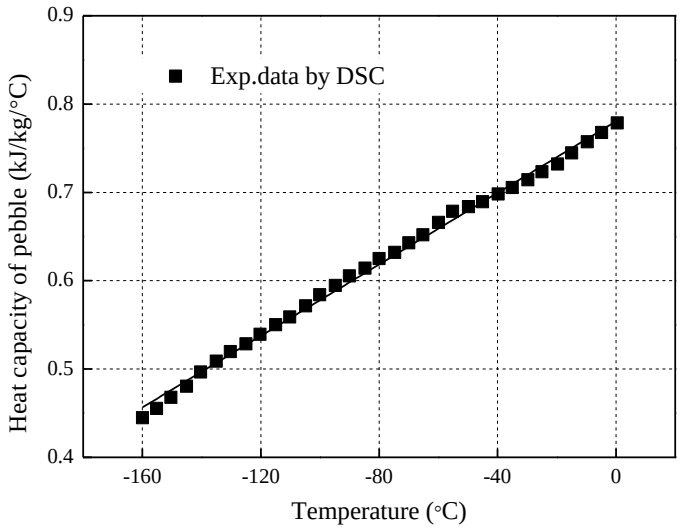

Fig. 5. Specific heat capacity variations of the pebble with temperature.

3.2. Experimental results

The experiments of the charging process of packed bed cryogenic storage with the mass flow ratio ranging from 80 kg/min to 200 kg/min were carried out under the pressure of 6.5 MPa and the inlet temperature of -166°C using nitrogen as the working media where a large difference in nitrogen density exists between the inlet (807 kg/m^3) and the outlet (73.1 kg/m^3). After every charging process, the packed bed was fully warmed to the ambient temperature by the compressed air. As shown in Fig.

6, the mass flow rate at the outlet is almost proportional to the inlet mass flow rate and the plot data by Eq. (14) fits well with the experiments and the deviation of less than ±8% under 6.5 MPa. Eq. (14) indicates that the density ratios between the gas to the packed bed material at the inlet ($\rho_{g,i}/\rho_s$) and the outlet ($\rho_{g,o}/\rho_s$) are the main factors influencing the mass flow ratio. In this experiment, the state of nitrogen change from subcooled to supercritical under a high pressure of 6.5 MPa where the high density ratios ($\rho_{g,i}/\rho_s$ and $\rho_{g,o}/\rho_s$) leading to a high mass flow ratio. As to the packed beds of PTES, owing to the small density difference of argon, the effect of mass flow ratio may be not as remarkable as this experiment.

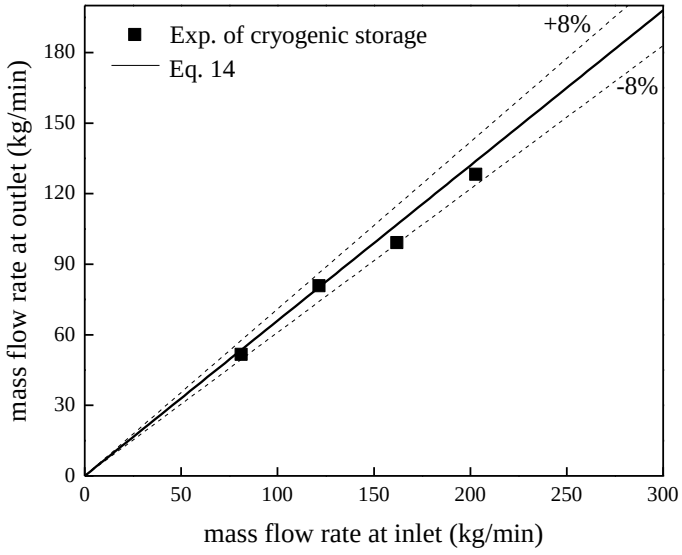

Fig. 6. Mass flow rate at outlet vs. inlet during cryogenic energy storage

Fig. 7 shows the axial temperature variation and the B-spline curves at the inlet mass flow rate of 80 kg/min at 6.5 MPa during the charging of cryogenic TES. It can be found that during the beginning 2000 s, the temperatures in packed bed decreased slowly as time passed, and then the thermocline occurred from the bottom and propagated upward from 4000 s to 10000 s, finally the thermocline vanished and the

packed bed was fully charged to below -130 °C at 12200 s. It can also found that, at the beginning of the charging process, nitrogen in the packed bed is under the supercritical state with a large temperature gradient (above -146.94 °C). And then the subcooled region (below -146.94 °C) with a small temperature gradient increases from the bottom gradually until the cryogenic energy is fully charged in the TES reservoir.

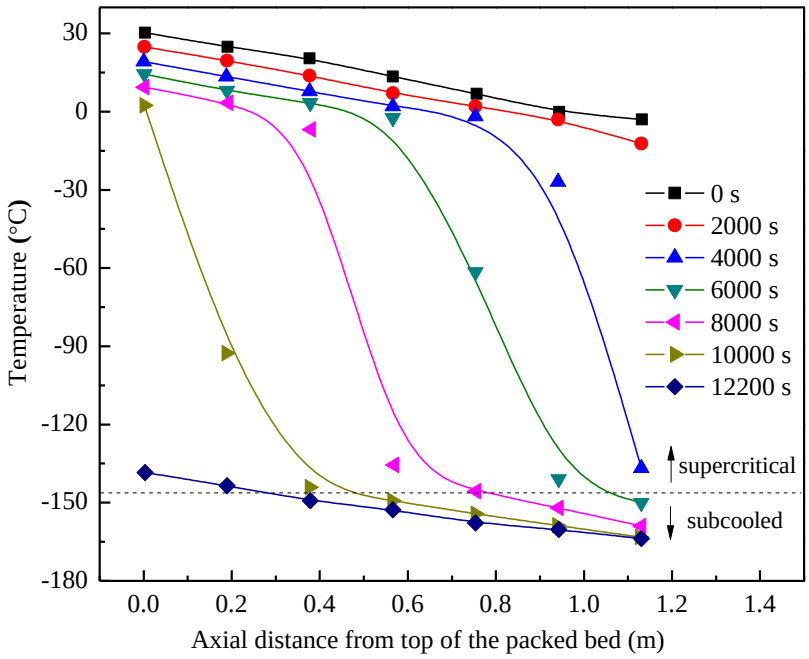

Fig. 7. Axial temperature during the charging of cryogenic energy

4. Discussion

4.1. Sensitivity of the mass flow rate

Due to the nature of density change inside the packed bed, there is a mass flow imbalance between the inflow and outflow during the charging and discharging process of the hot and cold reservoirs. For the Joule-Brayton based PTES system, as illustrated by McTigue et al. [30], the mass flow rate ratio of the outflow to inflow of

hot/cold TES reservoir exit during the charging process is 1.0062 and 0.9974 respectively, obtained by Eq. (14) based on the corresponding parameters is listed in Table 1, and the mass flow rate ratios during the discharging process are just the reciprocals of these.

Table 1. Hot and Cold reservoir detailed (storage material Fe_3O_4 with the void fraction of 0.35 and the density of 517.5 kg/m^3) [30]

Reservoir	Pressure (MPa)	Charge Temperature (K)	Discharge Temperature (K)	Charge Density (kg/m^3)	Discharge Density (kg/m^3)	Average c_g (J/kg/K)	Average c_s (J/kg/K)
Hot	1.05	778	310	6.46	16.36	527	860
Cold	0.105	123	310	4.15	1.63	528	520

From Eq. (14), it can be concluded that the porosity of the packed bed, the density ratio and heat capacity ratio of gas to TES material are the main factors influencing the ratio of mass flow rate between the outflow and inflow. The sensitivity of the mass flow rate ratio to the pressure ratio, the porosity and the heat capacity of TES material for the cold and hot reservoirs is shown in Fig. 8 (a)-(c). It can be found from Fig. 8(a) that for the high pressure reservoir, input of hot gas with low density and output of high density gas of the packed bed result in an outflow to inflow mass flow ratio higher than 1.0 and the mass flow ratio increases with increasing system pressure ratio, whereas increasing pressure ratio would lead to a colder input gas with higher density and a decreasing mass flow rate ratio between the output gas and the input gas.

As indicated in Table 1, normalized porosity (void fraction) of the packed bed is

0.35, and larger porosity leads to a larger mass flow ratio for the hot reservoir and a lower mass flow ratio for the cold reservoir as shown in Fig. 8(b). Also, as shown in Fig. 8(c) that the mass flow difference between the outflow and the inflow mass is decreased by increasing the heat capacity of TES material for both the hot and cold reservoirs. Generally, more influence of the factors on the mass flow ratio in the hot reservoir was found than that in the cold reservoir, mainly due to the larger change of gas density in the hot reservoir.

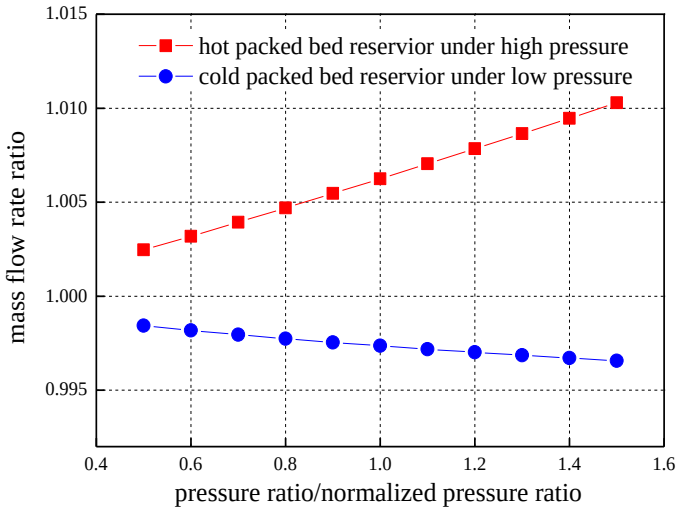

(a)

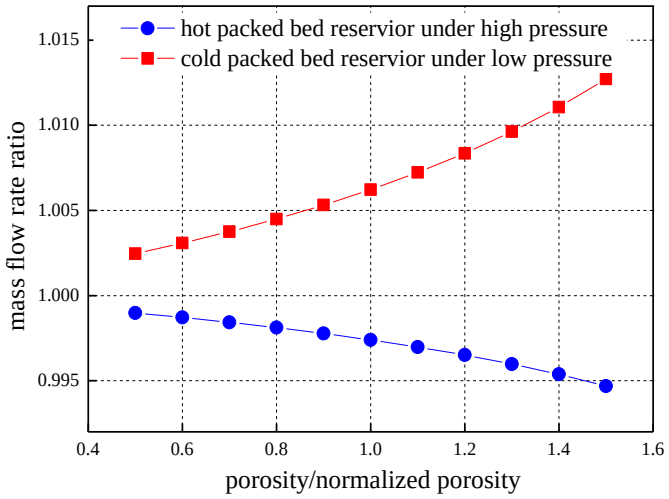

(b)

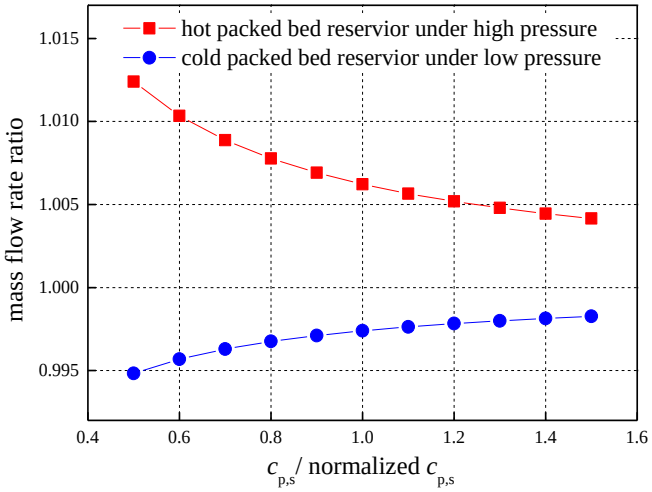

(c)

Fig. 8. Sensitivity to parameters: (a) Effect of pressure ratio; (b) Effect of porosity; (c) Effect of TES material $c_{p.}$

4.2. Mass flow of the PTES system

Although the hot reservoir releases gas and the cold reservoir absorbs gas simultaneously in the charging process of PTES system, the net mass flow out of the PTES is positive, but the PTES system is supposed to be a closed system of constant volume under stable pressure. For this, McTigue presents a buffer vessel (BV) to balance the total mass of gas as shown in Fig. 1(b) [30]. The mass flow of the PTES system in Fig. 1(b) is shown in Fig. 9, that when the mass flow rate of expander is 1.0, 0.36% of mass flow rate needs to be fed into the buffer vessel from the high pressure reservoir during the charging progress, and the same amount of mass flow rate feeds back to the low pressure reservoir from the buffer vessel during the discharging progress. On the other hand, we found that the mass flow rate ratios of expander to compressor in the PTES system are 99.74% and 100.26% for the charging cycle and discharging cycle, respectively.

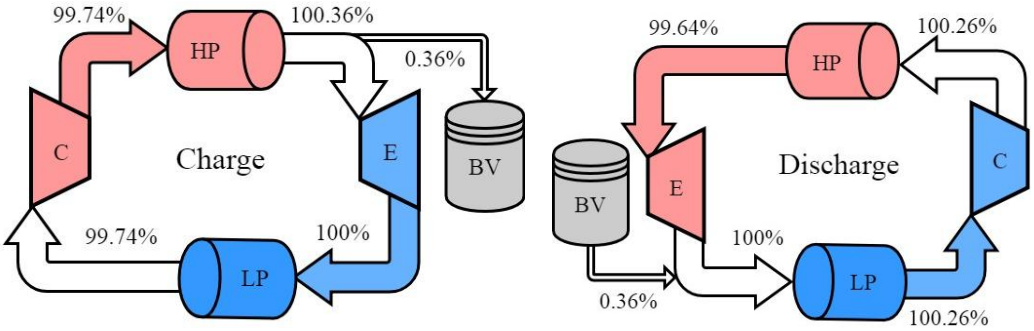

(a) (b)

Fig. 9. Mass flow of the PTES system: (a) charging; (b) discharging.

The feasible and self-balancing scheme to solve the imbalanced mass flow of the PTES system is to make the mass flow ratio of the hot reservoir and the cold reservoir reciprocal by selection of TES material with appropriate heat capacity and porosity, whose appearance is the same as Fig. 1(a) proposed by Desrues et al. [27] and White et al. [29]. Such a system has these potential benefits: no need for BV and complex control to maintain constant pressure; more gas participates in the energy storage cycle; increased round trip efficiency (there is exergy loss at the depressurization process from high pressure of hot reservoir to the BV and from the BV to the cold reservoir in the system in Fig. 1(b)); improved energy density due to reduced porosity. The mass flow of the self-balancing PTES system runs as shown in Fig. 10.

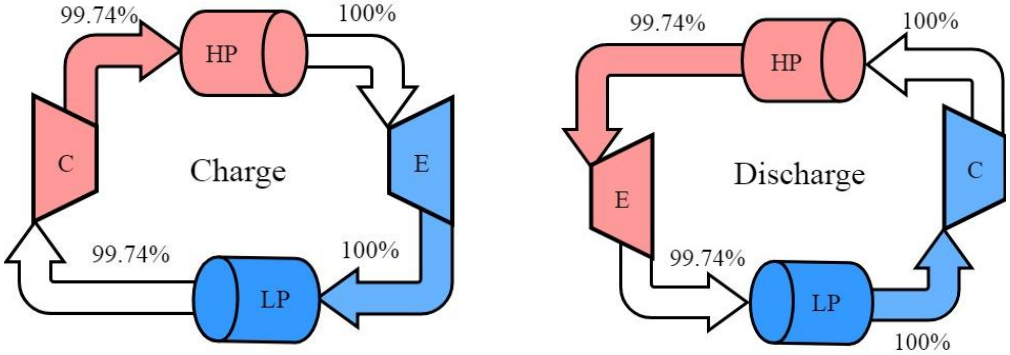

(a) (b)

Fig. 10. Mass flow of the modified PTES system: (a) charging; (b) discharging.

The mass flow relationship between the CR and HR of proposed self-balancing PTES system is as Eq. (15) that,

$$\frac{\dot{m}_{\mathrm{o,HR}}}{\dot{m}_{\mathrm{i,HR}}}\cdot\frac{\dot{m}_{\mathrm{o,CR}}}{\dot{m}_{\mathrm{i,CR}}}=1 \tag{15}$$

By analyzing Eq. (14) and Eq. (15) with a parameter $\delta=\varepsilon/(1-\varepsilon)$, we have the main influencing factors as shown in Eq. (16),

$$\frac{\left(\rho_{\mathrm{g,i,CR}}-\rho_{\mathrm{g,o,CR}}\right)}{\left(\rho_{\mathrm{g,o,HR}}-\rho_{\mathrm{g,i,HR}}\right)}\cdot\frac{\rho_{\mathrm{s,HR}}}{\rho_{\mathrm{s,CR}}}\cdot\frac{\bar{c}_{\mathrm{s,HR}}}{\bar{c}_{\mathrm{s,CR}}}\cdot\frac{\delta_{\mathrm{CR}}}{\delta_{\mathrm{HR}}}=1 \tag{16}$$

Where the gas densities have been decided in Table 1. Eq. (16) indicates that the self-balancing system can be obtained by: (1) selecting the suitable storage materials for HR and CR, and (2) adjusting the porosity of reservoirs.

One approach to adjust porosity is to utilize binary mixtures of particles with different sizes as the hot and cold energy storage material. The equation of the specific volume defined as the apparent volume occupied by a unit volume of solid particles for a binary mixture can be written as shown in Eq. (17) as [43, 44]

$$\left(\frac{V-V_{\mathrm{L}}X_{\mathrm{L}}}{V_{\mathrm{S}}}\right)^2+2G\left(\frac{V-V_{\mathrm{L}}X_{\mathrm{L}}}{V_{\mathrm{S}}}\right)\left(\frac{V-X_{\mathrm{L}}-V_{\mathrm{S}}X_{\mathrm{S}}}{V_{\mathrm{L}}-1}\right)+\left(\frac{V-X_{\mathrm{L}}-V_{\mathrm{S}}X_{\mathrm{S}}}{V_{\mathrm{L}}-1}\right)^2=1 \tag{17}$$

Where V is the specific volume of the binary mixture; V_{L} and V_{S} are the initial specific volumes, and X_{L} and X_{S} are the volume fractions of large and small particles, respectively. The relation of the coefficient G on the size ratio R ($R=d_{\mathrm{s}}/d_{\mathrm{l}}$) is [45]

$$G^{-1}=\begin{cases}1.355R^{1.566} & (R\le 0.824)\\ 1 & (R>0.824)\end{cases} \tag{18}$$

The packing of nonspherical particles and the characteristic size of nonspherical particles are then estimated by the correlation of Zou and Yu [46] as

$$d = \left(\frac{6V}{\pi}\right)^{\frac{1}{3}} \psi^{-2.875} \exp[-2.946(1-\psi)] \tag{19}$$

Where the Wadell's sphericity, Ψ, is defined as

$$\psi = \frac{\pi}{S}\left(\frac{6V}{\pi}\right)^{\frac{2}{3}} \tag{20}$$

Where S is the surface area and V is the volume.

Fig. 11 shows the calculated value of rock porosity by Eqs. (17)-(20) and the experimental results by Jeschar et al. for the ore and sinter of binary diameters [45]. The result indicates that significant reduction of porosity can be obtained by a large difference of size and a moderate volume ratio of binary pebbles.

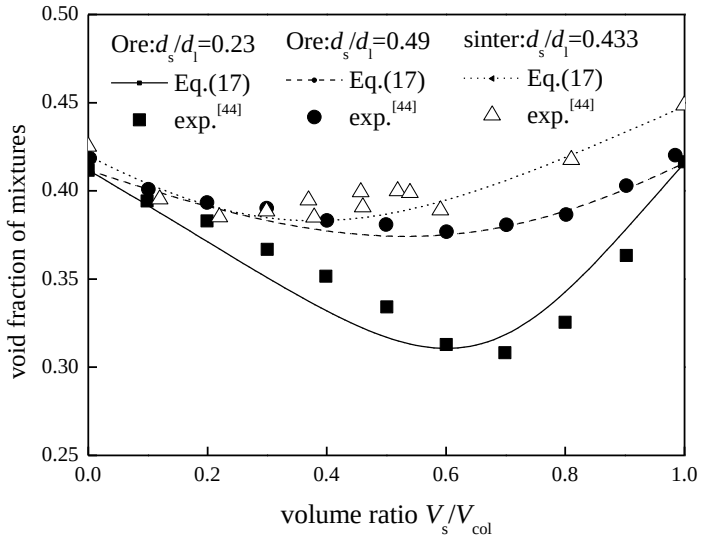

Fig. 11. Void fraction of mixtures of rocks with binary diameters.

There are many solutions to obtain a self-balancing PTES system by selecting different materials that meets Eq. (16). One solution is using granite as both the heat and cold storage material with the detailed parameters as shown in Table 2 where the temperature dependence of specific heat capacity of granite is from [47]. The TES material in HR is the packed bed of binary mixture with d_s/d_l=0.1 and V_s/V_{col}=0.65,

where the binary particles should be intensive mixed before installed in the HR.

Table 2. Designed hot and cold reservoir of the self-balancing PTES system (storage material granite with the density of 2650 kg/m^3)

Reservoir	Inflow gas Density (kg/m^3)	Outflow gas Density (kg/m^3)	Average c_s (J/kg/K)	Porosity	Packed bed particles
HR	6.46	16.36	1110	0.256	binary mixture with d_s/d_l=0.1 and V_s/V_{col}=0.65
CR	4.15	1.63	574	0.41	monosize particles

4.3. Round trip coefficient of the PTES system

As discussed above, the packed bed TES reservoir of PTES system would certainly cause the inequality of the mass flow rate between the hot side and cold side, as well as the mass flow through the compressor and expander. Taking the mass flow rate difference into account for the prediction of the round trip coefficient of PTES system will improve accuracy.

Supposing no mechanical loss or pressure loss, the round trip coefficient of the PTES system is obtained by the quotient of net shaft work output during the discharging process and the input shaft work during charging, as shown in Eq. (21)

$$\chi = \frac{\text{net work output}}{\text{net work input}} = \frac{\dot{m}_{e\_dis} c_p (T_2^{'} - T_1^{'}) - \dot{m}_{c\_dis} c_p (T_3^{'} - T_4^{'})}{\dot{m}_{c\_chg} c_p (T_2 - T_1) - \dot{m}_{e\_chg} c_p (T_3 - T_4)} \quad (21)$$

Where primes denote quantities during discharge, and $\dot{m}$ is the mass flow rate though the compressors and expanders. Polytropic process of compression and expansion occurs with the polytropic efficiencies η_c and η_t respectively. The parameter

κ is defined as $\kappa = (\gamma-1)/\gamma$.

$$T_2/T_1 = T_3^{'}/T_4^{'} = r_c^{\kappa/\eta_c} \tag{22}$$

$$T_4/T_3 = T_1^{'}/T_2^{'} = r_t^{\kappa\eta_t} \tag{23}$$

Where r_c and r_t are the pressure ratio of compressor and turbine.

$$\chi = \frac{\dot{m}_{e\_dis} T_2^{'}(1-r_t^{\eta_t\kappa}) - \dot{m}_{c\_dis} T_4^{'}(r_c^{\kappa/\eta_c}-1)}{\dot{m}_{c\_chg} T_1(r_c^{\kappa/\eta_c}-1) - \dot{m}_{e\_chg} T_3(1-r_t^{\eta_t\kappa})} \tag{24}$$

Ignoring losses due to heat storage and transfer, we have $T_2 = T_2'$ and $T_4 = T_4'$. After sufficient heat transfer of HX1 and HX2, T_1 and T_3 return to atmospheric temperature. And supposing the pressure ratio of compressor and turbine is the same during charging and discharging, we have the round trip efficiency as

$$\chi = \frac{\dot{m}_{e\_dis} r^{\kappa/\eta_c}(1-r^{\eta_t\kappa}) - \dot{m}_{c\_dis} r^{-\eta_t\kappa}(r^{\kappa/\eta_c}-1)}{\dot{m}_{c\_chg}(r^{\kappa/\eta_c}-1) - \dot{m}_{e\_chg}(1-r^{\eta_t\kappa})} \tag{25}$$

For the self-balancing PTES system shown in Fig. 1(a), the mass flow rate ratio e indicates the mass flow ratio of the compressor to the expander during the charging process as in Eq. (26)

$$e = \frac{\dot{m}_{e\_dis}}{\dot{m}_{c\_dis}} = \frac{\dot{m}_{c\_chg}}{\dot{m}_{e\_chg}} \tag{26}$$

And the round trip efficiency of the self-balancing PTES system is as in Eq. (27)

$$\chi = \frac{e\cdot r^{\kappa/\eta_c}(1-r^{\eta_t\kappa}) - r^{-\eta_t\kappa}(r^{\kappa/\eta_c}-1)}{e\cdot(r^{\kappa/\eta_c}-1) - (1-r^{\eta_t\kappa})} \tag{27}$$

For the PTES system balancing the mass with the BV as in Fig. 1(b), the mass flow rate ratio e is calculated as in Eq. (28)

$$e = \frac{\dot{m}_{e\_dis} + \dot{m}_{BV\_chg}}{\dot{m}_{c\_dis}} = \frac{\dot{m}_{c\_chg} + \dot{m}_{BV\_chg}}{\dot{m}_{e\_chg}} \tag{28}$$

Where the expressions of compressor and turbine polytropic efficiencies as

functions of pressure ratios provided by Wilson [48] as in Eqs. (29) and (30) are

$$\eta_c = 0.91 - \frac{r_c - 1}{300} \tag{29}$$

$$\eta_t = 0.90 - \frac{r_t - 1}{250} \tag{30}$$

The round trip efficiency of PTES systems under different conditions are predicted based on Eqs. (27)-(30), including: case 1, supposing the mass flow rate of the system is equal everywhere; case 2, balancing mass by the BV as shown in Fig.1 (b) and the mass flow shown in Fig. 9; case 3, balancing mass by making the mass flow ratio of the hot reservoir and the cold reservoir reciprocal as shown in Fig. 1 (c) and the mass flow shown in Fig. 10. As plotted in Fig. 12, the round trip efficiency of PTES system increases with the increasing of the pressure ratio. The effect of the mass flow rate imbalance is not significant and the coefficient of PTES systems considering the unequal mass flow rate is a little smaller than a coefficient produced under an assumption of equal mass flow rate. The round trip efficiency of PTES system as Fig. 1(a) and the mass flow as Fig. 10 is higher than that of the BV balancing system as Fig. 1 (b) and the mass flow as Fig. 9, and they are 57.42% and 57.30% at a pressure ratio of 15, respectively.

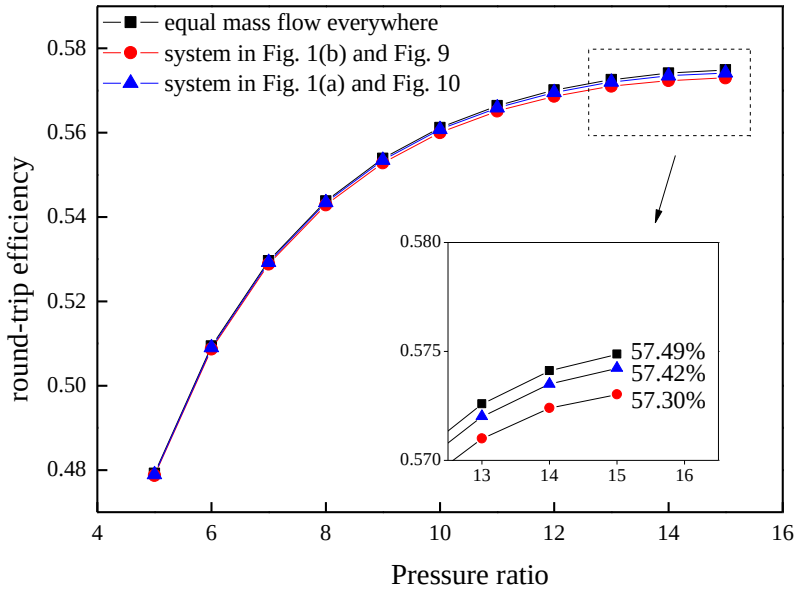

Fig. 12. Effect of pressure ratio on the round trip efficiency of PTES systems.

From the above studies, it can be found that 0.12% increase of round-trip efficiency obtained through the self-balancing method based on the system parameters in [29], which is not very significant. However, a large amount of initial cost of PTES can be saved by abolishing the components including the BV, pressure pipelines, valves and their controller. According to the parameters in [30], the volume of the high pressure BV need to be more than 12% of the HR volume, and the cost of the buffer vessel is comparable with the CR since the hot store is expected to cost between 11 and 17 Euro/kWh and the cold store 2 and 4 Euro/kWh [37]. Furthermore, the throttle loss of the regulating valve when gas fed into the BV is about 0.21% of the compression work, which can be saved in the self-balancing system.

5. Conclusion

For new-type pumped thermal electricity storage as a form of thermal energy storage, the issue of unbalanced mass flow rate between the inflow and the outflow of

packed beds under constant pressure has been analyzed. The correlations of the speed of thermal front propagation and the mass flow rate ratio between the inflow and the outflow have been developed. The cryogenic TES experiment of packed bed was carried out under the pressure of 6.5 MPa with nitrogen as the working fluid. It was found that steep cold thermal front propagated in the packed bed and the predicted mass flow rate ratio fit well with the experimental results with a deviation of less than ±8%. The influence of factors such as porosity, pressure ratio, and heat capacity ratio of gas to TES material on the ratio of mass flow rate was analyzed further.

The unbalanced mass flow behavior of the packed bed reservoirs and PTES system is found that, based on the designed PTES system parameters, the outflow mass flow rate of the hot and cold TES reservoir is 1.0062 and 0.9974 times of the inflow, respectively; and 0.36% of the total mass flow rate needs to be stored in BV of large volume owing to the cumulative charging over hours. And the expression of the round-trip efficiency is proposed where the unbalanced mass flow is taken into account.

Furthermore, a self-balancing PTES system is proposed with the methods including the selection of appropriate storage materials and the adjustment of porosity by pebble mixture of the binary diameters. Comparisons indicate that the self-balancing PTES system will not only improve the 0.12% of round-trip efficiency but also save the initial cost by voiding the components including the BV, pressure pipelines, valves and their controller. In addition, the mass flow ratio imbalance would be mitigated through the increase of heat capacity of TES material and the

decrease in porosity, so as to increase round trip efficiency and energy storage density.

6. Acknowledgements

The authors would like to thank the National Natural Science Foundation of China (NO.U1407205), Transformational Technologies for Clean Energy and Demonstration, the Strategic Priority Research Program of CAS (NO.XDA21070200), The Frontier Science Research Project of CAS (NO.QYZDB-SSW-JSC023) and the Youth Innovation Promotion Association CAS (NO.2016131). The authors would also like to thank Theo Carney for assistance in the manuscript revision process.

References

[1] Dale S. BP Statistical Review of World Energy June 2017, 2017.

[2] Sawin JL, Sverrisson F, Seyboth K, et al. Renewables 2017 Global Status Report. 2017.

[3] Chen H, Cong T N, Yang W, et al. Progress in electrical energy storage system: A critical review. Prog Nat Sci 2009; 19(3): 291-312.

[4] Luo X, Wang J, Dooner M, et al. Overview of current development in electrical energy storage technologies and the application potential in power system operation. Appl Energy 2015; 137: 511-36.

[5] Walawalkar R, Apt J, Mancini R. Economics of electric energy storage for energy arbitrage and regulation. Energ Policy 2007; 5: 2558-68.

[6] Dobie WC. Electrical energy storage. Power Eng J 1998; 12, 177-181.

[7] Aneke M, Wang M. Energy storage technologies and real life applications-A state of the art review. Appl Energy 2016; 179: 350-77.

[8] http://www.energystorageexchange.org/

[9] Barnes, Frank S., and Jonah G. Levine, eds. Large energy storage systems handbook. CRC press, 2011.

[10] https://www.highviewpower.com/

[11] Sciacovelli A, Vecchi A, Ding Y. Liquid air energy storage (LAES) with packed bed cold thermal storage – From component to system level performance through dynamic modelling. Appl Energy 2017; 190: 84-98.

[12] Advanced compressed air energy storage won the first prize of Beijing science and technology, http://www.escn.com.cn/news/show-222217.html.

[13] The 10MW compressed air energy storage is under integrated test, http://www.escn.com.cn/news/show-377349.html

[14] Thess A. Thermodynamic efficiency of pumped heat electricity storage. Phys Rev Lett 2013; 111(11):110602.

[15] Frate G F, Antonelli M, Desideri U. A novel pumped thermal electricity storage (PTES) system with thermal integration. Appl Therm Eng 2017; 121: 1051-8.

[16] Abarr M, Geels B, Hertzberg J, et al. Pumped thermal energy storage and bottoming system part A: Concept and model. Energy 2017; 120: 320-31.

[17] Abarr M, Hertzberg J, Montoya LD. Pumped thermal energy storage and Bottoming System Part B: Sensitivity analysis and baseline performance. Energy 2017; 119: 601-11.

[18] Benato A, Anna S. Energy and cost analysis of a new packed bed pumped thermal electricity storage unit. J Energ Resour-ASME 2018;140(2): 020904.

[19] Morandin M, Henchoz S, Mercangöz M. Thermo-electrical energy storage: a new type of large scale energy storage based on thermodynamic cycles. World Engineers' Convention 2011.

[20] Morandin M, Maréchal F, Mercangöz M, et al. Conceptual design of a thermo-electrical energy storage system based on heat integration of thermodynamic cycles–Part A: Methodology and base case. Energy 2012; 45: 375-85.

[21] Morandin M, Maréchal F, Mercangöz M, et al. Conceptual design of a thermo-electrical energy storage system based on heat integration of thermodynamic cycles–Part B: Alternative system configurations. Energy 2012; 45: 386-96.

[22] Steinmann WD. The CHEST (Compressed Heat Energy STorage) concept for facility scale thermo mechanical energy storage. Energy 2014; 69: 543-52.

[23] Guo J, Cai L, Chen J, et al. Performance optimization and comparison of pumped thermal and pumped cryogenic electricity storage systems. Energy 2016; 106: 260-9.

[24] Vinnemeier P, Wirsum M, Malpiece D, et al. Integration of heat pumps into thermal plants for creation of large-scale electricity storage capacities. Appl Energy 2016; 184: 506-22.

[25] Wang G B, Zhang X R. Thermodynamic analysis of a novel pumped thermal energy storage system utilizing ambient thermal energy and LNG cold energy. Energy Convers Manage 2017; 148: 1248-64.

[26] Roskosch D, Atakan B. Pumped heat electricity storage: potential analysis and

orc requirements. Energy Procedia 2017; 129: 1026-1033.

[27] Desrues T, Ruer J, Marty P, et al. A thermal energy storage process for large scale electric applications. Appl Therm Eng 2010; 30: 425-32.

[28] Howes J. Concept and development of a pumped heat electricity storage device. Proceedings of the IEEE 2012; 100(2): 493-503.

[29] White A, Parks G, Markides C. Thermodynamic analysis of pumped thermal electricity storage. Appl Therm Eng 2013; 53:291-8.

[30] McTigue J, White A, Markides C. Parametric studies and optimization of pumped thermal electricity storage. Appl Energy 2015; 137: 800-11.

[31] White A, McTigue J, Markides C. Analysis and optimisation of packed-bed thermal reservoirs for electricity storage applications, Proc. Inst. Mech. Eng. Part A J. Power Energy 2016; 230: 739-754.

[32] Davenne TR, Garvey SD, Cardenas B, et al. The cold store for a pumped thermal energy storage system. J Energ Storage 2017; 14: 295-310.

[33] Benato A. Performance and cost evaluation of an innovative pumped thermal electricity storage power system. Energy 2017; 138: 419-436.

[34] Benato A, Stoppato A. Heat transfer fluid and material selection for an innovative Pumped Thermal Electricity Storage system. Energy 2018; 147: 155-68.

[35] http://www.isentropic.co.uk/

[36] Hot rock solution to grid-scale energy storage, https://www.ncl.ac.uk/press/articles/archive/2017/11/isentropic/

[37] Smallbone A, Jülch V, Wardle R et al. Levelised Cost of Storage for Pumped

Heat Energy Storage in comparison with other energy storage technologies. Energy Convers Manag 2017; 152: 221-228.

[38] Solomos G, Shah N, Markides C. A thermo-economic analysis and comparison of pumped-thermal and liquid-air electricity storage systems. Appl Energy 2018; 226: 1119-1133.

[39] Steinmann WD. Thermo-mechanical concepts for bulk energy storage. Renewable Sustainable Energy Rev 2017; 75: 205-219.

[40] Benato A, Stoppato A. Pumped Thermal Electricity Storage: A technology overview. Therm Sci Eng Progress 2018; 6: 301-315.

[41] Gil A, Medrano M, Martorell I, et al. State of the art on high temperature thermal energy storage for power generation. Part 1-Concepts, materials and modellization. Renew Sustain Energy Rev 2009; 14: 31-55.

[42] White A, McTigue J, Markides C. Wave propagation and thermodynamic losses in packed-bed thermal reservoirs for energy storage. Appl Energy 2014; 130: 648-57.

[43] Westman AER. The packing of particles: empirical equations for intermediate diameter ratios. J Am Ceram Soc 1936; 19(1-12): 127-9.

[44] Yu AB, Standish N, McLean A. Porosity calculation of binary mixtures of nonspherical particles. Am Ceram Soc 1993; 76(11): 2813-6.

[45] Jeschar R, Potke W, Petersen V, et al. Blast furnace aerodynamics. Proceedings of the symposium on blast furnace aerodynamics 1975; 25-7.

[46] Zou RP, Yu AB. Evaluation of the packing characteristics of mono-sized non-spherical particles. Powder Technol 1996; 88(1): 71-9.

[47]Wen H, Lu J, Xiao Y, et al. Temperature dependence of thermal conductivity, diffusion and specific heat capacity for coal and rocks from coalfield. Thermochim Acta 2015; 619: 41-47.

[48] Wilson DG, Korakianitis T. The design of high-efficiency turbomachinery and gas turbines. MIT press; 2014.

Tables

Table 1. Hot and Cold reservoir detailed (storage material Fe_3O_4 with the void fraction of 0.35 and the density of 517.5 kg/m^3) [30]

Reservoir	Pressure (MPa)	Charge Temperature (K)	Discharge Temperature (K)	Charge Density (kg/m^3)	Discharge Density (kg/m^3)	Average c_g (J/kg/K)	Average c_s (J/kg/K)
Hot	1.05	778	310	6.46	16.36	527	860
Cold	0.105	123	310	4.15	1.63	528	520

Table 2. Designed hot and cold reservoir of the self-balancing PTES system (storage material granite with the density of 2650 kg/m^3)

Reservoir	Inflow gas Density (kg/m^3)	Outflow gas Density (kg/m^3)	Average c_s (J/kg/K)	Porosity	Packed bed particles
HR	6.46	16.36	1110	0.256	binary mixture with d_s/d_l=0.1 and V_s/V_{col}=0.65
CR	4.15	1.63	574	0.41	monosize particles

Figure 1a

Click here to download high resolution image

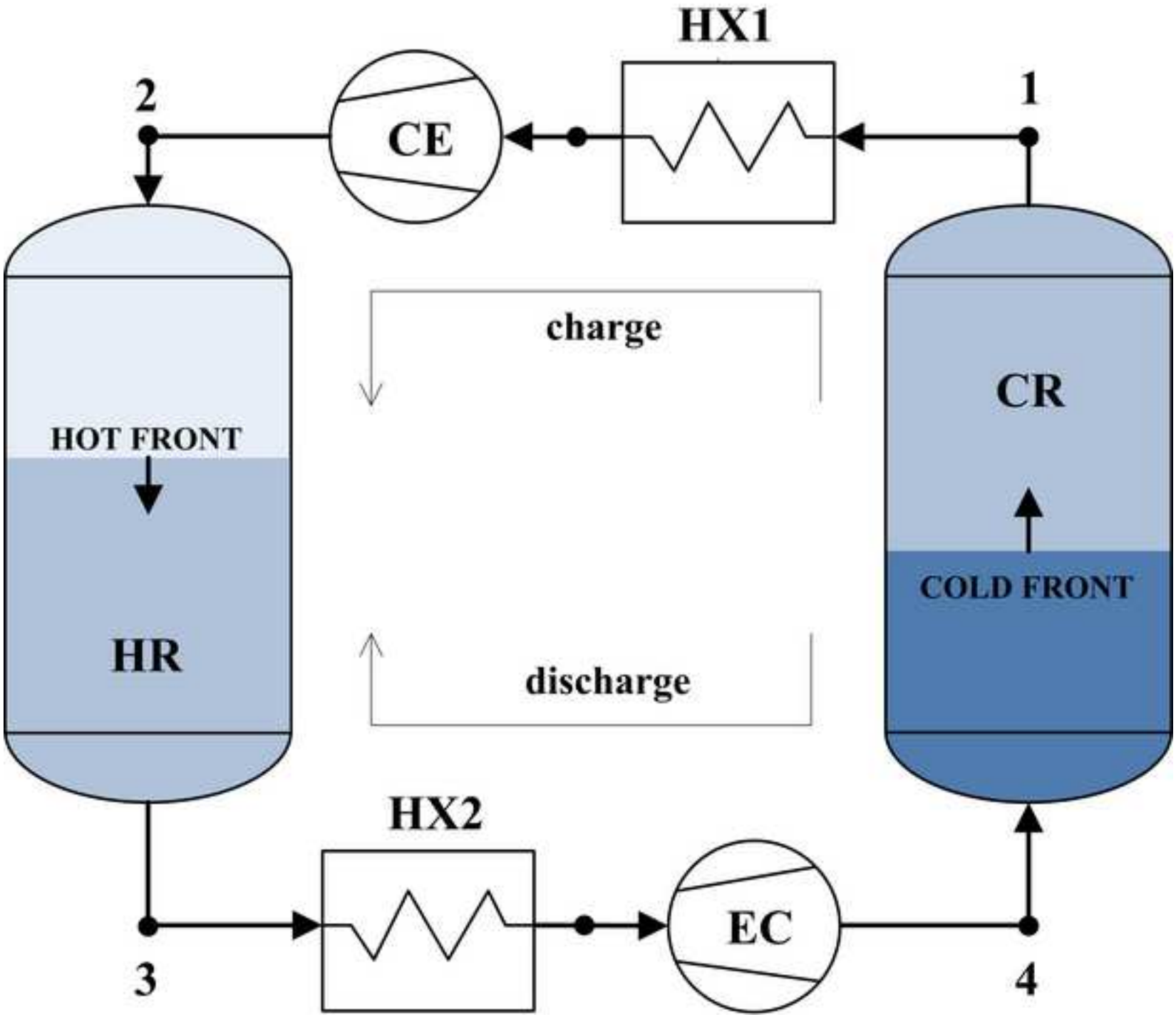

Figure 1b

Click here to download high resolution image

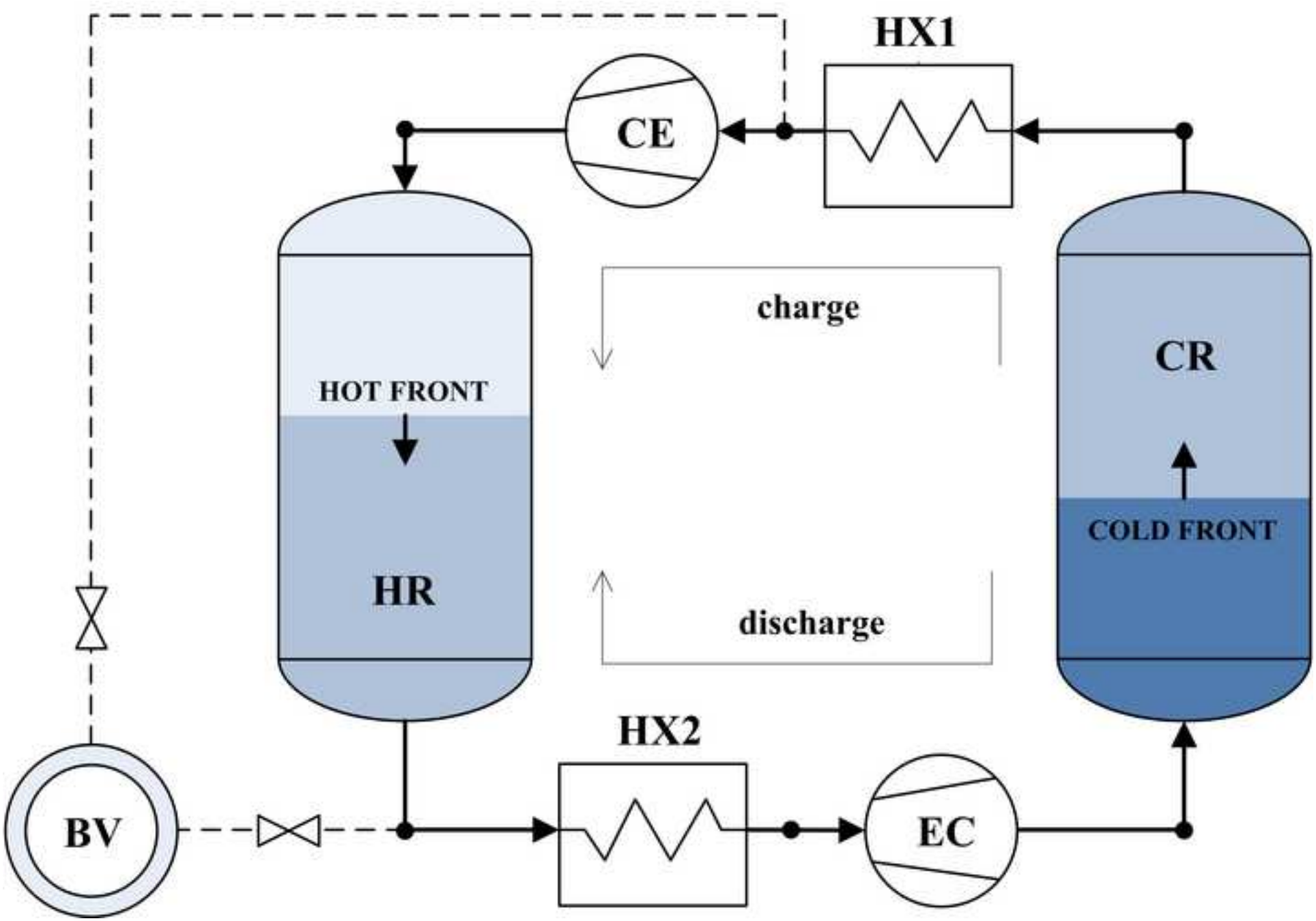

Figure 1c

Click here to download high resolution image

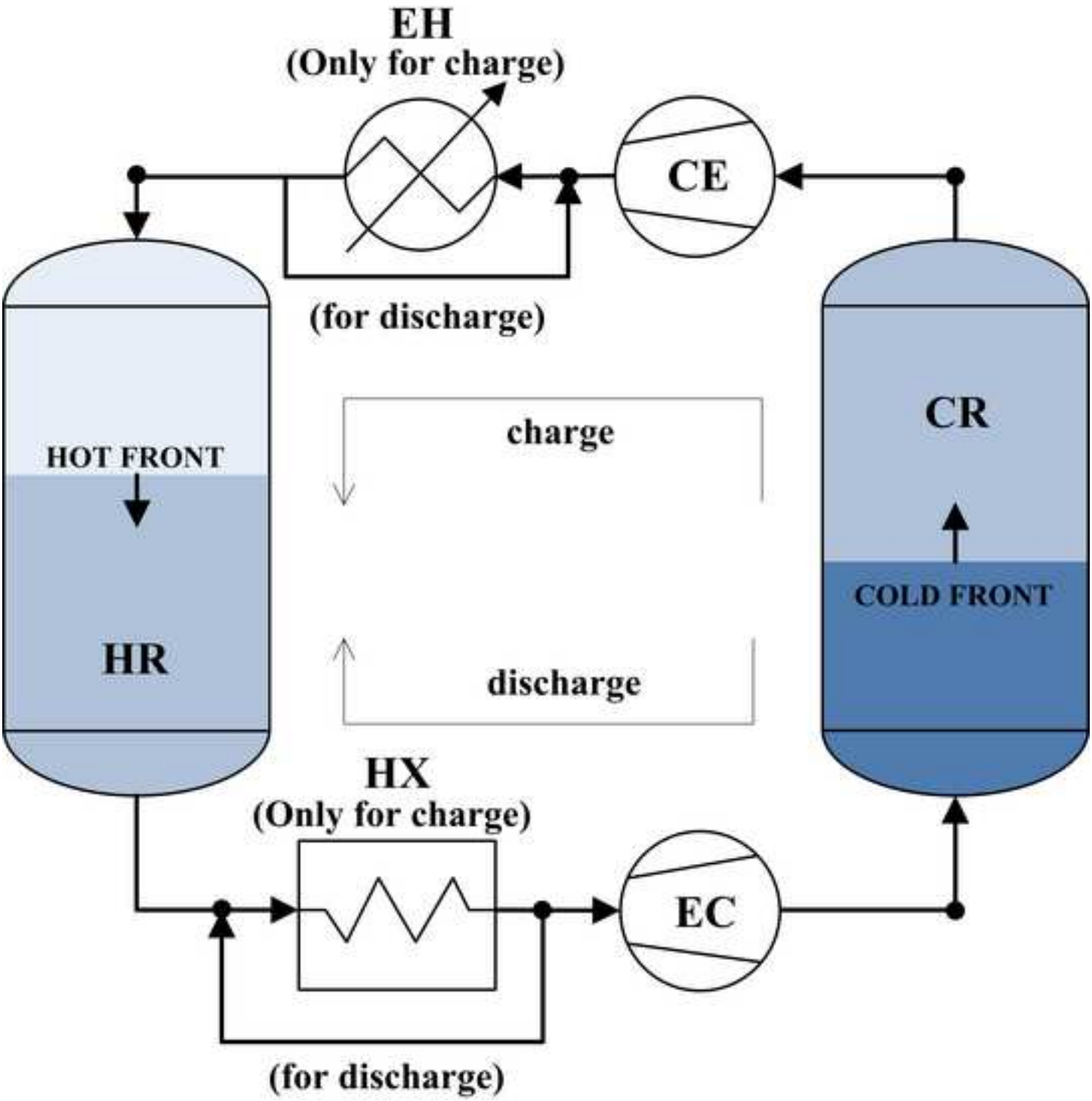

Figure 2

Click here to download high resolution image

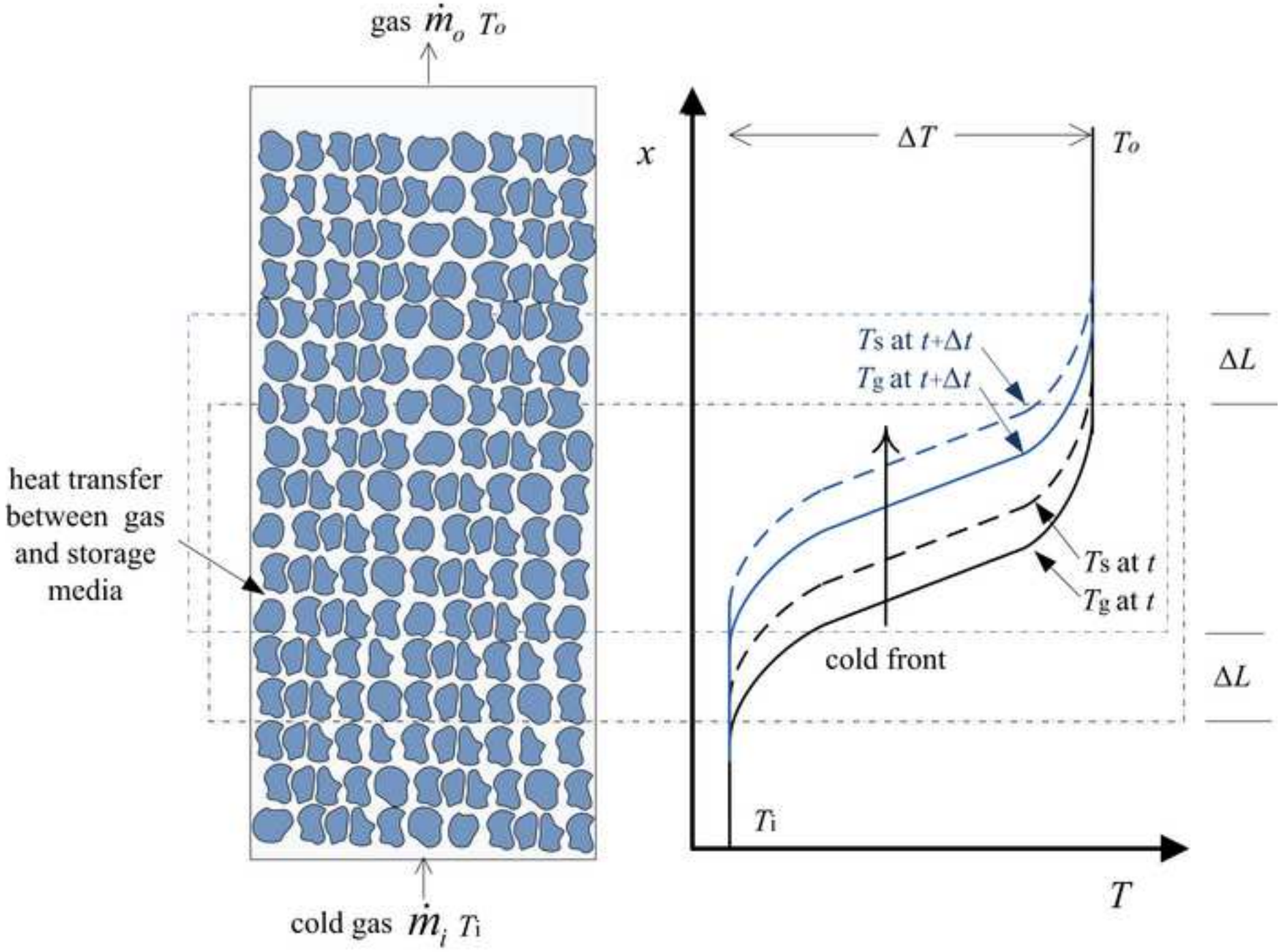

Figure 3

Click here to download high resolution image

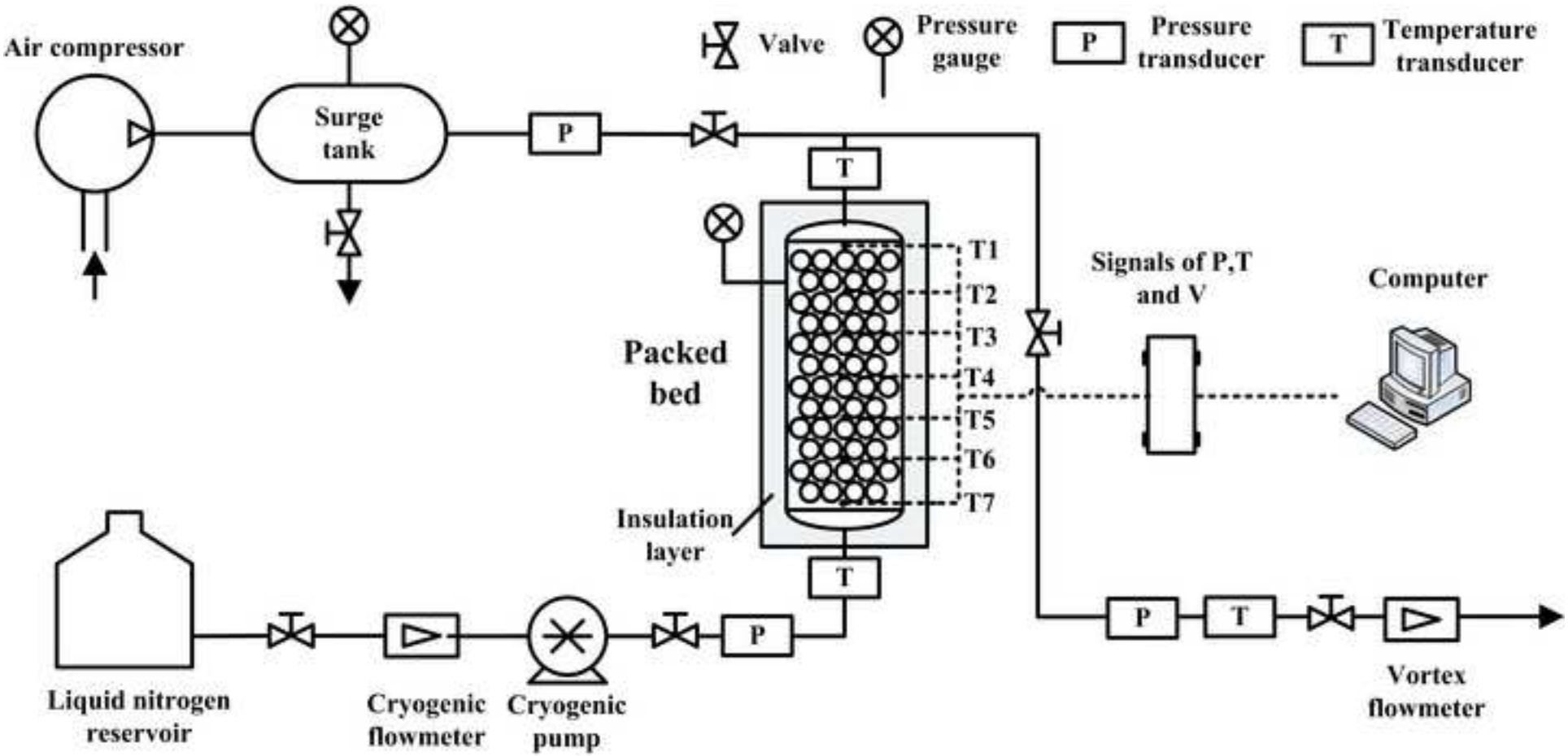

Figure 4
Click here to download high resolution image

compressor

data acquisition system

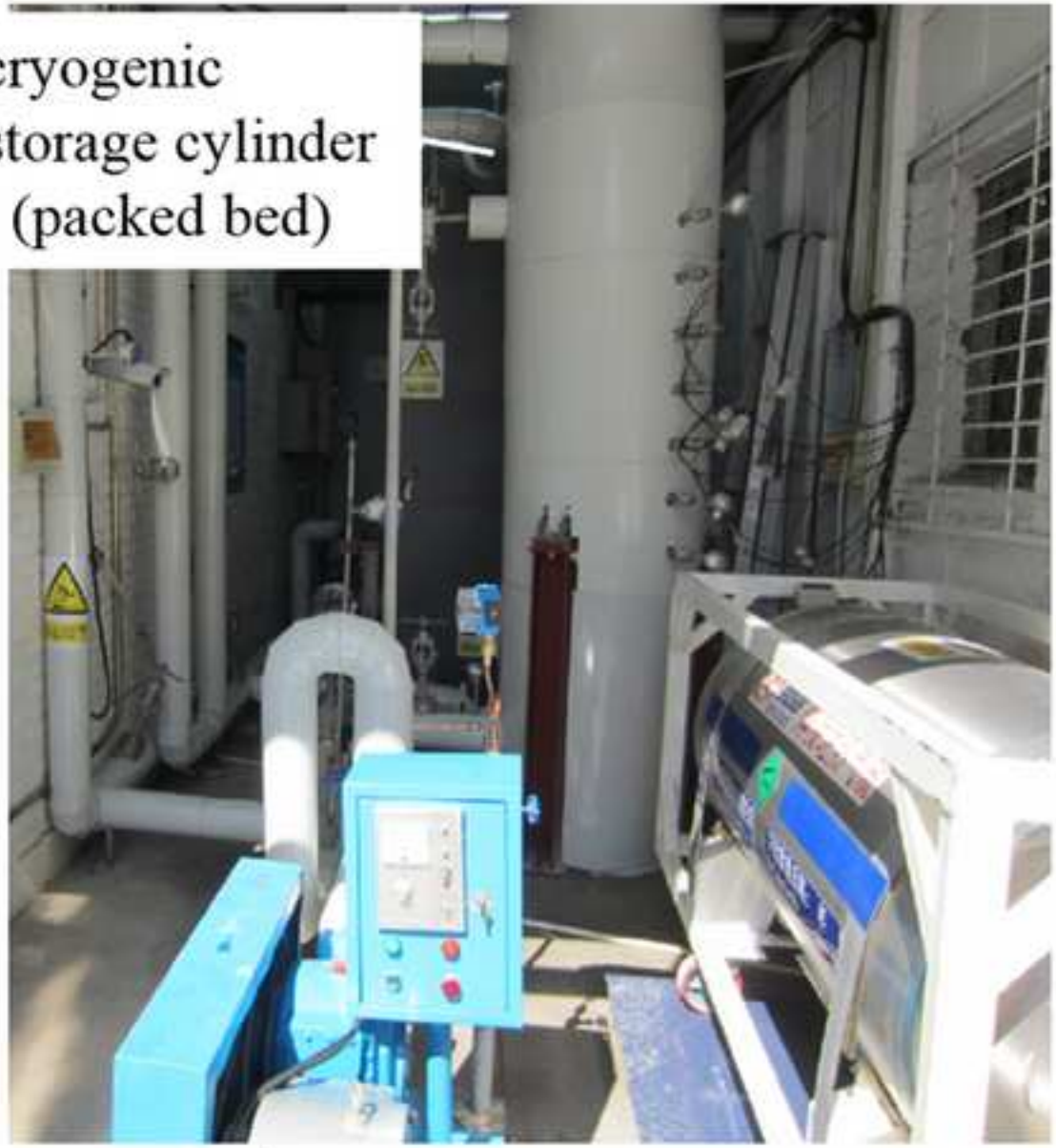

cryogenic pump

liquid nitrogen tank

Figure 5
Click here to download high resolution image

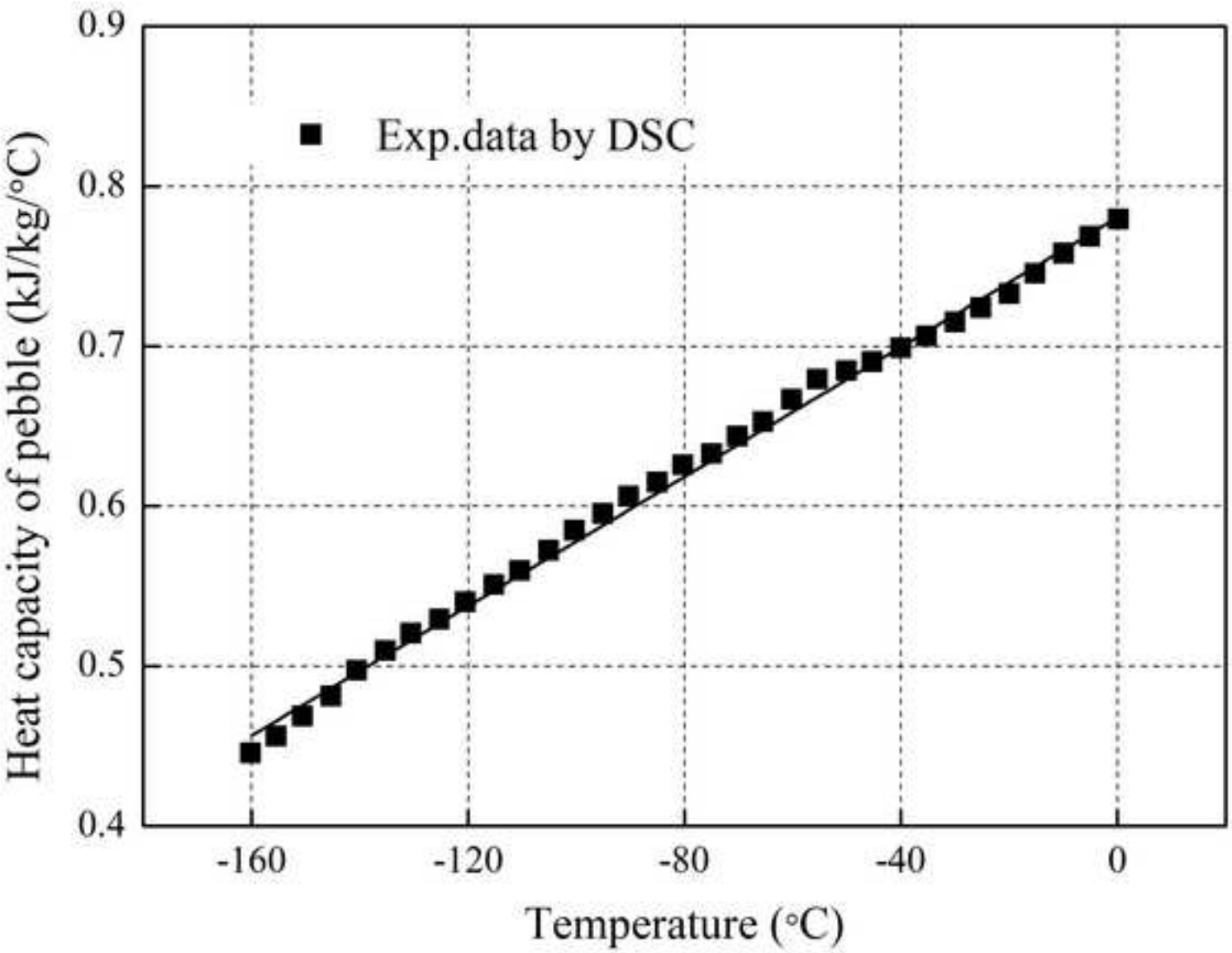

Figure 6
Click here to download high resolution image

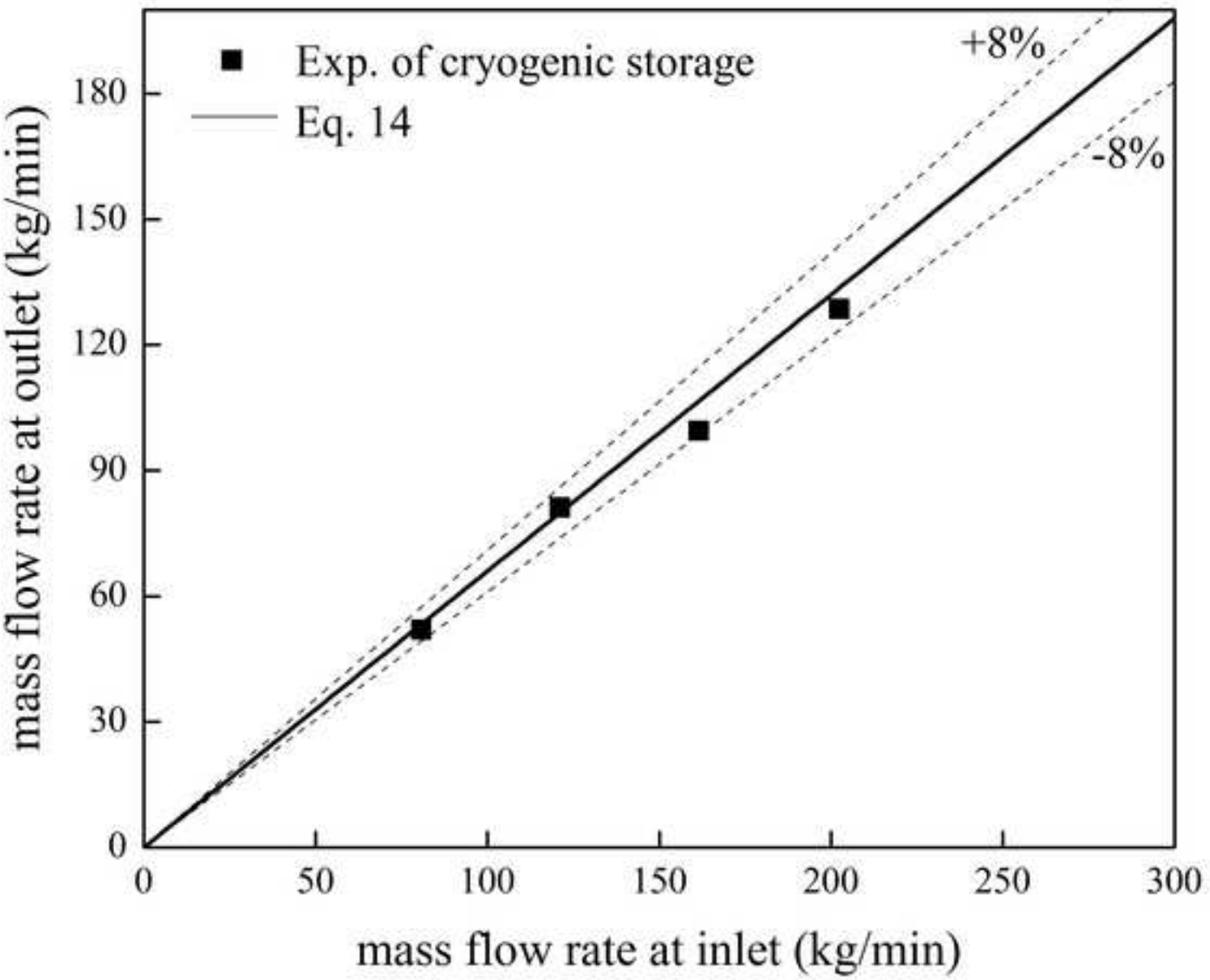

Figure 7

Click here to download high resolution image

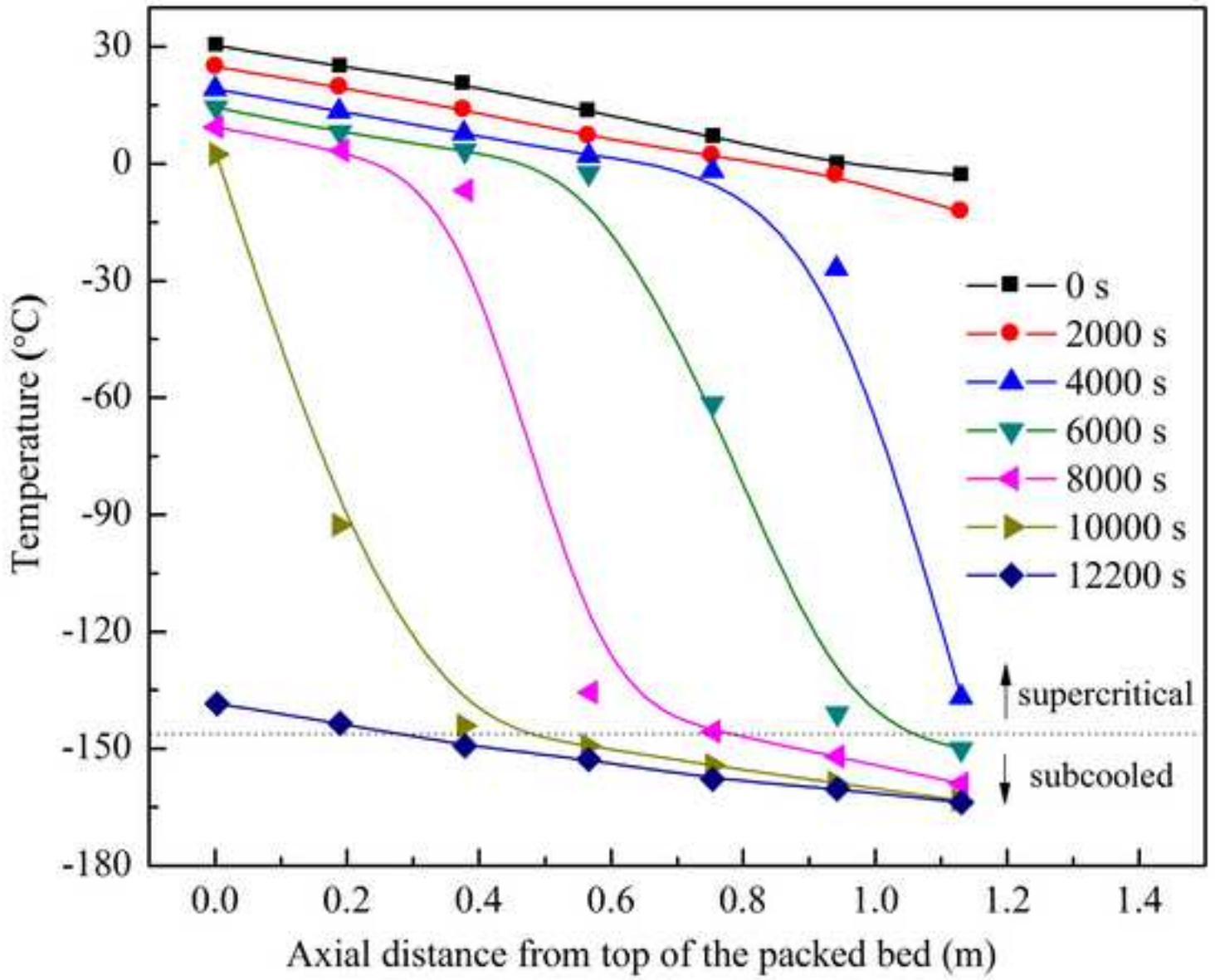

Figure 8a
Click here to download high resolution image

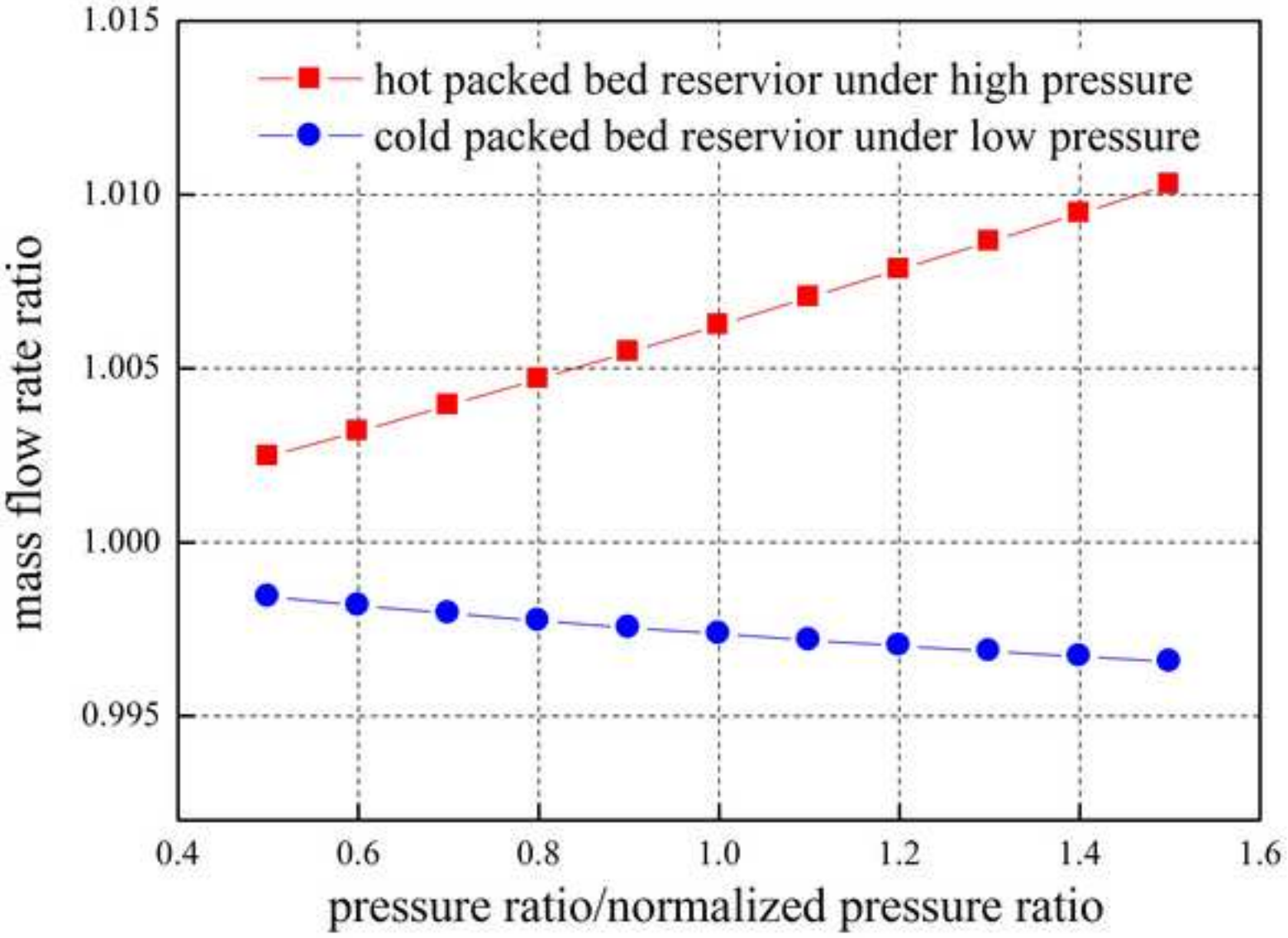

Figure 8b
Click here to download high resolution image

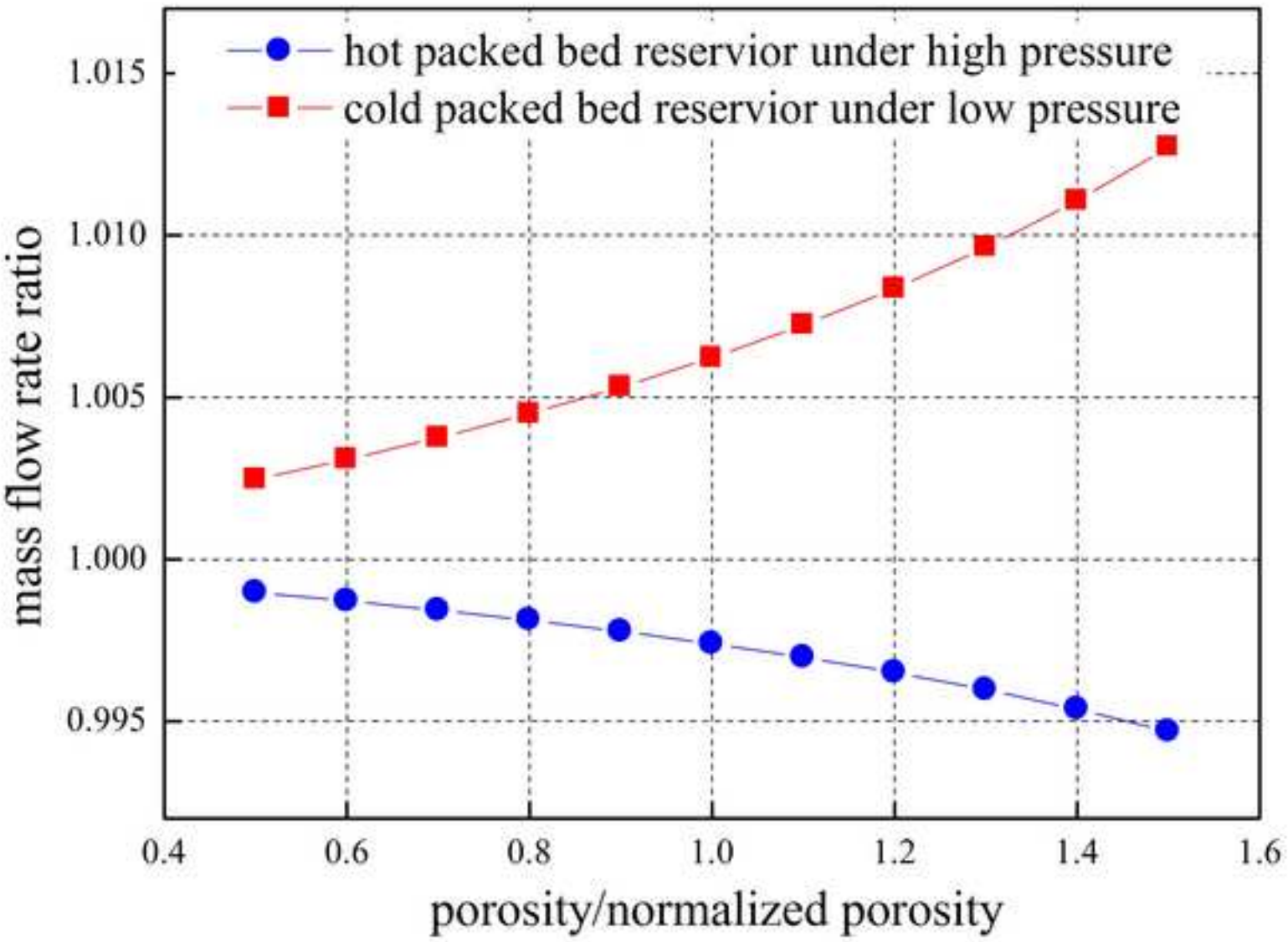

Figure 8c

Click here to download high resolution image

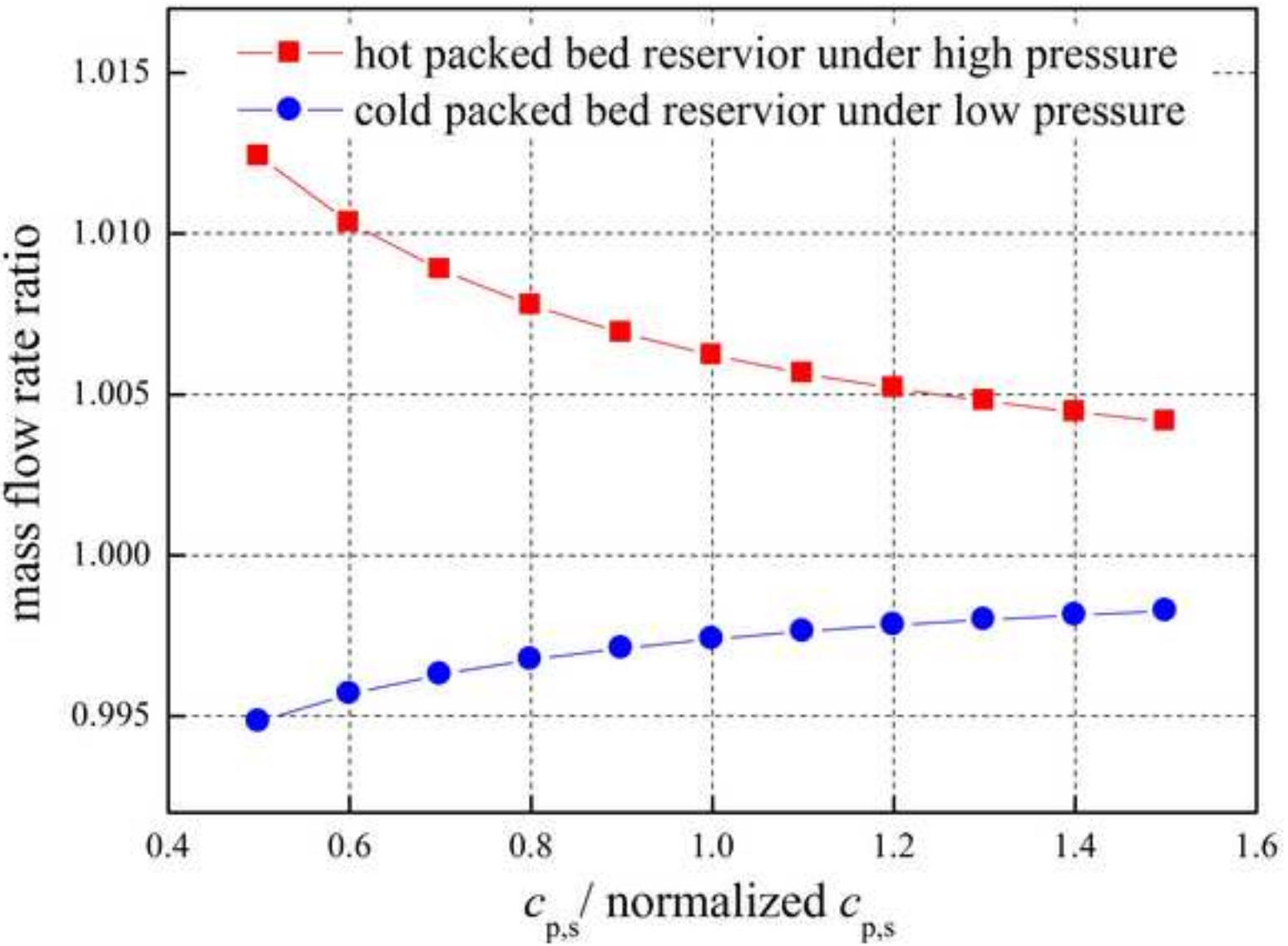

Figure 9a

Click here to download high resolution image

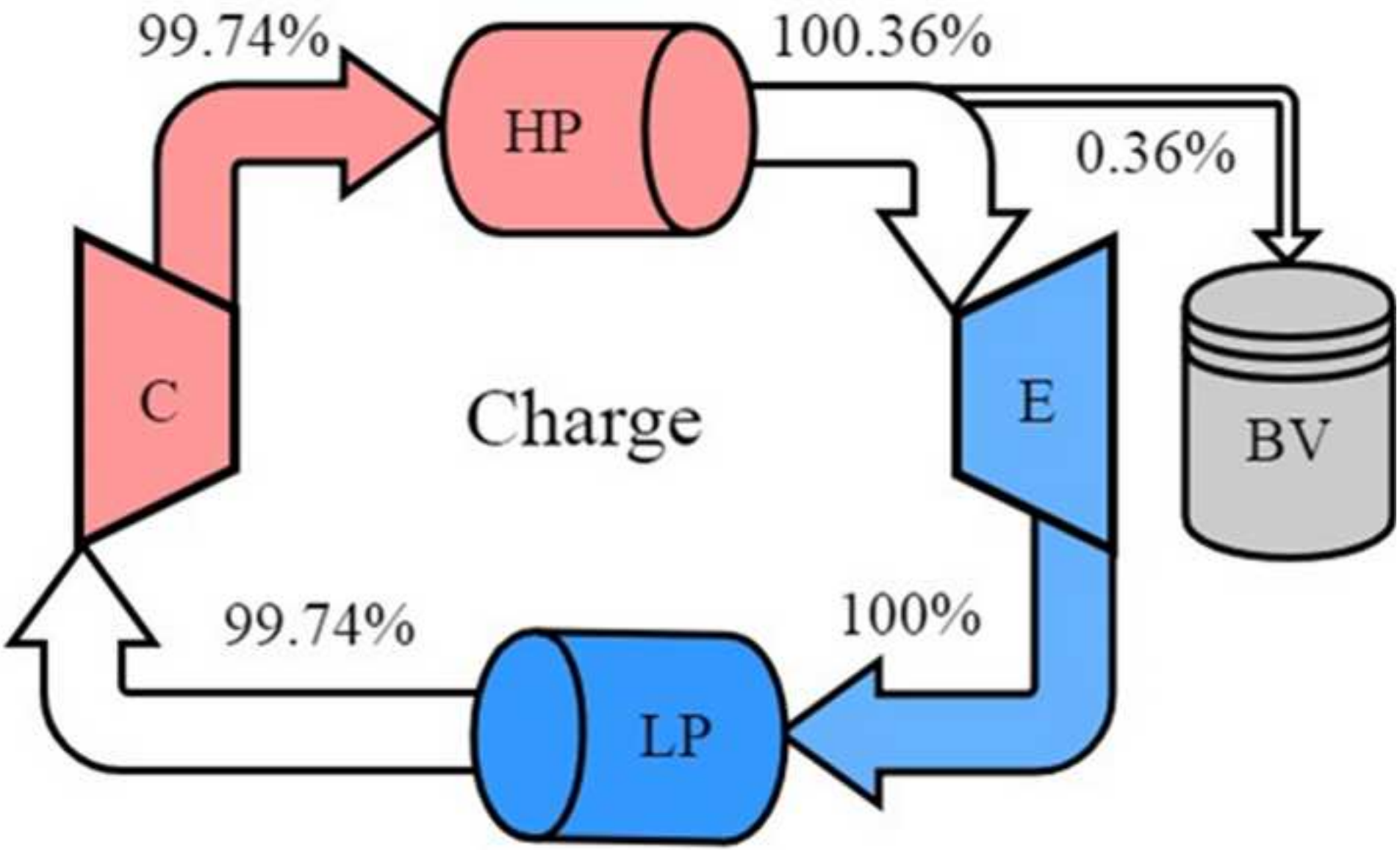

Figure 9b
Click here to download high resolution image

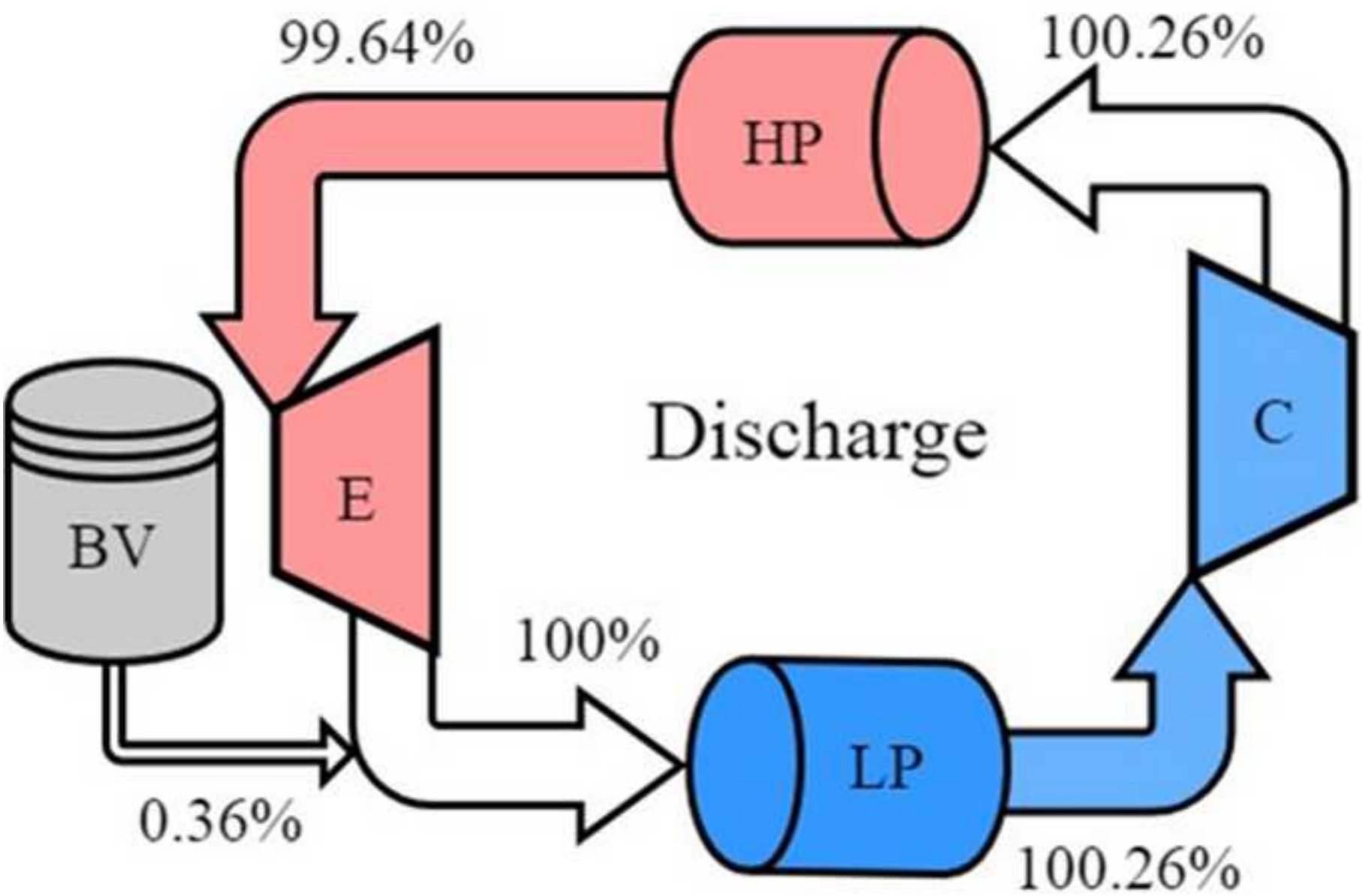

Figure 10a

Click here to download high resolution image

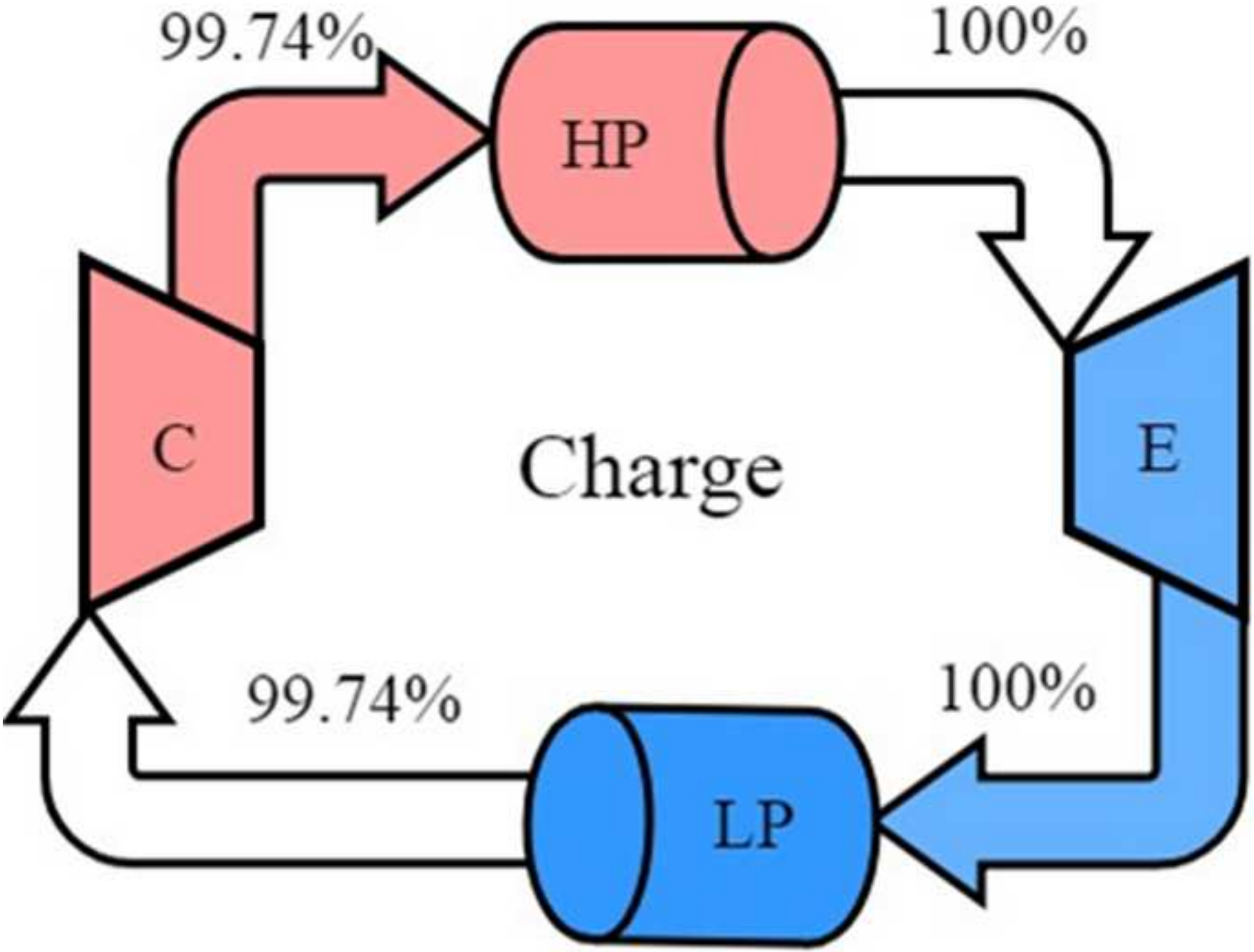

Figure 10b

Click here to download high resolution image

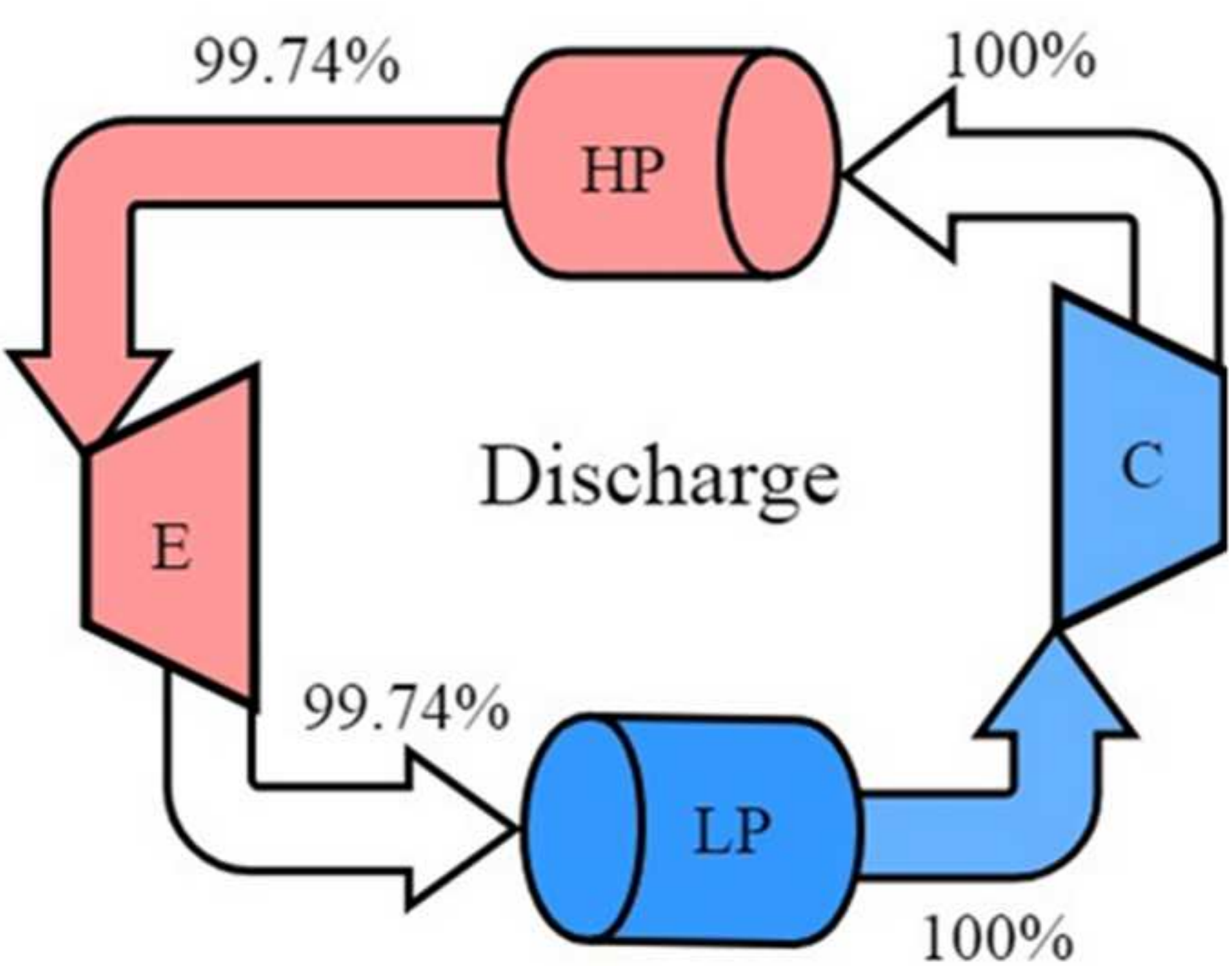

Figure 11

Click here to download high resolution image

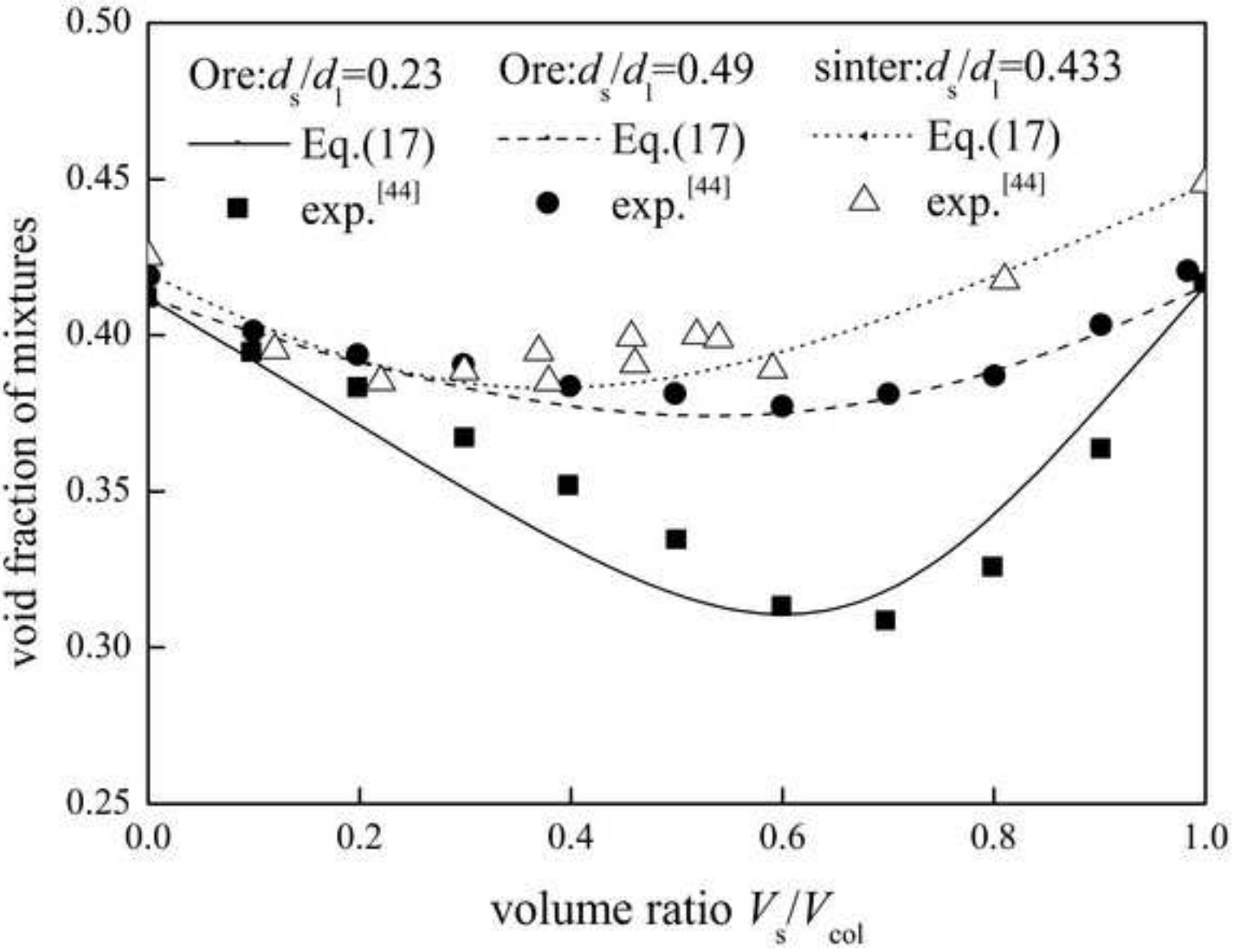

Figure 12

Click here to download high resolution image

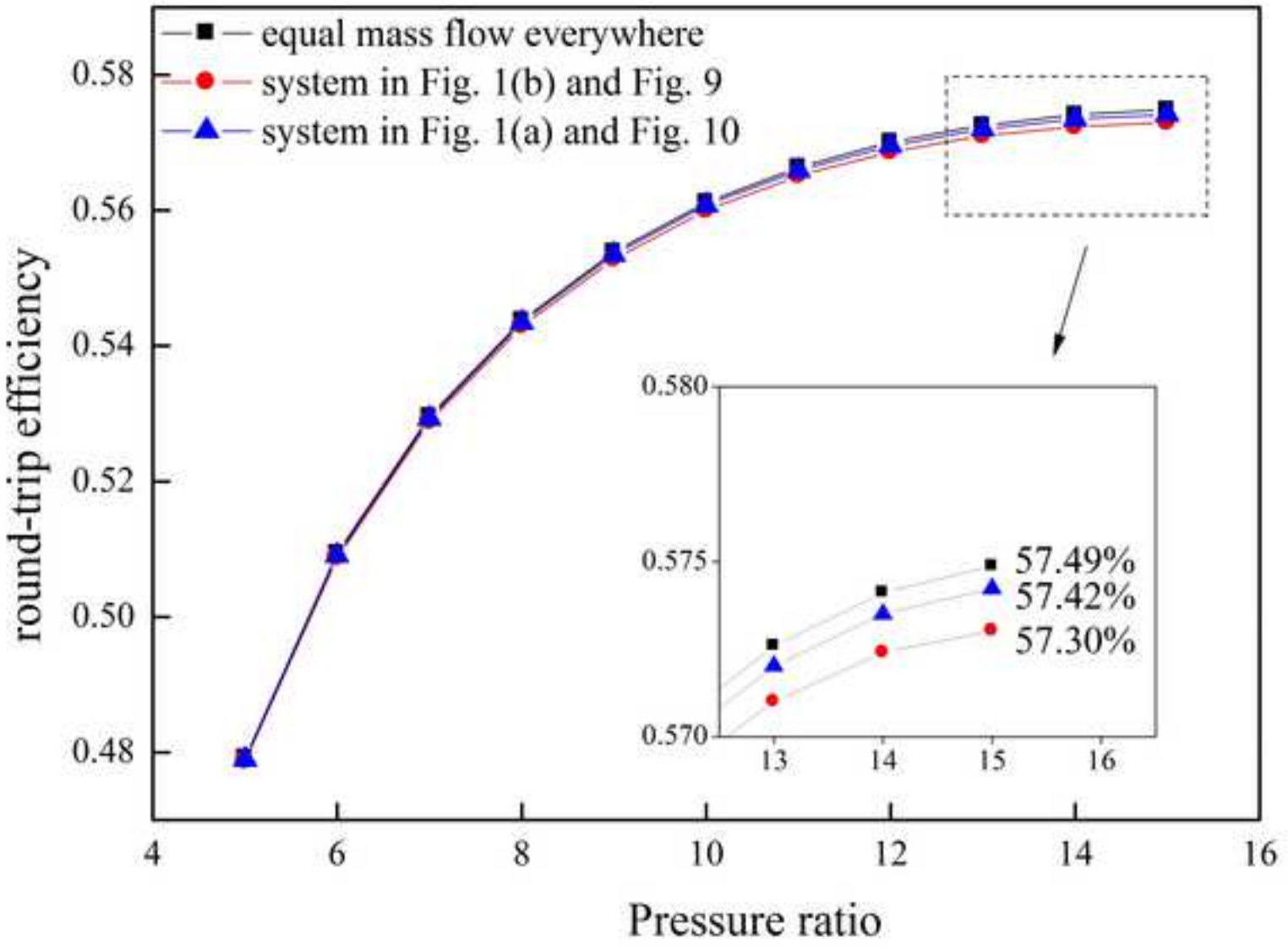

Response Letter

Manuscript number: ECM-D-18-07830

Dear Editor :

We thank you very much for your attention and the reviewers' evaluation and comments on our paper entitled "Unbalanced mass flow rate of packed bed thermal energy storage and its influence on the Joule-Brayton based Pumped Thermal Electricity Storage" (No.ECM-D-18-07830). We have revised the manuscript according to your kind advices and reviewers' detailed suggestions. All the revised parts have been marked in yellow. Enclosed please find the responses to the reviewers. We sincerely hope this manuscript will be finally acceptable to be published on Energy Conversion and Management. Thank you very much for all your help and looking forward to hearing from you soon.

Best regards

Sincerely yours

Dr. Liang Wang, Dr. Xipeng Lin, Dr. Lei Chai, Dr. Long Peng, Dr. Dong Yu, Dr. Jia Liu , Dr. Haisheng Chen

The response to the comments accordingly in the following:

Editor:

1) The text should be meticulously checked for accuracy and readability.

Reply: We thank the editor for the comments.

The text has been checked meticulously. Dozens of typos and mistakes have been corrected, and the readability has also been improved.

The revised parts in the manuscript have been marked in yellow.

2) The highlights are a stand-alone text for the readers' overall understanding. Unfamiliar abbreviations in the highlights should be avoided. Also, they should be rewritten to effectively reflect the main objective, findings and contributions in this paper.

Reply: The highlights have been rewritten to reflect the main objective, findings and contributions in this paper. The revised parts in the manuscript have been marked in yellow. We hope they meet the requirements of ECM.

3) Well-known information should not be overused in the abstract, even as background information. The abstract should be briefly written to describe the purpose of the research, the principal results, and major conclusions. Please revise.
Reply: Background information has been removed and the abstract has been written to describe the purpose of the research, the principal results, and major conclusions. The revised parts in the manuscript have been marked in yellow. We hope this version meet the requirements of ECM.

4) Please update the survey of related literature by referring to only the most recent and relevant references that have been published over the last 2-3years, particularly to draw the attention of Our Readers.
Reply: We retrieved for the relevant references carefully and found another 6 relevant papers. They are [26], [31], [37], [38], [39] and [40] in the reference which have been reviewed in the manuscript.

5) The introduction section is extremely long, which seems more like a review of the topic. It does not present a clear idea. This section should be focused on introducing the state of the art of the study and the gap in the literature that this work tries to cover.
Reply: We have rewritten the introduction, and more than 30% words in the introduction have been reduced compared with the previous version. Also the gap in the literature that this work tries to cover has been emphasized. We hope this version meet the requirements of ECM.

Reviewer #1:

Review:
Unbalanced mass flow rate of packed bed thermal energy storage and its influence of on the Joule-Brayton based Pumped Thermal Electricity Storage

In this paper, the authors describe how the mass flow rate differs between the inlet and outlet of a packed bed due to density differences. They develop an equation for this difference in mass flow rate and validate it against experimental results. The authors claim that this behavior is particularly important in an electricity storage system known as Pumped Thermal Electricity Storage (PTES) which uses a hot and cold packed bed. The authors propose a modifying the packed beds in PTES systems so that the mass flows are no longer "unbalanced".

This paper is generally well written and on a topic of considerable interest (packed beds and PTES). The behavior described is interesting from a scientific point of view and is relevant for the design of PTES systems, which so far use a buffer tank as a result of the unbalanced mass flows. The extent of the unbalanced mass flow on round-trip efficiencies and compressor/expander behavior is really quite small, and it would be better for the authors to quantify this earlier in the paper (e.g. abstract, introduction, conclusion) rather than giving the

impression that the effects are significant (see p.12 lines 10-17). The main result from this paper is being able to design a system that does not require a buffer vessel and this could be emphasized instead.

Reply: We thank the reviewer for the comments. Thank you very much! We have revised abstract, introduction where the unbalanced mass flow on round-trip efficiencies were quantitated, and will not give the impression that the effects are significant. Furthermore, it has been emphasized that the self-balancing system does not require a buffer vessel.

Major questions and comments are first listed, followed by minor corrections and typos.

Major comments:

1. I think it is necessary for the authors to state some results in the abstract and conclusion. For instance, they claim a self-balancing PTES system is proposed with a high efficiency. They should state the value of the efficiency, and how it compares to the unbalanced system. Also, when discussing the unbalanced mass flow they should state its magnitude - e.g. the imbalance is very small (the authors mention values of 1.0062 and 0.9972 on page 21), but over a long period of time a large mass of gas has to be stored.

Reply: The abstract and conclusion has been revised with some results including the magnitude of the imbalance effect. The revised parts in the manuscript have been marked in yellow.

2. The results do not seem to be that significant. The authors say that it is necessary to consider mass imbalance to correctly calculate the round-trip efficiency and that it might also affect the off-design performance of compressors and turbines. However, the authors own results suggest that the round-trip efficiency result changes a very small amount (0.19%) and that the fraction off-design of the components is also nearly insignificant (99.74% and 100.26%). Perhaps one aspect the authors could discuss further is the ability to get rid of the buffer tank. This tank stores a gas so it will have quite a large volume. The authors should quantify the volume (and maybe cost) that is being saved. Furthermore, the authors state that there is an exergy loss associated with the depressurization from the high pressure hot store to the buffer vessel (p24, line 18). The authors could quantify this exergy loss (or maybe the pumping power required) in order to clarify how important this loss for the round-trip efficiency.

Reply: According to your comments, a paragraph has been added in page 29 as below

"From the above studies, it can be found that 0.12% increase of round-trip efficiency obtained through the self-balancing method based on the system parameters in [29], which is not very significant. However, a large amount of initial cost of PTES can be saved by abolishing the components including the BV, pressure

pipelines, valves and their controller. According to the parameters in [30], the volume of the high pressure BV need to be more than 12% of the HR volume, and the cost of the buffer vessel is comparable with the CR since the hot store is expected to cost between 11 and 17 Euro/kWh and the cold store 2 and 4 Euro/kWh [37]. Furthermore, the throttle loss of the regulating valve when gas fed into the BV is about 0.21% of the compression work, which can be totally saved in the self-balancing system."

3. The idea to remove the need for a buffer vessel by altering the porosities of the packed beds is very interesting. However, the authors give no details about the design of these new packed beds. They should provide information on the porosities chosen for each packed bed (and the relative sizes of the two particles that are chosen). Do the packed beds still use the same filler material? (Different materials with different heat capacities might be another way to solve this problem). Since the difference in mass flows between the two stores is quite small, I would expect the two storage units to have quite similar porosities. The authors should discuss how achievable it would be to build a packed bed like this in practice. For instance, there is likely to be variance in the size of the particles, and the packed bed porosity will depend on this, and also on how the pebbles are placed into the bed when it is constructed. Thus, it may be difficult to control the porosity at tolerances of less than a few percent, which would make the execution of the proposed system challenging.

Reply: According to your comments, the design principle for the self-balancing PTES system has been presented in Page 24 line 1-9.

The detailed design of CR and HR using granite as storage material has been shown in Table 2 in Page 25 line 11- Page 26 line 2.

Other comments:

1. P.1, line 2: There seems to be a typo in the title! "… its influence [of] on the Joule-Brayton based …"

Reply: Corrected. Sorry for the typo.

2. P.6. Perhaps mention Liquid Air Energy Storage, since an LAES plants has recently been constructed by Highview Power.

Reply: In page 6 line 5-10, the present situations including that LAES plants built by Highview Power and the advanced CAES built by IET,CAS has been added in the text.

"By storing air at the liquid state to overcome this barrier, Highview Power Storage built a small pilot (350 kW/2.5 MWh) and a medium prototype LAES plant (5 MW/15 WMh) in the UK [10,11], and the Institute of Engineering Thermophysics, Chinese Academy of Sciences built a 1.5 MW and a 10MW advanced CAES demonstration in China [12, 13]."

3. P.7 line 10. What do the authors mean by Carnot cycles for PTES? A well-known (and trivial) result for PTES systems is that if both the heat pump and heat engine are reversible then the round-trip efficiency is 100% (COP of a heat pump multiplied by the Carnot efficiency of the heat engine). This result assumes there is no temperature difference between the storage systems and the power cycles. Thess and Guo's work - and also Mercangoz's [1] - use Carnot cycles but assume a temperature difference does exist between the storage and the power cycles. This is called endo-reversible thermodynamics.

Reply: According to your comments,the main finding and contribution of Thess and Guo's work has been added in page 6 line22-page 7 line 6。

Although Mercangöz et al. presented a simple discussion based on Carnot cycles in their paper: "M. Mercangöz, J. Hemrle, L. Kaufmann, A. Z'Graggen, C. Ohler, Electrothermal energy storage with transcritical CO2 cycles, Energy. 45 (2012) 407-415. doi:10.1016/j.energy.2012.03.013.", this paper mainly focuses the transcritical CO2 Rankine cycles. The research progress of the transcritical CO2 Rankine cycles of Mercangöz's group have been reviewed, they are reference [19], [20] and [21].

4. P9, line 10. Perhaps the authors could discuss Isentropic a little further. The company began to build a prototype but went into administration before it was complete. It now resides at Newcastle University, where it has been tested.

Reply: According to your comments, the Isentropic Ltd and the first 2 MW/16 MWh grid-scale PTES demonstration has been discussed in Page 8 line 18-20,that

"The first 2 MW/16 MWh grid-scale Brayton cycle based PTES demonstration was designed and manufactured by Isentropic Ltd and is being commissioned by Newcastle University [35, 36]"

5. P10, line 1. In an extension of McTigue's work, the packed beds were segmented into layers which was shown to reduce pressure losses [2]. This is the type of packed bed that was being developed by Isentropic.

Reply: According to your comments, the main finding from the paper [2]"Analysis and optimisation of packed-bed thermal reservoirs for electricity storage applications" has been added in Page 8 line 9-12 as below:

"And for the 2 MW/16 MWh PTES system, an extension study indicate that the radial-flow packed beds have a comparable thermodynamic performance to the axial-flow packed beds, but require additional volume"

6. P10, line 9. Perhaps the authors could discuss the recent cost analysis of PTES by Smallbone [3].

Reply: According to your comments, the analysis on the cost of PHES by Smallbone et al.[3] has been added in Page 8 line 20-22 as below:

"Based on the PTES demonstration plant, Smallbone et al. found the levelised cost of PHES is between 0.089 and 0.114 Euro/kWh."

7. There are a lot of typos (see below for a selection), and the abstract isn't particularly well written.

Reply: The typos have been corrected and the abstract have been improved.

8. P19, line 6. The authors specify the pressure of liquid nitrogen at 6.5 MPa. What is the temperature inlet to the packed bed?

Reply: The temperature at the inlet of the packed bed is -166°C. And the inlet temperature has been indicated in P17, line 6.

9. P19, line 7. In the experimental set up the authors investigate, the nitrogen changes phase from liquid to gas. As the authors note, the density difference between the inlet and outlet is large. The fractional change in mass is therefore quite large. However, this is unrepresentative of the packed beds that are discussed earlier in the paper for PTES applications (where the working fluid does not undergo a phase change). I understand the point of section 3.2 is to demonstrate the applicability of equation 14. However, the authors should discuss the difference between the experimental study and the typical fluids and density changes seen in sensible packed beds with ideal gas working fluids.

Reply: According to your comments, the difference between the experimental study and the typical fluids and density changes seen in the PTES system have been discussed in page 17 line 10-page 18 line 2, as below:

"Equation (14) indicates that the density ratios between the gas and the packed bed material at the inlet ($\rho_{g,i}/\rho_s$) and the outlet ($\rho_{g,o}/\rho_s$) are the main factors influencing the mass flow ratio. In this experiment, the state of nitrogen change from subcooled to supercritical under a high pressure of 6.5 MPa where the high density ratios ($\rho_{g,i}/\rho_s$ and $\rho_{g,o}/\rho_s$) leading to a high mass flow ratio. As to the packed beds of PTES, owing to the small density difference of argon, the effect of mass flow ratio may be not as remarkable as this experiment."

10. Figure 7: The points are presumably data points, but how were the lines generated? Are these some kind of curve fit, or were they generated with a model? If so, details are required.

Reply: The curves are B-spline curves generated based on the experimental points. It has been explained in page 18 line 5.

11. Figure 7: At this pressure, what is the temperature of the nitrogen phase change? Should the effect of this phase change be visible in Figure 7?

Reply: The critical temperature and pressure of nitrogen are 126.21K (-146.94°C) and 3.39 MPa. Under the pressure of 6.5 MPa which is above the critical pressure, nitrogen is at the subcooled state at the temperature below -146.94°C and nitrogen is at the supercritical state at the temperature above -146.94°C, but there is no obviously phase change phenomena. Furthermore, the effect has been added in Figure 7 with the explanation in page 18 line 10-15 as below

"It can also found that, at the beginning of the charging process, nitrogen in the packed bed is under the supercritical state with a large temperature gradient (above -146.94°C). And then the subcooled region (below -146.94°C) with a small temperature gradient increases from the bottom gradually until the cryogenic energy is fully charged in the TES reservoir."

12. P.24 line 1. PHES. The authors said they would use the term PTES throughout the paper

Reply: The "PHES"s have been corrected to "PTES"s.

13. Figure 9 title: "PHES". The authors said they would use the term PTES throughout the paper

Reply: The "PHES"s have been corrected to "PTES"s.

Comments on highlights:

1. "The unbalanced mass flow rate of the packed bed was raised". This is confusing and seems to indicate that the mass flow rate was increased. Presumably the authors mean that the issue of unequal mass flow rates between a packed bed inlet and outlet was raised.

Reply: The highlights have been rewritten to reflect the main objective, findings and contributions in this paper.

Additionally, a few typos should be corrected:

1. P.3 line 21. "An" should be "A"

Reply: This typo has been corrected.

2. P.8 line 15 Change "Joule-Brayron" to "Joule-Brayton"

Reply: This typo has been corrected.

3. P.8 line 21 Change "Joule-Brayron" to "Joule-Brayton"

Reply: This typo has been corrected.

4. P.9 line 1. Chage "ea" to "the" or "a"

Reply: "ea" has been changed to "the".

5. P.9 line 6. "Polytrophic" to "Polytropic"

Reply: This typo has been corrected.

6. P.9, line 9: Rephrase "Howes introduced three prototype PTES of company Isentropic .."

Reply: This sentences has been rewritten in page 8 line 1-3, that

"Based on the experimental studies on a series of working prototypes of Brayton based PTES, Howes developed a hypothetical 2 MW/16MWh PTES system with the calculated round-trip efficiency of 72% "

7. Figure 8b: Typo in x axis title. "prosity" should be "porosity"

Reply: This typo has been corrected.

8. P.28 line 6. "Polytrophic" to "Polytropic"

Reply: This typo has been corrected.

9. Sometimes the round trip efficiency is called a round trip coefficient. Perhaps it is better to be consistent with the terminology.

Reply: Four typos of "round trip coefficient" have been corrected to "round trip efficiency"

10. P 29 line 7: "pumped heat" should be "pumped thermal"

Reply: "pumped heat" has been corrected to pumped thermal"

References

[1] M. Mercangöz, J. Hemrle, L. Kaufmann, A. Z'Graggen, C. Ohler, Electrothermal energy storage with transcritical CO2 cycles, Energy. 45 (2012) 407-415. doi:10.1016/j.energy.2012.03.013.

[2] A.J. White, J.D. McTigue, C.N. Markides, Analysis and optimisation of packed-bed thermal reservoirs for electricity storage applications, Proc. Inst. Mech. Eng. Part A J. Power Energy. 230 (2016). doi:10.1177/0957650916668447.

[3] A. Smallbone, V. Jülch, R. Wardle, A. Paul, Levelised Cost of Storage for Pumped Heat Energy Storage in comparison with other energy storage technologies, Energy Convers. Manag. 152 (2017) 221-228. doi:10.1016/j.enconman.2017.09.047.

Reviewer #2:

This paper presents an interesting analysis of the differences observed in a packed bed for thermal energy storage when there is large differences in the densities of the HTF at the inlet and at the outlet of the bed. The theoretical analysis of the authors has been corroborated with experimental data and a sensitivity analysis has been also carried out. From my view the paper is suitable for publication if some minor aspects of the work are prior clarified. These points are:

1) Page 6. Lines 17-21. Please add the reference of the information about the two CAES units.

Reply: We thank the reviewer for the comments. The reference of the information about the two CAES units has been added in Page 6. Lines 3, they are reference [4] and [9].

2) Page 17. Line 20. Add more information about the measurement process and the uncertainty of the porosity and density values.

Reply: The porosity and the density of the granite pebbles were measured by the well-known water saturation method and the uncertainty of the porosity and density values are given in page 15 line 21-page 6 line 1,that

"With the water saturation method, the porosity and the density of the granite pebbles are measured to 0.40±0.0002 and 2688±11 kg/m^3, respectively"

Unbalanced mass flow rate of packed bed thermal energy storage and its influence on the Joule-Brayton based Pumped Thermal Electricity Storage

Liang Wang[1, 2], Xipeng Lin[1], Lei Chai[3], Long Peng[1], Dong Yu[1], Jia Liu[4], Haisheng Chen[1, 2,*]

(1 Institute of Engineering Thermophysics, Chinese Academy of Sciences, Beijing 100190, China; 2 University of Chinese Academy of Sciences, Beijing 100049, China

3 RCUK National Centre for Sustainable Energy Use in Food Chain (CSEF), Brunel University London, Uxbridge, Middlesex UB8 3PH, UK

4 China Huanqiu Contracting & Engineering Corporation, Beijing 100012, China)

*Corresponding author. Tel.: +86 10 82543148, E-mail: chen_hs@iet.cn

Abstract

As the most suitable thermal energy storage manner for the Joule-Brayton based Pumped Thermal Electricity Storage (PTES), packed beds thermal energy storage has the natural feature that a steep thermal front propagates with great difference of temperature and density, which lead to an unbalanced mass flow rate of packed bed reservoirs and the PTES close loop. In this paper, the expression of thermal front propagation and unbalanced mass flow rates between the inflow and the outflow of packed beds is developed and validated experimentally. The result indicates that there are 0.62%, 0.26% and 0.36% unbalanced mass flow for the hot reservoir, the cold reservoir and the PTES close loop respectively. The sensitivities of the factors such as

pressure ratio, heat capacity of TES material and porosity on the unbalanced mass flow rate and the round–trip efficiency of PTES system considering mass flow rate is discussed. Furthermore, a feasible and self-balancing PTES system without buffer vessel is proposed, with a round-trip efficiency 0.12% higher than the buffer vessel balancing PTES system.

***Keywords**:* pumped thermal electricity storage; thermal energy storage; packed bed; energy storage; unbalanced mass flow

Nomenclature

Abbreviations

CAES	Compressed air energy storage
CHEST	Compressed heat energy storage
DSC	Differential scanning calorimetry
EES	Electrical energy storage
ORC	Organic rankine cycle
PHS	Pumped hydro storage
PHES	Pumped heat electricity storage
PTES	Pumped thermal electricity storage
TES	Thermal energy storage

Symbols

C_F	Inertial coefficient of packed bed

1	c_p	Specific heat capacity, J K^{-1} kg^{-1}
2	D	Diameter of particles, m
3	E	Internal energy per unit mass, J kg^{-1}
4	G	Coefficient relating particles size ratio
5	h	Volumetric heat transfer coefficient, W m^{-3} K^{-1}
6	K	Intrinsic permeability of the porous medium
7	L	Length scale, m
8	m	Mass of gas, kg
9	V	Specific volume
10	r	Pressure/expansion ratio of compressor/expander
11	R	Size ratio of particles
12	S	The surface area, m^2
13	t	Time, s
14	T	Temperature, K
15	X	Volume fraction
16	u	Velocity, m s^{-1}
17	γ	Adiabatic exponent of gas
18	δ	A parameter, $\varepsilon/(1-\varepsilon)$
19	ε	Porosity of packed bed
20	η	Polytropic efficiency of compressor/expander
21	κ	A parameter, $(\gamma-1)/\gamma$
22	μ	Dynamic viscosity, Pa s

ρ	Density, kg m^{-3}	
χ	Round trip efficiency	
Ψ	Sphericity of particles	

Subscripts

BV_chg	Buffer vessel during charging
BV_dis	Buffer vessel during discharging
c_chg	Compressor during charging
c_dis	Compressor during discharging
e_dis	Expander during discharging
e_chg	Expander during charging
g	Gas
i	Inlet
L	Large
Nom	Nominal
o	Outlet
S	Small
v	Volume
x	X axial

1. Introduction

Over the past years, renewable power has grown rapidly: 161 GW of renewable

power (excluding hydro) capacity were added with the increase rate of nearly 9% in 2016, to almost 2017 GW [1, 2]. However, large quantities of grid-connected renewable energy bring challenges to the security and stability of the power network due to the fact that most renewable energy resources are characterized by intermittency and instability. Electrical Energy Storage (EES), which transforms electrical energy to another form of energy for storage and is later converted back to electrical energy when needed, has been referred to as one of the most promising approaches [3, 4]. Also, EES can provide substantial benefits for the conventional electricity industry, including load following, peaking power and standby reserve, hence improving the utilization rate of the power grid and the efficiency of thermal power generation [5, 6].

Nowadays, there are a lot of storage technologies of different maturation stages, including Pumped Hydro Storage (PHS), Compressed Air Energy Storage (CAES), Thermal energy storage (TES), and batteries including lithium ion, vanadium redox flow-cell etc. [3, 4]. Among the available storage technologies, only PHS and CAES are considered to be large-scale stand-alone electricity storage technologies with capacities over 100MW [3, 4, 7]. PHS is a mature technology with high capacity, long storage period, high efficiency and relatively low cost per unit of energy. With a round trip efficiency of about 71% to 85%, there are over 170GW of PHS in operation worldwide, which is about 94% of global energy storage capacity [3, 8]. The major constraints of PHS are suitable topological conditions for two large reservoirs with a certain fall head and one or two dams, as well as a long time and high cost for

construction. CAES is the other available technology suited for large scale energy storage. There are two CAES units under commercial operation in the world and they are 290 MW/2 h CAES in Huntorf, Germany and 110 MW/26 h CAES in McIntosh, Alabama, USA, with underground storage caverns of ~310,000 m^3 and ~500,000 m^3, respectively [4, 9]. Similar to PHS, appropriate geographical conditions for the enormous volume of storage caves is the main barrier for the construction of CAES systems. By storing air at the liquid state to overcome this barrier, Highview Power Storage Ltd built a small pilot (350 kW/2.5 MWh) and a medium prototype LAES plant (5 MW/15 WMh) in UK [10,11], and the Institute of Engineering Thermophysics, Chinese Academy of Sciences built a 1.5 MW and a 10MW advanced CAES demonstration in China [12, 13].

In recent years, relatively new energy storage technologies for large scale applications were studied, including "Pumped Heat Electricity Storage (PHES)" [14], "Pumped Thermal Electricity Storage (PTES)" [15-18], "Thermo-electric Energy Storage" [19-21], and "Compressed Heat Energy Storage (CHEST)" [22] etc. And the term PTES will be employed in this paper. Such technologies share similar working principles: in the charging process thermal (heat/cold) energy is generated by electricity through a heat pump cycle and stored; at the discharging process electricity is generated by the stored thermal energy through the heat-work conversion cycle. Such systems have the advantages of high efficiency, high energy storage density and no geographical restrictions.

There are two main PTES systems which have been investigated so far, based on

Joule-Brayton cycles and Rankine cycles. Few investigations have been made on the Carnot cycles although, Thess and Guo et al. carried out theoretical analysis on PHES and PCES systems using finite-time thermodynamics approaches and predicted the maximum round-trip efficiency with varying storage temperatures and other parameters, respectively [14, 23].

After the PTES system based on supercritical CO_2 Rankine cycle was firstly by ABB company [19], the PTES systems based on different thermodynamic cycles including subcritical NH_3 Rankine cycle [16, 17, 25], steam Rankine cycle [22], supercritical CO_2 Rankine cycle [20, 21, 24], supercritical air [24], supercritical argon [24] and the organic Rankine cycles (ORC) [15] were developed and the results show that the stand-alone round trip efficiency is between 51% and 70% under different temperatures of the hot and cold reservoirs [16, 17, 20-22], and achieve 130% when integrated with an 80°C~110°C heat source [15]. Roskosch et al. found the round trip efficiency of a PHES system consists of a compression heat pump and an ORC is between 56% and 37% and decrease with increasing storage temperatures [26].

On the Brayton based PTES, Desrues et al. firstly presented a PTES system based on the Joule-Brayton cycle consisting of two TES reservoirs connected by two compressor-turbine-pairs (one for charging and one for discharging) and two heat exchangers using argon as the working gas [27]. During the charging process, the hot reservoir is heated from 25°C to 1000°C under a pressure of 4.6 bar while the cold reservoir is cooled down from 500°C to -70°C under a pressure of 1.0 bar utilizing refractory material. By the numerical simulations and optimizations, a round-trip

efficiency of 66.7% was obtained for the 602.6 MWh PTES system based on the turbo machines' polytropic efficiency of 0.9. Based on the experimental studies on a series of working prototypes of Brayton based PTES, Howes developed a hypothetical 2 MW/16 MWh PTES system with the calculated round-trip efficiency of 72% [28]. White et al.'s thermodynamic study indicates that the round-trip efficiency and energy storage density increase with increasing temperature ratio between the hot and cold TES reservoirs [29]. Furthermore, McTigue et al. presented the theoretical analysis coupled with a Schumann-style packed bed model of the hot and cold reservoirs for the Brayton based PTES system. A buffer vessel was introduced in order to balance the total mass of gas in the hot and cold reservoirs [30]. For the 2 MW/16 MWh PTES system, the extension study indicates that the radial-flow packed beds have a comparable thermodynamic performance to the axial-flow packed beds, but require additional volume [31]. Davenne et al. introduced a liquid isopentane thermocline TES technology for cold storage for the PTES system driven by wind energy whose exergy loss was deduced to be smaller than the packed bed thermocline [32]. Benato proposed a new Brayton cycle based PTES system in which an electric heater is used after the compressor in order to maintain the hot tank temperature during the charging process with the cost ranges between 50 and 200 Euro/kWh while the energy density is from 60 to 285 kWh/m^3 [33, 34]. The first 2 MW/16 MWh grid-scale Brayton cycle based PTES demonstration was designed and manufactured by Isentropic Ltd and is being commissioned by Newcastle University [35, 36]. Based on the PTES demonstration plant, Smallbone et al. found the levelised cost of PHES is between

0.089 and 0.114 Euro/kWh [37]. And PTES become economically more competitive than LAES over a buy price of ~0.15 USD/kWh, primarily due to the higher round trip efficiency [38]. Detailed reviews of the principles and characteristics of these state of the art PHES technologies are presented in Refs. [39] and [40].

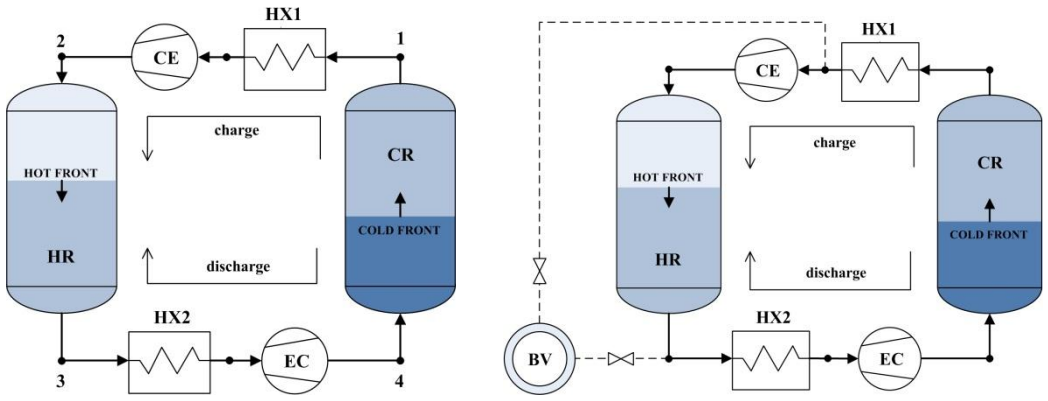

(a) (b)

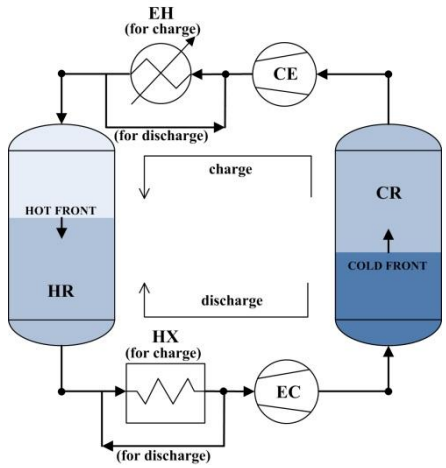

(c)

Fig.1. Layout of the Joule-Brayton cycle PTES system proposed by (a) Desrues et al. [27] and White et al.[29], (b) McTigue et al.[30], (c) Benato [33].

Low cost, high efficiency and high energy density TES is vital for the PTES system in order to compete with PHS and CAES. There are mainly three categories of heat storage: sensible, latent, and chemical heat storage [41]. Due to its low cost, wide

applicable temperature range (-200°C ~1000+°C), large specific surface area (which results in small temperature differences in heat transfer), non-toxicity, long life and other practical advantages, packed bed sensible TES has been identified as the most suitable technology for the PTES system [33]. The performance of PTES combining heat and cold packed bed reservoirs of different materials were adequately simulated and analyzed to determine round trip efficiency [27, 30, 33], energy density [33, 34], costs [33, 34] and other factors.

The existing studies on packed beds mainly focus on the thermal storage and thermodynamic loss [27-30, 34], whereas the characteristics of mass variation of gas has not been discussed before which is a basic but worthy to be noticed issue. During the charge/delivery process of packed bed TES, a large amount of heat transfer gas is stored or released in the pore volume of packed beds due to the great change in gas density owing to the translation of thermocline. In the PTES system, the total mass of argon in the hot reservoir decreases by about 60%, while that of the cold reservoir increases by about 150% [29, 30]. The mass variation of packed bed heat and cold reservoirs would certainly cause an unbalanced mass flow rate between the inflow and outflow in closed loop PTES systems, further lead to different gas flow rates between compressor and expander. Furthermore, taking the unbalanced mass flow rate into consideration would lead to an accurate calculation of round-trip efficiency and system optimization of PTES.

In this paper, therefore, both theoretical studies and experimental studies have been carried out on the propagation of the thermal front and the relation for the mass

flow rate ratio of packed bed between the outflow and the inflow. The unbalanced mass flow behavior of the packed bed reservoirs and Joule-Brayton based PTES system is found, and a series of related factors, such as PTES pressure ratio, packed bed porosity and heat capacity of TES materials, are investigated to understand their impact on unbalanced mass flow rate. Furthermore, the expression of the round-trip efficiency is proposed taking the unbalanced mass flow into account. Lastly, and a feasible and self-balancing PTES system are proposed, which can void the buffer vessel and have a little higher performance for future applications.

2. Theoretical Analysis

The packed bed region in the reservoir is chosen as the computational domain, and the x axis is the axial direction from the tank bottom to the tank top with x = 0 at the bottom of the packed bed region. The governing equations for heat transfer and fluid dynamics within the packed bed region include the continuity equation, the momentum equation, and the energy equations of the gas phase and the solid phase, which are Eqs. (1)–(4), shown below:

$$\varepsilon\frac{\partial\rho_{\mathrm{g}}}{\partial t}+\frac{\partial\left(\rho_{\mathrm{g}}u_{\mathrm{x}}\right)}{\partial x}=0 \tag{1}$$

$$\frac{\partial\left(\rho_{\mathrm{g}}u_{\mathrm{x}}\right)}{\varepsilon\partial t}+\frac{\partial\left(\rho_{\mathrm{g}}u_{\mathrm{x}}u_{\mathrm{x}}\right)}{\varepsilon^{2}\partial x}=\frac{\partial}{\partial x}\left(\mu\frac{\partial u_{\mathrm{x}}}{\partial x}\right)-\frac{\partial p}{\partial x}-\rho_{\mathrm{g}}g-\left(\frac{\mu}{K}+\frac{C_{\mathrm{F}}}{\sqrt{K}}\left|u_{\mathrm{x}}\right|\right)u_{\mathrm{x}} \tag{2}$$

$$\varepsilon\frac{\partial\left(\rho_{\mathrm{g}}c_{\mathrm{p,g}}T_{\mathrm{g}}\right)}{\partial t}+\frac{\partial\left(\rho_{\mathrm{g}}c_{\mathrm{p,g}}u_{\mathrm{x}}T_{\mathrm{g}}\right)}{\partial x}=h_{\mathrm{v}}\left(T_{\mathrm{s}}-T_{\mathrm{g}}\right) \tag{3}$$

$$\left(1-\varepsilon\right)\frac{\partial\left(\rho_{\mathrm{s}}c_{\mathrm{p,s}}T_{\mathrm{s}}\right)}{\partial t}=h_{\mathrm{v}}\left(T_{\mathrm{g}}-T_{\mathrm{s}}\right) \tag{4}$$

where ε is the porosity of the packed bed, u_x represents the superficial velocity based on the total cross-sectional area of gas and porous medium, K is the intrinsic permeability of the porous medium, μ is the dynamic viscosity of gas, C_F is the inertial coefficient of the packed bed, and h_v represents the volumetric interstitial heat transfer coefficient between gas and the packed bed.

Based on Eqs. (3) and (4), we have

$$\frac{\partial\left(\rho_g c_{p,g} u_x T_g\right)}{\partial x}+\varepsilon\frac{\partial\left(\rho_g c_{p,g} T_g\right)}{\partial t}+\left(1-\varepsilon\right)\frac{\partial\left(\rho_s c_{p,s} T_s\right)}{\partial t}=0 \tag{5}$$

Combining this equation with the progress of the thermal front in this ideal case determined with the wave propagation speed of the thermal front U by Eqs. (6) and (7) [41] we derive

$$\frac{\partial\left(\rho_g c_{p,g} T_g\right)}{\partial t}+U\frac{\partial\left(\rho_g c_{p,g} T_g\right)}{\partial x}=0 \tag{6}$$

$$\frac{\partial T_s}{\partial t}+U\frac{\partial T_s}{\partial x}=0 \tag{7}$$

Integrated in the region of thermocline, the propagation speed of the thermal front U can be obtained as shown in Eq. (8)

$$U=\frac{u_x\left(\rho_{g,o}e_{g,o}-\rho_{g,i}e_{g,i}\right)}{\left(1-\varepsilon\right)\rho_s\left(e_{s,o}-e_{s,i}\right)+\varepsilon\left(\rho_{g,o}e_{g,o}-\rho_{g,i}e_{g,i}\right)} \tag{8}$$

when neglecting the variation of density and internal energy of gas inside the packed bed pore, the thermal wave speed can be reduced to

$$U=\frac{u_x\left(\rho_{g,o}e_{g,o}-\rho_{g,i}e_{g,i}\right)}{\left(1-\varepsilon\right)\rho_s\left(e_{s,o}-e_{s,i}\right)}=\frac{u_x\rho_g c_{p,g}}{\left(1-\varepsilon\right)\rho_s c_s} \tag{9}$$

as achieved by White et al.[42].

For ideal cases of thermal front propagation in the packed bed as shown in Fig. 2,

during the charging process of cold energy, the thermal front moves upward with a distance of Δx over the time Δt. Under a constant pressure, the mass change of gas Δm for the whole reservoir due to temperature and density variation extend as shown in Eq. (10)

$$\Delta m=\left(\dot{m}_{\mathrm{i}}-\dot{m}_{\mathrm{o}}\right)\Delta t=\left(\rho_{\mathrm{g,i}}-\rho_{\mathrm{g,o}}\right)\varepsilon UA\Delta t \tag{10}$$

where A is the area of the cross section.

As to the energy balance of the whole reservoir, the energy change of the thermal storage reservoir ΔE is

$$\Delta E=\left(\dot{m}_{\mathrm{i}}e_{\mathrm{g,i}}-\dot{m}_{\mathrm{o}}e_{\mathrm{g,o}}\right)\Delta t=\left(\rho_{\mathrm{g,i}}e_{\mathrm{g,i}}-\rho_{\mathrm{g,o}}e_{\mathrm{g,o}}\right)u_{\mathrm{x}}A\Delta t \tag{11}$$

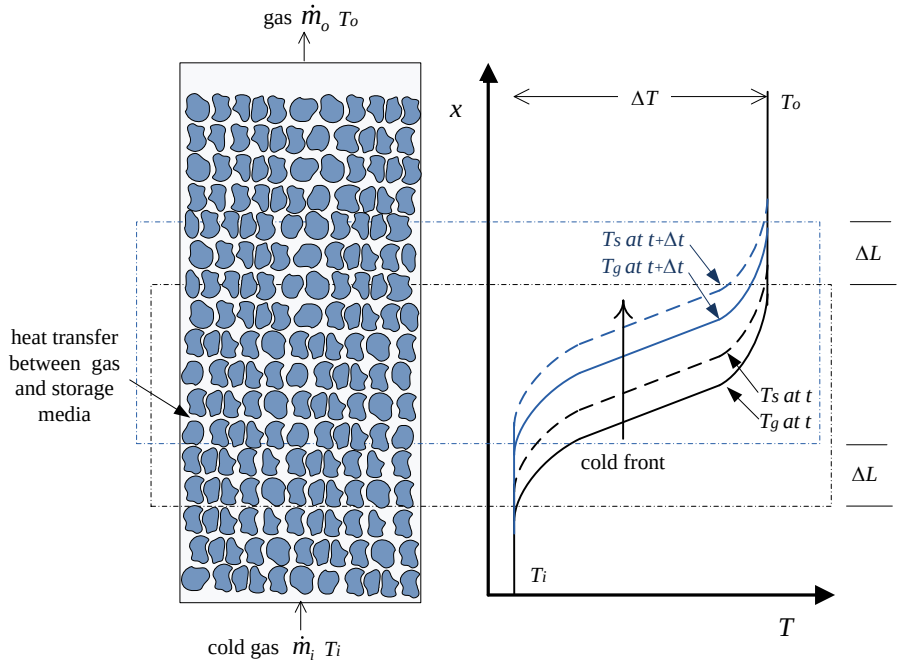

Fig. 2. Schematic diagram of thermal front in packed bed.

For thermal front propagation in the packed bed over time Δt, the variation of packed bed internal energy with volume of ΔxA including the packed solid storage medium and the gas in the pore, is as shown in Eq. (12) as below

$$\Delta E = \Delta L A\left[\rho_{\mathrm{s}}(1-\varepsilon)\left(e_{\mathrm{s,i}}-e_{\mathrm{s,o}}\right)+\varepsilon\left(\rho_{\mathrm{g,i}}e_{\mathrm{g,i}}-\rho_{\mathrm{o}}e_{\mathrm{g,o}}\right)\right] \tag{12}$$

From Eqs. (10) and (12), we have

$$U=\frac{\Delta L}{\Delta t}=\frac{u_{\mathrm{x}}\left(\rho_{\mathrm{g,o}}e_{\mathrm{g,o}}-\rho_{\mathrm{g,i}}e_{\mathrm{g,i}}\right)}{(1-\varepsilon)\rho_{\mathrm{s}}\left(e_{\mathrm{s,o}}-e_{\mathrm{s,i}}\right)+\varepsilon\left(\rho_{\mathrm{g,o}}e_{\mathrm{g,o}}-\rho_{\mathrm{g,i}}e_{\mathrm{g,i}}\right)} \tag{13}$$

which is as the same as Eq. (9). Combining Eqs. (10), (12) and (13), the mass flow ratio of the outflow to inflow for the packed bed reservoir is shown in Eq. (14) as

$$\frac{\dot{m}_o}{\dot{m}_i}=\frac{1+\dfrac{\rho_{\mathrm{g,o}}\bar{c}_{\mathrm{g}}}{\rho_{\mathrm{s}}\bar{c}_{\mathrm{s}}}\dfrac{\varepsilon}{1-\varepsilon}}{1+\dfrac{\rho_{\mathrm{g,i}}\bar{c}_{\mathrm{g}}}{\rho_{\mathrm{s}}\bar{c}_{\mathrm{s}}}\dfrac{\varepsilon}{1-\varepsilon}} \tag{14}$$

The mass flow ratio is mainly related to the gas density and gas heat capacity at the inlet and outlet, the volumetric heat capacity of TES material and the porosity of packed bed.

3 Validation experiment

In order to verify the mass flow correlations of Eq. (14) and study the cold thermal energy storage characteristics in the packed bed reservoir, the experimental study was performed using nitrogen as the working media.

3.1 Experimental apparatus

As shown in Fig. 3, the experimental system consists of two branches, i.e. the air branch and the nitrogen branch. In the air branch, dried air is first compressed from atmospheric pressure to the necessary pressure with a reciprocating compressor, and then goes through a surge tank to smooth the pulse air flow. Then it enters the packed bed reservoir from the top to provide the target pressure of the packed bed before the

cryogenic energy storage process. In order to decrease the thermal energy loss to the environment, high quality heat insulation material 100 mm thick was wrapped around the outer surface of the cryogenic storage packed bed reservoir, the cryogenic liquid pump and the corresponding connection tubes. In the nitrogen branch, liquid nitrogen forms a Dewar reservoir flow through a cryogenic flow meter to measure the flow rate, is pumped to the target pressure by a cryogenic liquid pump, and then enters the packed bed reservoir from the bottom. During the charging period, the valve at the outlet is adjusted by the feedback of a pressure signal to keep the pressure of the packed bed reservoir at a constant value. When the liquid nitrogen flows upward through the packed bed, the cryogenic energy is absorbed by packed pebbles, the liquid nitrogen changes to a gas state, and the flow rate is measured before delivered to the atmosphere. At the inlet and the outlet of the packed bed tank, the flow rate of liquid nitrogen is determined by a Shakic cryogenic electromagnetic flow meter with a range of 0-300 L/h and an accuracy of ±1%, and by a Collihigh vortex flow meter with a range of 36-320 m^3/h and an accuracy of ±1%. Three Collihigh piezoresistance pressure transducers with a range of 0-10 MPa and accuracies of ±0.5% are installed in the top and bottom of the cryogenic storage cylinder and at the end of the vent pipe.

The cryogenic storage cylinder is a 1500 mm height, 345 mm internal diameter and 32mm thickness stainless steel cylinder, wrapped with 200 mm thick magnesium silicate wool for insulation. The main apparatuses, such as the compressor, data acquisition system, cryogenic liquid pump, Dewar reservoir, and the cryogenic storage cylinder, are shown in Fig. 4. Granite pebbles of 7~11 mm in size with the

equivalent diameter of 9 mm are packed in the cryogenic storage cylinder. With the water saturation method, the porosity and the density of the granite pebbles are measured to 0.4±0.002 and 2688±11 kg/m^3, respectively. As shown in Fig. 5, the specific heat capacity of the pebbles is found to depend heavily on temperature from 0.45 kJ/(kgK) at -160°C to 0.82 kJ/(kgK) at 0°C, as measured by TA Q2000 DSC. Seven Pt100 platinum-thermal resistors with a range of -200 to 450^{o}C and accuracy of ±0.1% located in the interior of the packed bed at 0, 188, 376, 564, 752, 940 and 1128 mm below the upper surface of the pebble were used to measure the axial temperature distribution of the packed bed.

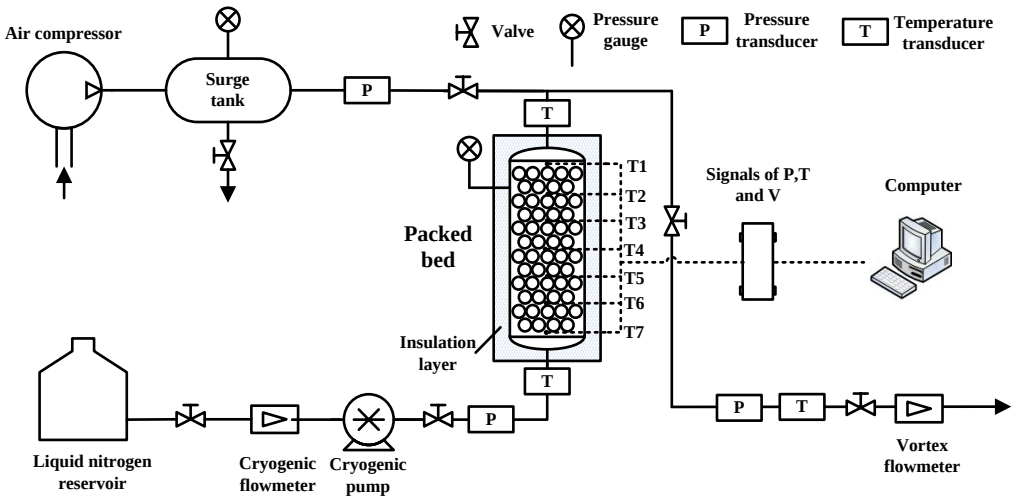

Fig. 3. Experiment setup and apparatus.

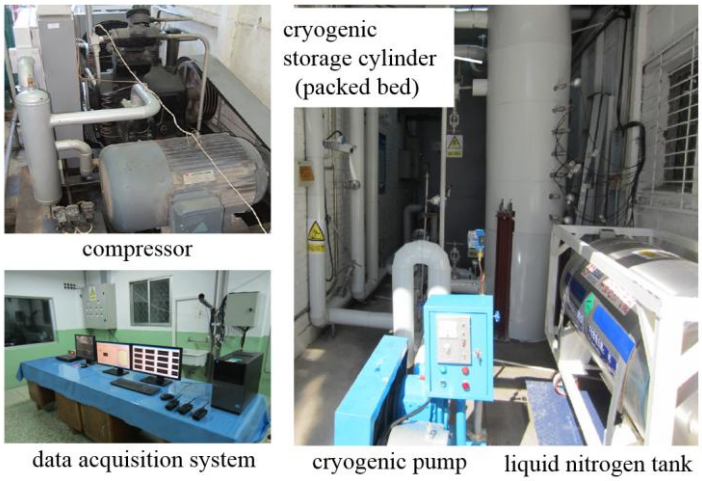

Fig. 4. Some of the experiment apparatus.

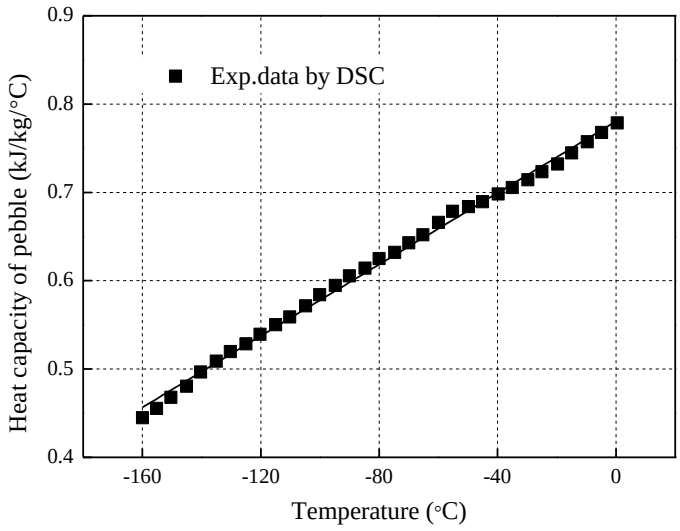

Fig. 5. Specific heat capacity variations of the pebble with temperature.

3.2. Experimental results

The experiments of the charging process of packed bed cryogenic storage with the mass flow ratio ranging from 80 kg/min to 200 kg/min were carried out under the pressure of 6.5 MPa and the inlet temperature of -166°C using nitrogen as the working media where a large difference in nitrogen density exists between the inlet (807 kg/m^3) and the outlet (73.1 kg/m^3). After every charging process, the packed bed was fully warmed to the ambient temperature by the compressed air. As shown in Fig.

6, the mass flow rate at the outlet is almost proportional to the inlet mass flow rate and the plot data by Eq. (14) fits well with the experiments and the deviation of less than ±8% under 6.5 MPa. Eq. (14) indicates that the density ratios between the gas to the packed bed material at the inlet ($\rho_{g,i}/\rho_s$) and the outlet ($\rho_{g,o}/\rho_s$) are the main factors influencing the mass flow ratio. In this experiment, the state of nitrogen change from subcooled to supercritical under a high pressure of 6.5 MPa where the high density ratios ($\rho_{g,i}/\rho_s$ and $\rho_{g,o}/\rho_s$) leading to a high mass flow ratio. As to the packed beds of PTES, owing to the small density difference of argon, the effect of mass flow ratio may be not as remarkable as this experiment.

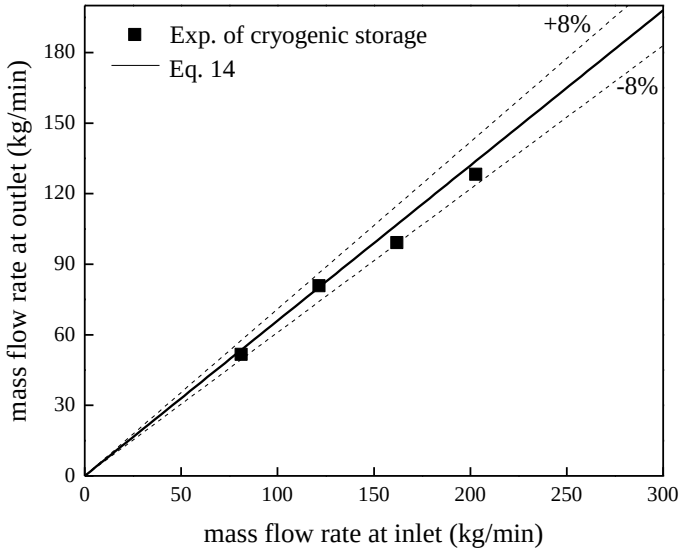

Fig. 6. Mass flow rate at outlet vs. inlet during cryogenic energy storage

Fig. 7 shows the axial temperature variation and the B-spline curves at the inlet mass flow rate of 80 kg/min at 6.5 MPa during the charging of cryogenic TES. It can be found that during the beginning 2000 s, the temperatures in packed bed decreased slowly as time passed, and then the thermocline occurred from the bottom and propagated upward from 4000 s to 10000 s, finally the thermocline vanished and the

packed bed was fully charged to below -130 °C at 12200 s. It can also found that, at the beginning of the charging process, nitrogen in the packed bed is under the supercritical state with a large temperature gradient (above -146.94 °C). And then the subcooled region (below -146.94 °C) with a small temperature gradient increases from the bottom gradually until the cryogenic energy is fully charged in the TES reservoir.

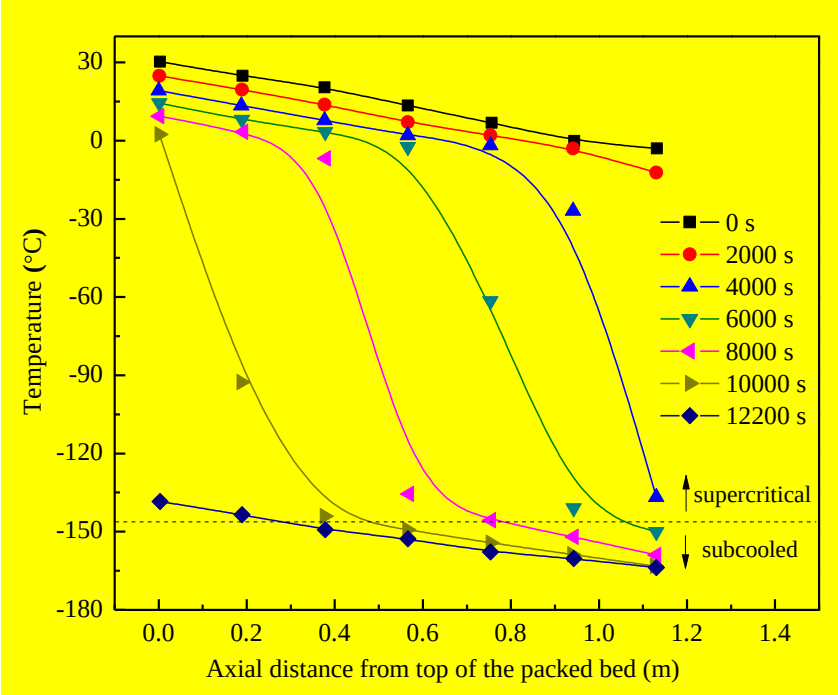

Fig. 7. Axial temperature during the charging of cryogenic energy

4. Discussion

4.1. Sensitivity of the mass flow rate

Due to the nature of density change inside the packed bed, there is a mass flow imbalance between the inflow and outflow during the charging and discharging process of the hot and cold reservoirs. For the Joule-Brayton based PTES system, as illustrated by McTigue et al. [30], the mass flow rate ratio of the outflow to inflow of

hot/cold TES reservoir exit during the charging process is 1.0062 and 0.9974 respectively, obtained by Eq. (14) based on the corresponding parameters is listed in Table 1, and the mass flow rate ratios during the discharging process are just the reciprocals of these.

Table 1. Hot and Cold reservoir detailed (storage material Fe_3O_4 with the void fraction of 0.35 and the density of 517.5 kg/m^3) [30]

Reservoir	Pressure (MPa)	Charge Temperature (K)	Discharge Temperature (K)	Charge Density (kg/m^3)	Discharge Density (kg/m^3)	Average c_g (J/kg/K)	Average c_s (J/kg/K)
Hot	1.05	778	310	6.46	16.36	527	860
Cold	0.105	123	310	4.15	1.63	528	520

From Eq. (14), it can be concluded that the porosity of the packed bed, the density ratio and heat capacity ratio of gas to TES material are the main factors influencing the ratio of mass flow rate between the outflow and inflow. The sensitivity of the mass flow rate ratio to the pressure ratio, the porosity and the heat capacity of TES material for the cold and hot reservoirs is shown in Fig. 8 (a)-(c). It can be found from Fig. 8(a) that for the high pressure reservoir, input of hot gas with low density and output of high density gas of the packed bed result in an outflow to inflow mass flow ratio higher than 1.0 and the mass flow ratio increases with increasing system pressure ratio, whereas increasing pressure ratio would lead to a colder input gas with higher density and a decreasing mass flow rate ratio between the output gas and the input gas.

As indicated in Table 1, normalized porosity (void fraction) of the packed bed is

0.35, and larger porosity leads to a larger mass flow ratio for the hot reservoir and a lower mass flow ratio for the cold reservoir as shown in Fig. 8(b). Also, as shown in Fig. 8(c) that the mass flow difference between the outflow and the inflow mass is decreased by increasing the heat capacity of TES material for both the hot and cold reservoirs. Generally, more influence of the factors on the mass flow ratio in the hot reservoir was found than that in the cold reservoir, mainly due to the larger change of gas density in the hot reservoir.

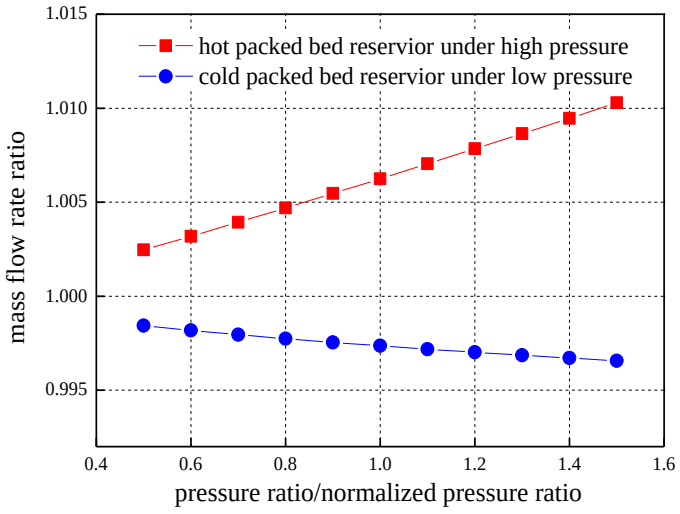

(a)

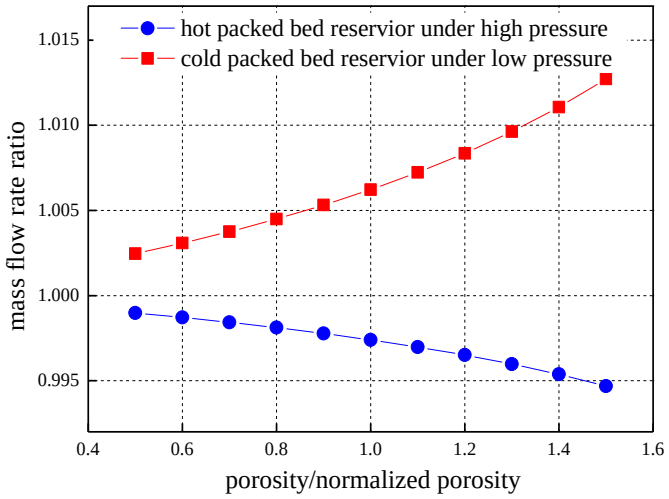

(b)

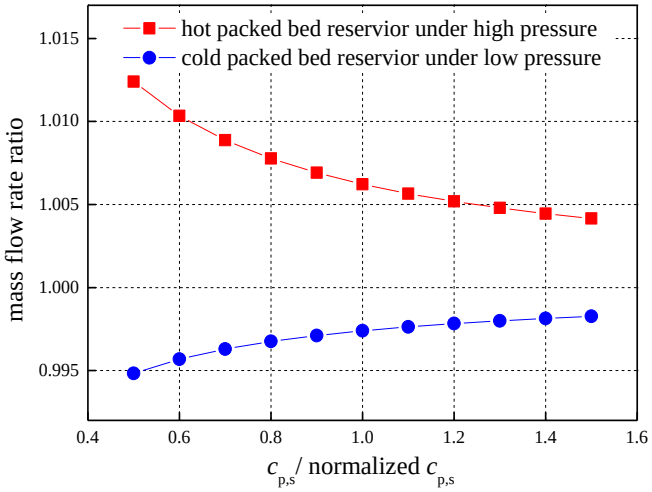

(c)

Fig. 8. Sensitivity to parameters: (a) Effect of pressure ratio; (b) Effect of porosity; (c) Effect of TES material $c_{p.}$

4.2. Mass flow of the PTES system

Although the hot reservoir releases gas and the cold reservoir absorbs gas simultaneously in the charging process of PTES system, the net mass flow out of the PTES is positive, but the PTES system is supposed to be a closed system of constant volume under stable pressure. For this, McTigue presents a buffer vessel (BV) to balance the total mass of gas as shown in Fig. 1(b) [30]. The mass flow of the PTES system in Fig. 1(b) is shown in Fig. 9, that when the mass flow rate of expander is 1.0, 0.36% of mass flow rate needs to be fed into the buffer vessel from the high pressure reservoir during the charging progress, and the same amount of mass flow rate feeds back to the low pressure reservoir from the buffer vessel during the discharging progress. On the other hand, we found that the mass flow rate ratios of expander to compressor in the PTES system are 99.74% and 100.26% for the charging cycle and discharging cycle, respectively.

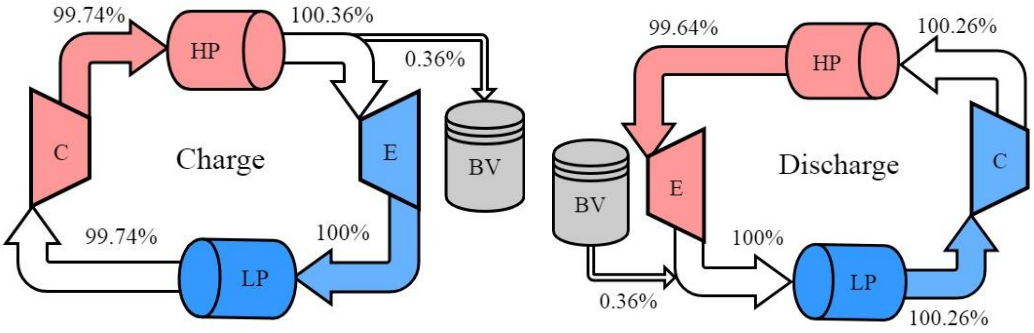

(a) (b)

Fig. 9. Mass flow of the PTES system: (a) charging; (b) discharging.

The feasible and self-balancing scheme to solve the imbalanced mass flow of the PTES system is to make the mass flow ratio of the hot reservoir and the cold reservoir reciprocal by selection of TES material with appropriate heat capacity and porosity, whose appearance is the same as Fig. 1(a) proposed by Desrues et al. [27] and White et al. [29]. Such a system has these potential benefits: no need for BV and complex control to maintain constant pressure; more gas participates in the energy storage cycle; increased round trip efficiency (there is exergy loss at the depressurization process from high pressure of hot reservoir to the BV and from the BV to the cold reservoir in the system in Fig. 1(b)); improved energy density due to reduced porosity. The mass flow of the self-balancing PTES system runs as shown in Fig. 10.

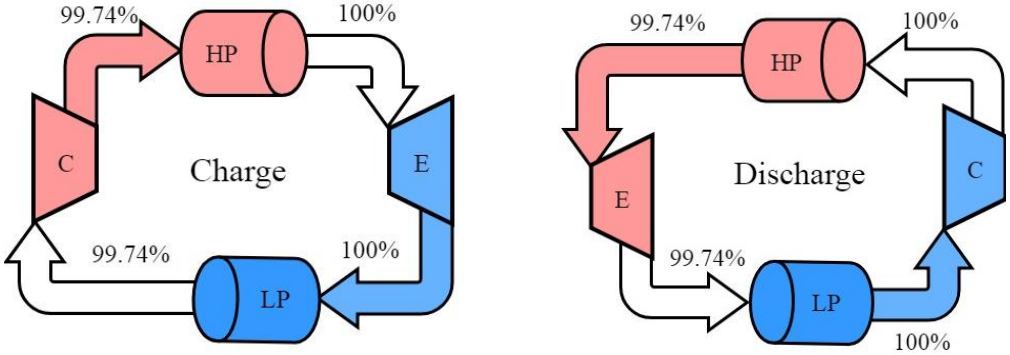

(a) (b)

Fig. 10. Mass flow of the modified PTES system: (a) charging; (b) discharging.

The mass flow relationship between the CR and HR of proposed self-balancing PTES system is as Eq. (15) that,

$$\frac{\dot{m}_{\mathrm{o,HR}}}{\dot{m}_{\mathrm{i,HR}}}\cdot\frac{\dot{m}_{\mathrm{o,CR}}}{\dot{m}_{\mathrm{i,CR}}}=1 \tag{15}$$

By analyzing Eq. (14) and Eq. (15) with a parameter $\delta=\varepsilon/(1-\varepsilon)$, we have the main influencing factors as shown in Eq. (16),

$$\frac{\left(\rho_{\mathrm{g,i,CR}}-\rho_{\mathrm{g,o,CR}}\right)}{\left(\rho_{\mathrm{g,o,HR}}-\rho_{\mathrm{g,i,HR}}\right)}\cdot\frac{\rho_{\mathrm{s,HR}}}{\rho_{\mathrm{s,CR}}}\cdot\frac{\bar{c}_{\mathrm{s,HR}}}{\bar{c}_{\mathrm{s,CR}}}\cdot\frac{\delta_{\mathrm{CR}}}{\delta_{\mathrm{HR}}}=1 \tag{16}$$

Where the gas densities have been decided in Table 1. Eq. (16) indicates that the self-balancing system can be obtained by: (1) selecting the suitable storage materials for HR and CR, and (2) adjusting the porosity of reservoirs.

One approach to adjust porosity is to utilize binary mixtures of particles with different sizes as the hot and cold energy storage material. The equation of the specific volume defined as the apparent volume occupied by a unit volume of solid particles for a binary mixture can be written as shown in Eq. (17) as [43, 44]

$$\left(\frac{V-V_{\mathrm{L}}X_{\mathrm{L}}}{V_{\mathrm{S}}}\right)^2+2G\left(\frac{V-V_{\mathrm{L}}X_{\mathrm{L}}}{V_{\mathrm{S}}}\right)\left(\frac{V-X_{\mathrm{L}}-V_{\mathrm{S}}X_{\mathrm{S}}}{V_{\mathrm{L}}-1}\right)+\left(\frac{V-X_{\mathrm{L}}-V_{\mathrm{S}}X_{\mathrm{S}}}{V_{\mathrm{L}}-1}\right)^2=1 \tag{17}$$

Where V is the specific volume of the binary mixture; V_{L} and V_{S} are the initial specific volumes, and X_{L} and X_{S} are the volume fractions of large and small particles, respectively. The relation of the coefficient G on the size ratio R ($R=d_{\mathrm{s}}/d_{\mathrm{l}}$) is [45]

$$G^{-1}=\begin{cases}1.355R^{1.566} & (R\le 0.824)\\ 1 & (R>0.824)\end{cases} \tag{18}$$

The packing of nonspherical particles and the characteristic size of nonspherical particles are then estimated by the correlation of Zou and Yu [46] as

$$d = \left(\frac{6V}{\pi}\right)^{\frac{1}{3}} \psi^{-2.875} \exp[-2.946(1-\psi)] \tag{19}$$

Where the Wadell's sphericity, Ψ, is defined as

$$\psi = \frac{\pi}{S}\left(\frac{6V}{\pi}\right)^{\frac{2}{3}} \tag{20}$$

Where S is the surface area and V is the volume.

Fig. 11 shows the calculated value of rock porosity by Eqs. (17)-(20) and the experimental results by Jeschar et al. for the ore and sinter of binary diameters [45]. The result indicates that significant reduction of porosity can be obtained by a large difference of size and a moderate volume ratio of binary pebbles.

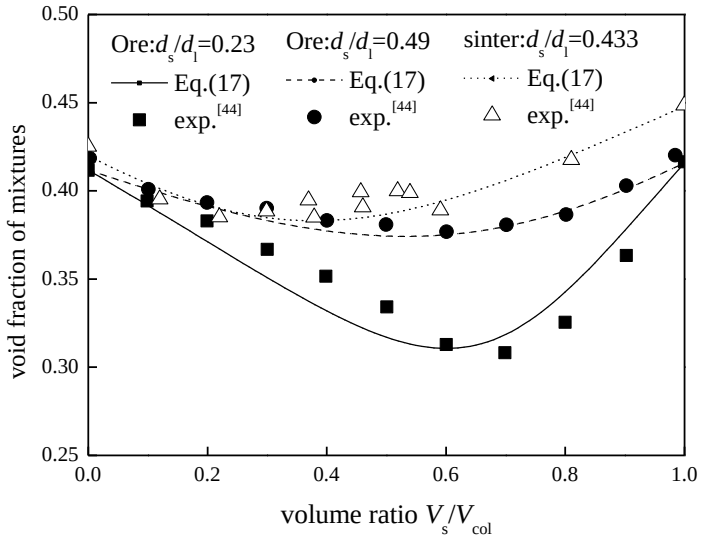

Fig. 11. Void fraction of mixtures of rocks with binary diameters.

There are many solutions to obtain a self-balancing PTES system by selecting different materials that meets Eq. (16). One solution is using granite as both the heat and cold storage material with the detailed parameters as shown in Table 2 where the temperature dependence of specific heat capacity of granite is from [47]. The TES material in HR is the packed bed of binary mixture with d_s/d_l=0.1 and V_s/V_{col}=0.65,

where the binary particles should be intensive mixed before installed in the HR.

Table 2. Designed hot and cold reservoir of the self-balancing PTES system (storage material granite with the density of 2650 kg/m^3)

Reservoir	Inflow gas Density (kg/m^3)	Outflow gas Density (kg/m^3)	Average c_s (J/kg/K)	Porosity	Packed bed particles
HR	6.46	16.36	1110	0.256	binary mixture with d_s/d_l=0.1 and V_s/V_{col}=0.65
CR	4.15	1.63	574	0.41	monosize particles

4.3. Round trip coefficient of the PTES system

As discussed above, the packed bed TES reservoir of PTES system would certainly cause the inequality of the mass flow rate between the hot side and cold side, as well as the mass flow through the compressor and expander. Taking the mass flow rate difference into account for the prediction of the round trip coefficient of PTES system will improve accuracy.

Supposing no mechanical loss or pressure loss, the round trip coefficient of the PTES system is obtained by the quotient of net shaft work output during the discharging process and the input shaft work during charging, as shown in Eq. (21)

$$\chi = \frac{\text{net work output}}{\text{net work input}} = \frac{\dot{m}_{e\_dis} c_p (T_2^{'} - T_1^{'}) - \dot{m}_{c\_dis} c_p (T_3^{'} - T_4^{'})}{\dot{m}_{c\_chg} c_p (T_2 - T_1) - \dot{m}_{e\_chg} c_p (T_3 - T_4)} \quad (21)$$

Where primes denote quantities during discharge, and $\dot{m}$ is the mass flow rate though the compressors and expanders. Polytropic process of compression and expansion occurs with the polytropic efficiencies η_c and η_t respectively. The parameter

κ is defined as $\kappa = (\gamma-1)/\gamma$.

$$T_2/T_1 = T_3^{'}/T_4^{'} = r_c^{\kappa/\eta_c} \tag{22}$$

$$T_4/T_3 = T_1^{'}/T_2^{'} = r_t^{\kappa\eta_t} \tag{23}$$

Where r_c and r_t are the pressure ratio of compressor and turbine.

$$\chi = \frac{\dot{m}_{e\_dis} T_2^{'}(1-r_t^{\eta_t\kappa}) - \dot{m}_{c\_dis} T_4^{'}(r_c^{\kappa/\eta_c}-1)}{\dot{m}_{c\_chg} T_1 (r_c^{\kappa/\eta_c}-1) - \dot{m}_{e\_chg} T_3 (1-r_t^{\eta_t\kappa})} \tag{24}$$

Ignoring losses due to heat storage and transfer, we have $T_2 = T_2'$ and $T_4 = T_4'$. After sufficient heat transfer of HX1 and HX2, T_1 and T_3 return to atmospheric temperature. And supposing the pressure ratio of compressor and turbine is the same during charging and discharging, we have the round trip efficiency as

$$\chi = \frac{\dot{m}_{e\_dis} r^{\kappa/\eta_c}(1-r^{\eta_t\kappa}) - \dot{m}_{c\_dis} r^{-\eta_t\kappa}(r^{\kappa/\eta_c}-1)}{\dot{m}_{c\_chg}(r^{\kappa/\eta_c}-1) - \dot{m}_{e\_chg}(1-r^{\eta_t\kappa})} \tag{25}$$

For the self-balancing PTES system shown in Fig. 1(a), the mass flow rate ratio e indicates the mass flow ratio of the compressor to the expander during the charging process as in Eq. (26)

$$e = \frac{\dot{m}_{e\_dis}}{\dot{m}_{c\_dis}} = \frac{\dot{m}_{c\_chg}}{\dot{m}_{e\_chg}} \tag{26}$$

And the round trip efficiency of the self-balancing PTES system is as in Eq. (27)

$$\chi = \frac{e\cdot r^{\kappa/\eta_c}(1-r^{\eta_t\kappa}) - r^{-\eta_t\kappa}(r^{\kappa/\eta_c}-1)}{e\cdot(r^{\kappa/\eta_c}-1) - (1-r^{\eta_t\kappa})} \tag{27}$$

For the PTES system balancing the mass with the BV as in Fig. 1(b), the mass flow rate ratio e is calculated as in Eq. (28)

$$e = \frac{\dot{m}_{e\_dis} + \dot{m}_{BV\_chg}}{\dot{m}_{c\_dis}} = \frac{\dot{m}_{c\_chg} + \dot{m}_{BV\_chg}}{\dot{m}_{e\_chg}} \tag{28}$$

Where the expressions of compressor and turbine polytropic efficiencies as

functions of pressure ratios provided by Wilson [48] as in Eqs. (29) and (30) are

$$\eta_c = 0.91 - \frac{r_c - 1}{300} \tag{29}$$

$$\eta_t = 0.90 - \frac{r_t - 1}{250} \tag{30}$$

The round trip efficiency of PTES systems under different conditions are predicted based on Eqs. (27)-(30), including: case 1, supposing the mass flow rate of the system is equal everywhere; case 2, balancing mass by the BV as shown in Fig.1 (b) and the mass flow shown in Fig. 9; case 3, balancing mass by making the mass flow ratio of the hot reservoir and the cold reservoir reciprocal as shown in Fig. 1 (c) and the mass flow shown in Fig. 10. As plotted in Fig. 12, the round trip efficiency of PTES system increases with the increasing of the pressure ratio. The effect of the mass flow rate imbalance is not significant and the coefficient of PTES systems considering the unequal mass flow rate is a little smaller than a coefficient produced under an assumption of equal mass flow rate. The round trip efficiency of PTES system as Fig. 1(a) and the mass flow as Fig. 10 is higher than that of the BV balancing system as Fig. 1 (b) and the mass flow as Fig. 9, and they are 57.42% and 57.30% at a pressure ratio of 15, respectively.

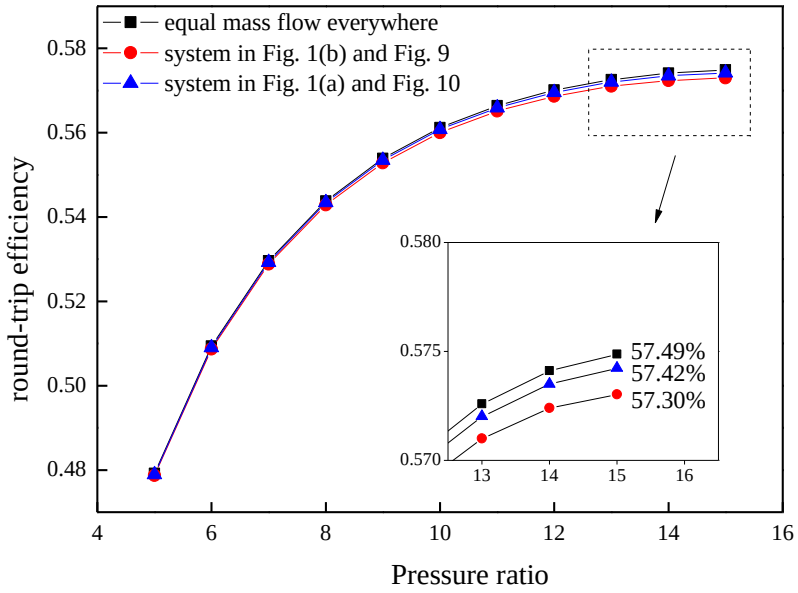

Fig. 12. Effect of pressure ratio on the round trip efficiency of PTES systems.

From the above studies, it can be found that 0.12% increase of round-trip efficiency obtained through the self-balancing method based on the system parameters in [29], which is not very significant. However, a large amount of initial cost of PTES can be saved by abolishing the components including the BV, pressure pipelines, valves and their controller. According to the parameters in [30], the volume of the high pressure BV need to be more than 12% of the HR volume, and the cost of the buffer vessel is comparable with the CR since the hot store is expected to cost between 11 and 17 Euro/kWh and the cold store 2 and 4 Euro/kWh [37]. Furthermore, the throttle loss of the regulating valve when gas fed into the BV is about 0.21% of the compression work, which can be saved in the self-balancing system.

5. Conclusion

For new-type pumped thermal electricity storage as a form of thermal energy storage, the issue of unbalanced mass flow rate between the inflow and the outflow of

packed beds under constant pressure has been analyzed. The correlations of the speed of thermal front propagation and the mass flow rate ratio between the inflow and the outflow have been developed. The cryogenic TES experiment of packed bed was carried out under the pressure of 6.5 MPa with nitrogen as the working fluid. It was found that steep cold thermal front propagated in the packed bed and the predicted mass flow rate ratio fit well with the experimental results with a deviation of less than ±8%. The influence of factors such as porosity, pressure ratio, and heat capacity ratio of gas to TES material on the ratio of mass flow rate was analyzed further.

The unbalanced mass flow behavior of the packed bed reservoirs and PTES system is found that, based on the designed PTES system parameters, the outflow mass flow rate of the hot and cold TES reservoir is 1.0062 and 0.9974 times of the inflow, respectively; and 0.36% of the total mass flow rate needs to be stored in BV of large volume owing to the cumulative charging over hours. And the expression of the round-trip efficiency is proposed where the unbalanced mass flow is taken into account.

Furthermore, a self-balancing PTES system is proposed with the methods including the selection of appropriate storage materials and the adjustment of porosity by pebble mixture of the binary diameters. Comparisons indicate that the self-balancing PTES system will not only improve the 0.12% of round-trip efficiency but also save the initial cost by voiding the components including the BV, pressure pipelines, valves and their controller. In addition, the mass flow ratio imbalance would be mitigated through the increase of heat capacity of TES material and the

decrease in porosity, so as to increase round trip efficiency and energy storage density.

6. Acknowledgements

The authors would like to thank the National Natural Science Foundation of China (NO.U1407205), Transformational Technologies for Clean Energy and Demonstration, the Strategic Priority Research Program of CAS (NO.XDA21070200), The Frontier Science Research Project of CAS (NO.QYZDB-SSW-JSC023) and the Youth Innovation Promotion Association CAS (NO.2016131). The authors would also like to thank Theo Carney for assistance in the manuscript revision process.

References

[1] Dale S. BP Statistical Review of World Energy June 2017, 2017.

[2] Sawin JL, Sverrisson F, Seyboth K, et al. Renewables 2017 Global Status Report. 2017.

[3] Chen H, Cong T N, Yang W, et al. Progress in electrical energy storage system: A critical review. Prog Nat Sci 2009; 19(3): 291-312.

[4] Luo X, Wang J, Dooner M, et al. Overview of current development in electrical energy storage technologies and the application potential in power system operation. Appl Energy 2015; 137: 511-36.

[5] Walawalkar R, Apt J, Mancini R. Economics of electric energy storage for energy arbitrage and regulation. Energ Policy 2007; 5: 2558-68.

[6] Dobie WC. Electrical energy storage. Power Eng J 1998; 12, 177-181.

[7] Aneke M, Wang M. Energy storage technologies and real life applications-A state of the art review. Appl Energy 2016; 179: 350-77.

[8] http://www.energystorageexchange.org/

[9] Barnes, Frank S., and Jonah G. Levine, eds. Large energy storage systems handbook. CRC press, 2011.

[10] https://www.highviewpower.com/

[11] Sciacovelli A, Vecchi A, Ding Y. Liquid air energy storage (LAES) with packed bed cold thermal storage – From component to system level performance through dynamic modelling. Appl Energy 2017; 190: 84-98.

[12] Advanced compressed air energy storage won the first prize of Beijing science and technology, http://www.escn.com.cn/news/show-222217.html.

[13] The 10MW compressed air energy storage is under integrated test, http://www.escn.com.cn/news/show-377349.html

[14] Thess A. Thermodynamic efficiency of pumped heat electricity storage. Phys Rev Lett 2013; 111(11):110602.

[15] Frate G F, Antonelli M, Desideri U. A novel pumped thermal electricity storage (PTES) system with thermal integration. Appl Therm Eng 2017; 121: 1051-8.

[16] Abarr M, Geels B, Hertzberg J, et al. Pumped thermal energy storage and bottoming system part A: Concept and model. Energy 2017; 120: 320-31.

[17] Abarr M, Hertzberg J, Montoya LD. Pumped thermal energy storage and Bottoming System Part B: Sensitivity analysis and baseline performance. Energy 2017; 119: 601-11.

[18] Benato A, Anna S. Energy and cost analysis of a new packed bed pumped thermal electricity storage unit. J Energ Resour-ASME 2018;140(2): 020904.

[19] Morandin M, Henchoz S, Mercangöz M. Thermo-electrical energy storage: a new type of large scale energy storage based on thermodynamic cycles. World Engineers' Convention 2011.

[20] Morandin M, Maréchal F, Mercangöz M, et al. Conceptual design of a thermo-electrical energy storage system based on heat integration of thermodynamic cycles–Part A: Methodology and base case. Energy 2012; 45: 375-85.

[21] Morandin M, Maréchal F, Mercangöz M, et al. Conceptual design of a thermo-electrical energy storage system based on heat integration of thermodynamic cycles–Part B: Alternative system configurations. Energy 2012; 45: 386-96.

[22] Steinmann WD. The CHEST (Compressed Heat Energy STorage) concept for facility scale thermo mechanical energy storage. Energy 2014; 69: 543-52.

[23] Guo J, Cai L, Chen J, et al. Performance optimization and comparison of pumped thermal and pumped cryogenic electricity storage systems. Energy 2016; 106: 260-9.

[24] Vinnemeier P, Wirsum M, Malpiece D, et al. Integration of heat pumps into thermal plants for creation of large-scale electricity storage capacities. Appl Energy 2016; 184: 506-22.

[25] Wang G B, Zhang X R. Thermodynamic analysis of a novel pumped thermal energy storage system utilizing ambient thermal energy and LNG cold energy. Energy Convers Manage 2017; 148: 1248-64.

[26] Roskosch D, Atakan B. Pumped heat electricity storage: potential analysis and

orc requirements. Energy Procedia 2017; 129: 1026-1033.

[27] Desrues T, Ruer J, Marty P, et al. A thermal energy storage process for large scale electric applications. Appl Therm Eng 2010; 30: 425-32.

[28] Howes J. Concept and development of a pumped heat electricity storage device. Proceedings of the IEEE 2012; 100(2): 493-503.

[29] White A, Parks G, Markides C. Thermodynamic analysis of pumped thermal electricity storage. Appl Therm Eng 2013; 53:291-8.

[30] McTigue J, White A, Markides C. Parametric studies and optimization of pumped thermal electricity storage. Appl Energy 2015; 137: 800-11.

[31] White A, McTigue J, Markides C. Analysis and optimisation of packed-bed thermal reservoirs for electricity storage applications, Proc. Inst. Mech. Eng. Part A J. Power Energy 2016; 230: 739-754.

[32] Davenne TR, Garvey SD, Cardenas B, et al. The cold store for a pumped thermal energy storage system. J Energ Storage 2017; 14: 295-310.

[33] Benato A. Performance and cost evaluation of an innovative pumped thermal electricity storage power system. Energy 2017; 138: 419-436.

[34] Benato A, Stoppato A. Heat transfer fluid and material selection for an innovative Pumped Thermal Electricity Storage system. Energy 2018; 147: 155-68.

[35] http://www.isentropic.co.uk/

[36] Hot rock solution to grid-scale energy storage, https://www.ncl.ac.uk/press/articles/archive/2017/11/isentropic/

[37] Smallbone A, Jülch V, Wardle R et al. Levelised Cost of Storage for Pumped

Heat Energy Storage in comparison with other energy storage technologies. Energy Convers Manag 2017; 152: 221-228.

[38] Solomos G, Shah N, Markides C. A thermo-economic analysis and comparison of pumped-thermal and liquid-air electricity storage systems. Appl Energy 2018; 226: 1119-1133.

[39] Steinmann WD. Thermo-mechanical concepts for bulk energy storage. Renewable Sustainable Energy Rev 2017; 75: 205-219.

[40] Benato A, Stoppato A. Pumped Thermal Electricity Storage: A technology overview. Therm Sci Eng Progress 2018; 6: 301-315.

[41] Gil A, Medrano M, Martorell I, et al. State of the art on high temperature thermal energy storage for power generation. Part 1-Concepts, materials and modellization. Renew Sustain Energy Rev 2009; 14: 31-55.

[42] White A, McTigue J, Markides C. Wave propagation and thermodynamic losses in packed-bed thermal reservoirs for energy storage. Appl Energy 2014; 130: 648-57.

[43] Westman AER. The packing of particles: empirical equations for intermediate diameter ratios. J Am Ceram Soc 1936; 19(1-12): 127-9.

[44] Yu AB, Standish N, McLean A. Porosity calculation of binary mixtures of nonspherical particles. Am Ceram Soc 1993; 76(11): 2813-6.

[45] Jeschar R, Potke W, Petersen V, et al. Blast furnace aerodynamics. Proceedings of the symposium on blast furnace aerodynamics 1975; 25-7.

[46] Zou RP, Yu AB. Evaluation of the packing characteristics of mono-sized non-spherical particles. Powder Technol 1996; 88(1): 71-9.

[47]Wen H, Lu J, Xiao Y, et al. Temperature dependence of thermal conductivity, diffusion and specific heat capacity for coal and rocks from coalfield. Thermochim Acta 2015; 619: 41-47.

[48] Wilson DG, Korakianitis T. The design of high-efficiency turbomachinery and gas turbines. MIT press; 2014.

***Declaration of Interest Statement**

Declaration of interests

☒ The authors declare that they have no known competing financial interests or personal relationships that could have appeared to influence the work reported in this paper.

☐The authors declare the following financial interests/personal relationships which may be considered as potential competing interests: